12-3-2014 12:00 AM

Investigating Cortical Changes in Cervical Spondylotic Myelopathy Using Functional Magnetic Resonance Imaging, Proton Magnetic Resonance Spectroscopy and Diffusion Tensor Imaging

Izabela Kowalczyk
The University of Western Ontario

Supervisor
Dr. Robert Bartha
The University of Western Ontario Joint Supervisor
Dr. Neil Duggal
The University of Western Ontario

Graduate Program in Medical Biophysics
A thesis submitted in partial fulfillment of the requirements for the degree in Doctor of Philosophy

INVESTIGATING CORTICAL CHANGES IN CERVICAL SPONDYLOTIC MYELOPATHY USING FUNCTIONAL MAGNETIC RESONANCE IMAGING, PROTON MAGNETIC RESONANCE SPECTROSCOPY AND DIFFUSION TENSOR IMAGING

by

Izabela Aleksanderek

Graduate Program in Medical Biophysics

A thesis submitted in partial fulfillment
of the requirements for the degree of
Doctor of Philosophy

The School of Graduate and Postdoctoral Studies
The University of Western Ontario
London, Ontario, Canada

ABSTRACT

Cervical spondylotic myelopathy (CSM) is the most common cause of spinal cord dysfunction in older adults and results in motor and sensory dysfunction. CSM can present abruptly with severe symptoms of neurological impairment or insidiously with a slow stepwise deterioration. There is no current imaging modality or biomarker that can help predict which patient will successfully respond to conservative versus surgical treatment. Previous research suggests that surgical intervention triggers functional alterations in the CSM patient sensorimotor cortex. The goal of this thesis was to follow a group of CSM patients longitudinally to assess how brain function, metabolism, and structure correlate to clinical outcomes in the context of recovering neurological function following surgery.

Chapter 1 of this thesis provides a detailed literature review of the current controversies in treating CSM, specifically between mild and moderate severities of CSM. Novel imaging techniques that can elucidate cortical adaptations in CSM patients are discussed. In chapter 2, the cortical metabolite profile was characterized in a group of CSM patients using proton magnetic resonance spectroscopy (MRS). A lower *N*-Acetylaspartate (NAA) to creatine (Cr) ratio was found in the CSM patients with decreased neurological function compared to controls, indicative of neuronal death or mitochondrial dysfunction. In chapter 3, the metabolite changes in the primary motor cortex of CSM patients are shown to recover following successful surgical intervention. The structural integrity of the white matter adjacent to the primary motor and sensory cortices was also assessed using diffusion tensor imaging (DTI). The DTI results indicated maintenance of white matter and axonal integrity, while a decrease in NAA/Cr following surgery suggested neuronal mitochondrial impairment. Our findings of a clear neurological improvement in CSM patients following surgery support the hypothesis that

neurological recovery may require the recruitment of surrounding cortex, given that focal recovery in the motor cortex may be metabolically unattainable. In chapter 4, functional MRI is used to study the cortical adaptation and reorganization that occurs in mild and moderate CSM severities, prior to and following decompressive surgery. The goal was to determine whether there are critical factors (metabolite and/or functional) that can classify patients along a spectrum of injury severity, and predict successful surgical outcome. This study found distinct metabolic and functional profiles in the motor cortex that discriminate between mild and moderate CSM patients prior to surgery. We propose mitochondrial dysfunction, indicated by low levels of NAA/Cr, as the primary trigger for cortical reorganization and recruitment leading to functional improvement. Collectively, this thesis utilizes novel imaging methods to explore how the cortex adapts and compensates for neurological deficits, distal to the site of injury, and attempts to identify new imaging biomarkers to characterize the severity of CSM and predict functional recovery.

Keywords:

cervical spondylotic myelopathy; spinal cord compression, neuroimaging, functional MRI, magnetic resonance spectroscopy, diffusion tensor imaging, *N*-Acetylaspartate, white matter, brain reorganization, disease severity

CO-AUTHORSHIP STATEMENT

The following thesis contains material from previously published and submitted manuscripts, as well as material from a third manuscript that is in preparation for submission. Permission was obtained from the publishers to reproduce each manuscript, and appears in Appendix C and D. The contributions of co-authors for each chapter are summarized below. With the exception of the co-author contributions listed below, Izabela Aleksanderek performed all of the protocol development, patient recruitment and follow-up, data acquisition and analysis, statistical analysis, interpretation of the results, and preparation and submission of manuscripts.

The material contained in Chapter 2 has been published in *Brain* in a manuscript entitled, 'Proton magnetic resonance spectroscopy of the motor cortex in Cervical Spondylotic Myelopathy' (135(Pt 2):461-468, 2012). Co-authors were Izabela Aleksanderek (nee Kowalczyk), Neil Duggal, and Robert Bartha. N Duggal performed the clinical assessments and the decompressive surgery in all CSM patients. N Duggal and R Bartha were responsible for the design of the study. R Bartha and N Duggal provided guidance and support in the analysis and interpretation of the data. N Duggal and R Bartha provided critical review and revision of the manuscript.

The material contained in Chapter 3 is in preparation for submission in a manuscript entitled, 'Metabolite changes in the primary motor cortex after surgery in Cervical Spondylotic Myelopathy'. Co-authors were Izabela Aleksanderek, Stuart M McGregor, Todd K Stevens, Sandy Goncalves, Robert Bartha, and Neil Duggal. SM McGregor performed the diffusion tensor imaging data analysis. TK Stevens completed the secondary magnetic resonance spectroscopy data analysis. S Goncalves recruited and scanned a subset of patients. R Bartha and N Duggal

were involved in the design and oversight of the study and provided guidance and support in the analysis and interpretation of the data. N Duggal performed the clinical assessments and the decompression surgery in all CSM patients. N Duggal and R Bartha provided critical review and revision of the manuscript.

The material contained in Chapter 4 is in preparation for submission in a manuscript Entitled, 'Mild and moderate Cervical Spondylotic Myelopathy: Are they metabolically and functionally different?' Co-authors were Izabela Aleksanderek, Todd K Stevens, S Goncalves, R Bartha and N Duggal. TK Stevens completed the secondary MRS data analysis. S Goncalves recruited and scanned a subset of patients. R Bartha and N Duggal were involved in the design and oversight of the study and provided guidance and support in the analysis and interpretation of the data. N Duggal performed the clinical assessments and the decompression surgery in all CSM patients. N Duggal and R Bartha provided critical review and revision of the manuscript.

ACKNOWLEDGMENTS

My doctoral studies and thesis writing has been a long journey, one I could not have completed without a few special people in my life. To begin, I would like to thank my family for being a pilar of support during my pursuit of my studies. The biggest thank you goes to my parents, Grażyna and Edward Kowalczyk, who have been my motivation and inspiration for as long as I can remember. You have both taught me about hard work, persistence, and perseverance to reach your goals. Thank you for being great role models of resilience, strength and character. Your continuous and never-ending love, and encouragement has helped me complete my studies and made me the person I am today. Thank you with all my heart.

I am particularly grateful to my wonderful husband, Filip Aleksanderek, for being by my side during my very long graduate education years. Thank you for being there from the start of my experiments and being my guinea pig by laying in the MRI scanner for over 4 hours while I perfected my protocol, helping me with physics assignments, and quizzing me for all my tests and exams. Thank you for your love and motivation and keeping a sense of humor when I lost mine. Thank you for coming to my presentations and cheering me on in this journey. For all these reasons and many, many more, I am eternally grateful. Thank you for believing in me. And to my husband's family who have all been supportive and caring.

This thesis would not have been possible without the mentorship of my supervisors: Dr. Neil Duggal and Dr. Robert Bartha. Dr. Duggal has been a great mentor for the past 9 years, starting with my second year in my undergraduate studies where I started working for him as a research assistant. Dr. Duggal was the reason why I decided to pursue a career in research. His enthusiasm is contagious. He has been helpful in providing advice many times during my undergraduate and

graduate school career. He's been motivating, encouraging, and enlightening. For this, I cannot thank him enough. I am forever grateful. Dr. Bartha taught me numerous skill sets that I will carry throughout my career. He has instilled in me the confidence I need to be a successful clinician scientist. Dr. Bartha is a great teacher , is patient and has encouraged me to think critically about my experiments and data analysis. He taught me leadership and time management by responding to my MANY emails, even to the very end of my thesis submission. He remains my best role model for a scientist, and teacher. Thank you.

I am indebted to the members of my advisory committee: Jody Culham and Ravi Menon. Your academic support, and stimulating questions you asked at each meeting are greatly appreciated.

Next, I would like to thank Joy Williams, Kim Krueger, and Adam McLean for their assistance with MRI data collection and all the evening and weekend scans they agreed to that kept my patient recruitment on track.

I would also like to thank all my lab group members, and Todd Stevens, Stuart McGregor and Jacob Penner in particular. Aspects of my data collection and analysis would not have been possible without your collaboration. Thank you for all the challenging discussions and wonderful friendships.

Special gratitude goes towards Patricia Doyle-Pettypiece for being one of the first friendly faces to greet me in Outpatient Neurosurgery Clinics when I first began as a research assistant in my undergraduate studies and continued on as a PhD student. She took me under her wing and taught

me how to first and foremost, listen to the patient, and how to convey sensitive and sometimes heartbreaking information. Thank you Pat.

Thank you Jennifer Long for your friendship during my work as a research assistant and helping me transition into my doctoral studies. Your quick responses to my numerous emails, and your organization skills have helped me keep on track with data collection and patient follow-up appointments.

I would like to thank my dear friends Dzvena Krivoglavyi and Magda Zdunek, who have played the parts of roommate, confidant, phone comrade, and study buddies. You have both played so many roles in my life that I cannot express enough gratitude to you for being tough on me, supportive, and caring. Dzvena, I am indebted to you for countless discussions and late study night that helped me to focus and complete the writing of my thesis. You are both true life-long friends.

Thank you to all my other dear friends who have affectionately referred to my thesis as “The Paper,” and asked, “Are you done yet?” and calling me the “eternal student.” Thank you for your support, and humor that kept me smiling.

TABLE OF CONTENTS

LIST OF FIGURES

LIST OF TABLES

LIST OF ABBREVIATIONS

^{1}H	Hydrogen
^{1}H-MRS	Proton Magnetic Resonance Spectroscopy
^{13}C	Carbon
^{19}F	Fluorine
^{23}Na	Sodium
^{31}P	Phosphorus
ADC	Apparent diffusion coefficient
ASIA	American Spinal Injury Association Impairment Scale
ATP	Adenosine triphosphate
BOLD	Blood Oxygen Level Dependent
Cho	Choline
Cho/Cr	Choline/Creatine
CK	Creatine kinase
CNS	Central nervous system
Cr	Creatine
CSF	Cerebrospinal fluid
CSM	Cervical Spondylotic Myelopathy
CT	Computerised tomography
dHb	deoxygenated hemoglobin
DTI	Diffusion Tensor Imaging
DWI	Diffusion Weighted Imaging
fMRI	functional Magnetic Resonance Imaging
FA	Fractional anisotropy
GABA	Gamma-aminobutyric acid
Gln	Glutamine
Glu	Glutamate
Glx	Glutamine and Glutamate
Glx/Cr	Glutamine and Glutamate/Creatine
GPCho	Glycerophosphorylcholine
H_20	Water
Hb	oxygenated hemoglobin
HDR	Hemodynamic response
JOACMEQ-L	Japanese Orthopaedic Association Cervical Myelopathy Evaluation Questionnaire
K+	Potassium
MD	Mean diffusivity
M1	Primary motor cortex
mJOA	modified Japanese Orthopaedic Association score
MRI	Magnetic Resonance Imaging
MRS	Magnetic Resonance Spectroscopy
Myo	Myo-inositol
Myo/Cr	Myo-inositol/Creatine
M_z	Net magnetization
NAA	*N*-Acetylaspartate
NAA/Cr	*N*-Acetylaspartate/Creatine
NAAG	*N*-Acetylaspartylglutamate

NDI	Neck Disability Index
NO·	Nitric Oxide
PCho	Phosphocholine
PCr	Phosphocreatine
PD	Proton density
ppm	parts per million
RF	Radiofrequency
S1	Primary sensory cortex
SCC	Spinal cord compression
SCI	Spinal cord injury
SF-36	36-Item Short Form Health Survey
SNR	signal-to-noise ratio
T_1	Longitudinal magnetization
T_2	Transverse magnetization
TE	Echo time
TMS	Transcranial magnetic stimulation
TR	Repetition time
VOA	Volume of activation
VOI	Volume of interest
WM	White matter

CHAPTER 1:

INTRODUCTION AND GOAL OF THESIS

1. 1 Cervical Spondylotic Myelopathy

Cervical spondylosis is used to describe the degenerative changes of the spine that become increasingly more prevalent with aging. In its most severe form, spondylosis can lead to compression of the spinal cord referred to as cervical spondylotic myelopathy (CSM).[1-3] CSM is the most common form of spinal cord dysfunction in people over the age of 55.[2,3] Male patients are preferentially affected at a ratio of 2.7:1 and spinal cord compression can occur at multiple levels with C5-C6 being the most common.[2,4-5] A majority of the older population will show signs of pathological or radiographic evidence of cervical degeneration, and the progression to CSM with symptoms of neurological impairment becomes more prevalent with increasing age.[2,6] The CSM population is heterogeneous with symptoms ranging from mild dysfunction, such as numbness or problems with dexterity, to severe, such as quadraparesis and incontinence.[1-4] The diagnosis of CSM can be difficult as the onset of symptoms is usually insidious with long periods of disability and short episodes of worsening.[2] Each year thousands of Canadians with worsening spinal cord compression, debilitating symptoms and failure to respond to alternative treatments will require surgical intervention. Current assessments include patient history, physical examination, x-ray, and magnetic resonance imaging (MRI). Nonetheless, clinical improvement is difficult to predict. There is a need for improved pre-operative screening to predict the outcome of decompressive surgery in this debilitating disease.

1.1.1 Pathophysiology and Pathology of CSM

As part of normal aging, degenerative changes occur in various components of the spine such as the vertebral body, intervertebral disc, supporting ligaments and facet joints, eventually leading to narrowing of the spinal canal at one or more levels.[2,5-6] CSM results from this degeneration and the primary mechanism of injury is secondary to compression of the spinal cord (Figure

1.1).[2] The degenerative cascade typically begins with the deterioration of the intervertebral disc. The disc collapses and the annulus bulges posteriorly causing narrowing of the spinal canal. These changes can lead to osteophyte formation and increase the stress on the facets.[2,6] Decreased disc height also causes the spinal column to shorten, leading to alignment changes.[2,5] The ligamentum flavum thickens and buckles into the spinal canal. Ossification of the posterior longitudinal ligament, most commonly seen in Asian populations, can also lead to CSM by direct compression of the spinal cord.[7] In conjunction, hypermobility and abnormal spine biomechanics cause hypertrophy and ossification of the facets, posterior longitudinal ligament and ligamentum flavum.[2,5-6] Congenital narrowing or acquired subluxation, uncovertebral joint thickening and osteoarthritis can also play a part in narrowing of the spinal canal.[2] As the degenerative cascade continues, the affected vertebrae become stiffer, and initiate hypermobility at adjacent vertebrae.[2]

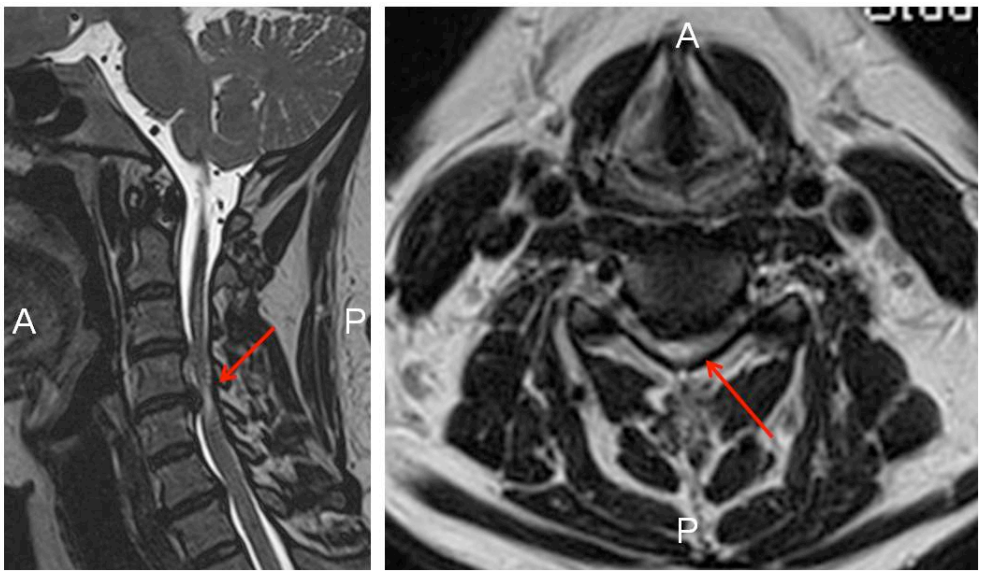

Figure 1.1: A sagittal *(left)* and axial (*right*) T_2-weighted image of the cervical spine. The red arrows point to the cord compression at the C4-C5 level due to intervertebral disc bulging.

Spondylotic changes happen concurrently with static factors responsible for stenosis, and dynamic factors causing repetitive injury to the cord and ischemia. Static factors include a congenitally narrow canal, osteophyte formation, hypertrophy of the ligamentum flavum, ossification of the posterior longitudinal ligament and subluxation.[2,3] Static factors cause structural degenerative changes that decrease the size of the spinal canal from its normal cervical canal diameter of 17-18 mm in Caucasians from the C3-C7 levels (with some variation between genders).[8] Dynamic factors refer to abnormal repetitive movement of the cervical spine during flexion and extension causing nerve root and spinal cord irritation and compression. During flexion, the spinal cord stretches and can be compressed against anterior osteophytic spurs and intervertebral discs.[2,7,9] Hyperextension may lead to spinal cord "pinching" between the posterior margin of the vertebral body anteriorly and the hypertrophied ligamentum flavum posteriorly.[2,7,9] The third factor, ischemia, occurs when the blood vessels that supply the spinal cord and nerve roots are compressed by degenerative structures.[9] The ischemia and the decreased blood flow may initiate apoptosis, which is suggested to be the primary cellular process underlying the disappearance of oligodendrocytes in CSM.[10-11] Oligodendrocytes aid in neurological development, repair of axonal injury and in the formation of myelin.[11]

Pathological findings due to mechanical compression and restricted microvasculature likely result in gray and white matter degeneration, cystic cavitation, gliosis, posterolateral white matter demyelination, sparing of anterior columns, and atrophy of the anterior horns.[8,12]

1.1.2 Clinical Presentation

The onset of symptoms is usually insidious with long periods of disability and short episodes of worsening, however symptoms can develop acutely or transiently.[2] Pain is not always associated with the progressive loss of function and patients learn to adapt, attributing the slow progression to natural aging.[3] In the early stages of CSM, common presentation includes neck stiffness, changes in muscle tone, superficial sensory loss, deteriorations in gait, balance and manual dexterity.[3,7] Symptoms can progress to quadraparesis, incontinence and loss of urethral sphincter control.[3,7] Patients who do progress, experience a large functional decline leading to a reduced quality of life.

1.1.3 Natural History

The natural history of CSM is unpredictable.[13-16] Clarke and Robinson observed 120 CSM patients without treatment and found that 75% worsened in a stepwise fashion, 20% slowly worsened and 5% experienced rapid onset of symptoms without further progression.[13] Epstein *et al*. found that in a series of 1355 patients, 36% reported improvement and 64% either remained stable or deteriorated in function.[14] There are few predictors to determine which patients will experience spontaneous improvement and which will have progressive deterioration over time.

1.1.4 Clinical Measurements

Validated instruments for assessing disability resulting from spinal cord compression include the American Spinal Injury Association Impairment Classification (ASIA) Scale (Figure 1.2) and the modified Japanese Orthopaedic Association Score for CSM (mJOA).[17] For the ASIA scale, the maximum motor score is 100 (50 for upper limb and 50 for lower limb) and the maximum sensory score is 112 for light touch and 112 for pin prick (Figure 1.2).

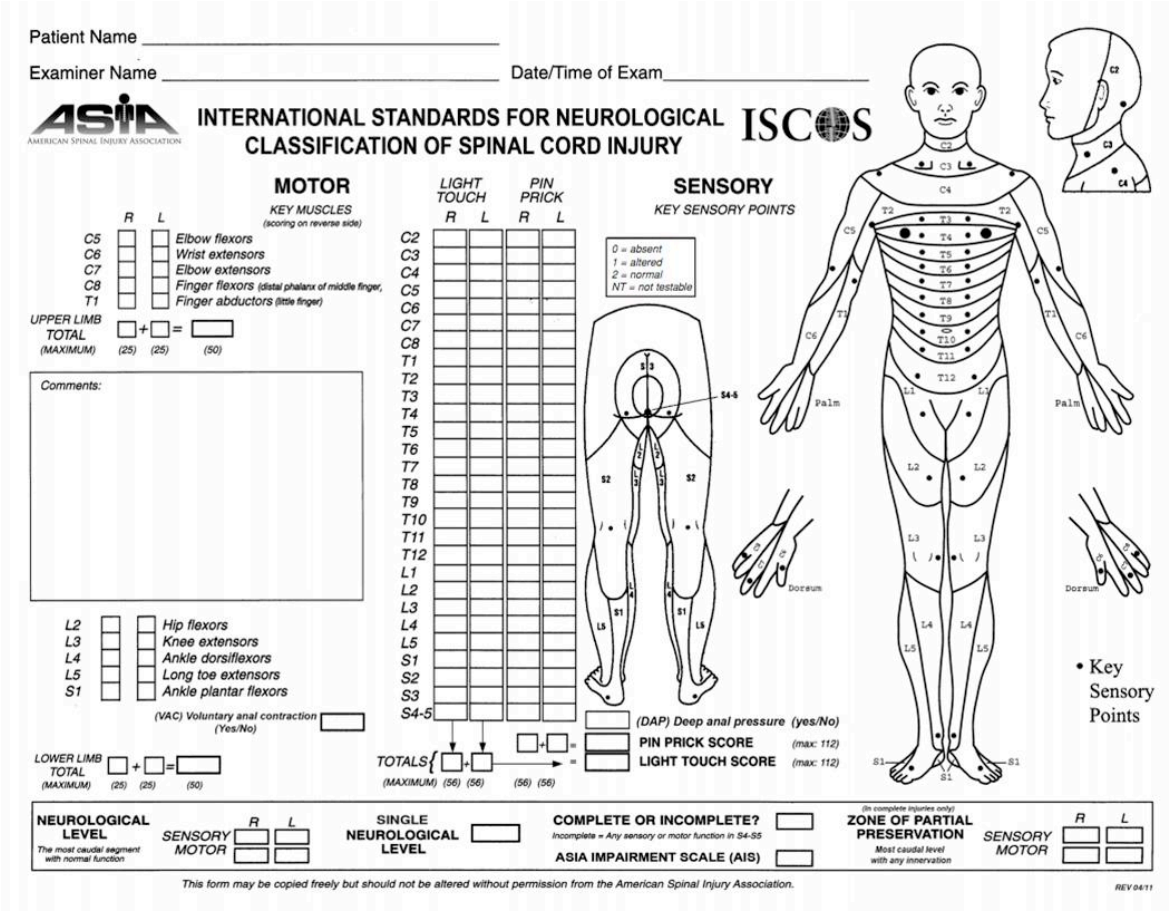

Figure 1.2: American Spinal Injury Association (ASIA) clinical assessment form. Source: http://asiaspinalinjury.org/elearning/ISNCSCI.php (accessed September 2014, available for free download)

The mJOA scale ranges from 3 to 18 points (with 18 representing the maximum score) and identifies upper and lower motor, upper sensory and sphincter function.[18] To better understand this population, studies separate the CSM group into mild, moderate and severe based on the initial mJOA score.[19] Mild CSM is defined as having a mJOA score of >12, moderate CSM patients present with a mJOA score between 9 and 12, and severe CSM cases have a mJOA<9.[19] Patient derived outcome tools commonly used for self-perceived measures of improvement

include the 36-item Short-Form Health Survey (SF-36)[20] and Neck Disability Index (NDI).[21] The SF-36 measures general health and is divided into two components: Physical component summary and Mental component summary. The NDI score has a total of 10 questions that range from 0 to 100 (with 100 representing the maximum score).

1.1.5 Imaging (Diagnostic Evaluations)

Cervical radiographs (plain x-rays) are often used to examine the narrowing of the disc space, presence and size of osteophyte formations, global sagittal alignment and focal translation or kyphosis.[3,22] Computed tomography (CT) is also used to assess bony anatomy and ossification of the posterior longitudinal ligament. However, x-rays and CT scans provide limited information regarding the condition of the spinal cord. Currently, the most useful diagnostic tool remains MRI of the cervical spine, which shows the size and shape of the spinal cord in the sagittal, axial, and coronal planes. Signal changes, such as T_2-hyperintensity or T_1-hypointensity, within the cord can reflect atrophy of the cord or rule out other differential diagnoses.[3] T_2-hyperintensity at the level of the compression has been shown to correlate with symptom severity and represent oedema and inflammation.[23-24] T_1-hypointensity in images has been shown to correlate with worse prognosis and represent ischemia, myelomalacia or gliosis.[23,25] The accuracy of T_2 and/or T_1-weighted signal changes as predictors of recovery of function are highly debated.[23-25]

1.1.6 Conservative Treatment, Surgical Intervention and Predicting Outcome

Conservative treatment is aimed at controlling pain and protecting the spinal cord from additional injury when there is radiographic evidence of spinal canal narrowing but limited signs or symptoms.[2] This may include cervical immobilization with a soft collar, medications, avoidance of certain activities, acupuncture, physical and massage therapy. In a cohort of 45 patients, 82%

and 56% of CSM patients who undertook conservative treatment did not experience neurological deterioration at 5 and 10 years, respectively.[26] Surgical decompression is reserved for patients with moderate or severe CSM exhibited by neurologic deficits during a clinical exam, severity of symptoms, rate of progression, and findings on x-ray and MRI.[2] The goal of surgery is to decompress the spinal cord, preserve the alignment of the vertebra and prevent any further neurologic injury. However, surgical outcomes are unpredictable. Some studies report a 60% improvement while others suggest that the success rate of surgery is more variable with a third improving, 40% showing no change and 25% worsening.[27-28] In addition, the complication rate has an average of 18.7%, with the most common complication being postoperative dysphagia.[29] Several factors have been suggested as predictors of surgical outcome such as: age, duration of symptoms, severity of myelopathy, mJOA score, cross-sectional area of spinal cord and high-signal intensity changes on T_2-weighted MRI.[29-33]

1.1.7 Cortical Changes due to CSM

The pathologic changes occurring in the spinal cord due to CSM have been studied extensively, but remain relatively unexplored in the cortex. In CSM, the spinal cord is compressed and the corticospinal tract is compromised. The pathways mediating the efferent and afferent flow of communication between the brain and spinal cord are disrupted and alterations within neural circuits may occur.

When an injury to the spinal cord is sustained, a process called Wallerian degeneration occurs where axons distal to the site of injury undergo progressive retrograde deterioration.[34] Wallerian degeneration occurs at the local injury site, however, whether there are significant changes that occur upstream in the cortical neurons is debated.[35-37] Some animal studies report the majority of

neurons in the cortex are unaffected following a disrupted corticospinal tract and continue to remain receptive to incoming signals.[36] In contrast, primate studies show apoptosis of corticospinal neurons in the motor cortex, and decreased synaptic spine density.[35,37] Similarly, human studies following SCI demonstrated cortical atrophy in the somatosensory areas which related to the degree of sensory impairment.[38]

Although little is known about the pathological changes in CSM, there is evidence that the maintenance of residual motor function and the recovery process involves reorganization of the cortex and the spared spinal motor neuron pools.[39-40] The adaptive process may occur by the modification of pre-existing connections (synaptic plasticity) or the development of new circuits through sprouting of axons and dendrites.[40] Reorganization of the cerebral cortex due to CSM and SCI will be discussed in further detail in the next sections.

1.1.8 Limitations and the Solution

With arthritis of the spine increasing in both prevalence and severity in our aging population, a precise and accurate tool is required to tailor the treatment of CSM and to ensure appropriate and efficient use of medical resources and technology. CSM is a unique model of reversible SCI providing an opportunity to examine mechanisms involved in injury, recovery, and possibly neuronal plasticity. Even though these factors are currently used to predict the extent of recovery following surgery, the existing evidence lacks the scientific rigor to present consistent and confident conclusions. Results from this heterogeneous group presenting with mild and moderate symptoms are variable using the current evaluation and follow-up criteria. For patients with early, mild symptoms of CSM, the timing of intervention is particularly controversial as select patients can stabilize clinically without operative intervention.

Management of mild CSM patients remains controversial. Kadanka *et al.* compared conservative and surgical treatment in mild-to-moderate CSM patients and showed no significant differences at 10 years with respect to mJOA score, score of daily activities, subjective assessment by patients and ability to walk 10-m track.[41] Oshima *et al*. reported that 82% and 56% of mild CSM patients who undertook conservative treatment did not experience neurological deterioration at 5 and 10 years, respectively.[26] A recent study, however, reported that surgery resulted in improved functional, disability-related, and quality-of-life outcomes at 1 year in symptomatic CSM, even when the disease is mild.[29] These results suggest that early surgical intervention may be preferable in cases of early, mild CSM.

Although MRI remains the best imaging modality to visualize the spinal cord and the impact of spondylotic changes, the accuracy of T_2 and/or T_1-weighted signal changes as a predictor of the recovery of function following surgery are highly debated.[24-25,32] Advanced MRI techniques, however, can be used to study the biochemistry, microstructure, and functional reorganization of the brain using techniques such as magnetic resonance spectroscopy (MRS), diffusion tensor imaging (DTI), and functional MRI (fMRI). Our group has shown cortical changes, distal to the site of injury in the spinal cord.[42] Duggal *et al*. illustrated that reversible spinal cord compression (SCC) leads to an increased activated area within the primary motor cortex in comparison to controls.[42] Surgical decompression resulted in cortical reorganization that was accompanied by a significant return of clinical function.[42] This novel approach examined the problem of CSM from a different perspective and may provide biomarkers *in the brain* to help predict which patients require early intervention.

1.2 Magnetic Resonance Imaging

MRI is an imaging technique that provides anatomic, functional, and physiologic information from the body (Figure 1.3). The images provide detailed information from soft tissues that can be used for diagnosis, treatment planning, and disease monitoring.

Figure 1.3: The 3 Tesla Siemens Magnetom Tim Trio MRI scanner at Robarts Research Institute.

MRI is a safe technique that uses magnetic fields and radio-frequency waves to create images. It is preferred over CT imaging in many instances as it does not use any form of ionizing radiation, and provides more detailed soft-tissue anatomical information. Due to its ability to provide soft-tissue contrast, particularly between grey and white matter, MRI can be used to investigate the central nervous system (CNS) to show areas of injury or demyelination.

1.2.1 The MR Signal

Hydrogen nuclei (protons) found in water and fat in the body are used to produce magnetic resonance images.[43] Hydrogen is the most abundant nucleus in the human body and found in water which makes up 60% of the body weight. The interaction between the hydrogen nuclei and the magnetic fields used to produce magnetic resonance images can be explained using a simple classical physics description. Briefly, the hydrogen protons have a property called spin, which produces a magnetic field. Each hydrogen behaves like a bar magnet where, without any external influences, the magnetic fields would be randomly oriented. However, in the presence of a magnetic field, such as the one produced by the MRI scanner, a component of the magnetic field produced by hydrogen tends to align along the main magnetic field direction of the MRI scanner. In the presence of the external magnetic field produced by the MRI, the hydrogen nuclei are all in a mixed state that can be decomposed on the basis of two eigenvectors: parallel (low energy state) or anti-parallel (high energy state) (Figure 1.4).

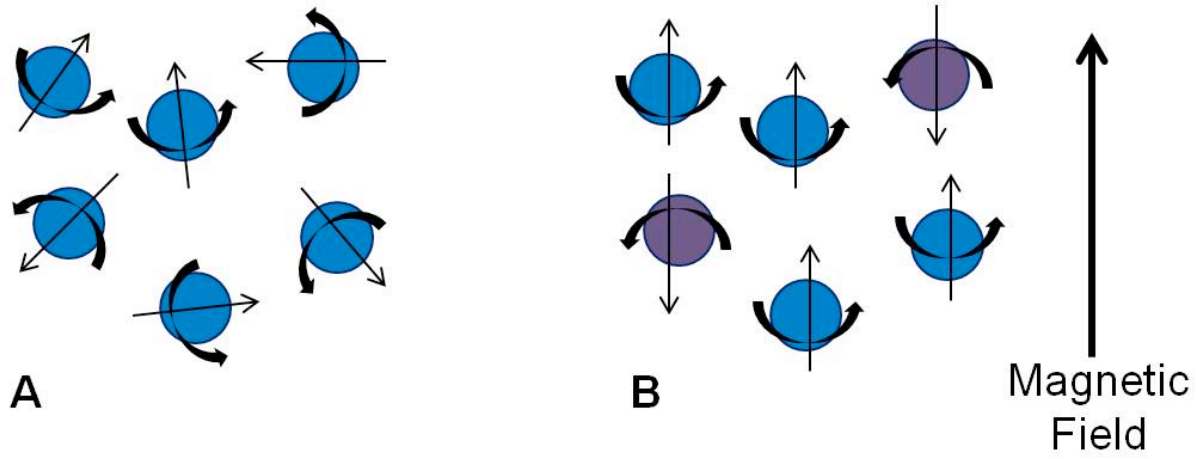

Figure 1.4: A) Protons spin in random orientation along their own axis. B) In the presence of a magnetic field, a component of the magnetic field produced by the hydrogen nuclei align either parallel, or anti-parallel to the external field.

Protons prefer to be in a low energy state. The number of excess protons in the parallel orientation is proportional to the magnetic field where there are 6 per million on a 1.0 Tesla and 9 per million on a 1.5 Tesla MRI. With higher magnetic field strengths, a larger net magnetization occurs, called M_z, which represents the longitudinal component of the magnetization. Higher magnetic fields also cause the nucleus to precess faster described by the Larmor Equation:

$$\omega = \gamma B$$

where ω is the precession or the Larmor frequency in MHz, γ is the gyromagnetic ratio, a fundamental property of each nucleus (the hydrogen nucleus has a gyromagnetic ratio of 267.52×10^6 rad s^{-1} T^{-1}), and B is the external magnetic field strength in Tesla.

1.2.2 Excitation

Excitation occurs when energy from an externally applied oscillating magnetic field is absorbed by the hydrogen nuclei in a low energy state, elevating them into a high energy state. Usually a short burst of energy is used called a pulse. The energy delivered must occur at the resonant frequency, typically in the radio-frequency (RF) range, which is determined by the Larmor equation. When a RF pulse is applied at the resonant frequency, using a classical description of the system, the vector sum of the magnetic moments from the individual hydrogen nuclei (the net magnetization) is rotated from it's equilibrium direction parallel to the static magnetic field of the MRI, to produce components that are perpendicular to the main field (the transverse plane). If all the magnetization is rotated into the transverse plane, then a 90° RF excitation pulse has occurred. In principle, RF excitation pulses can produce any arbitrary rotation (flip angle) of the net magnetization. The RF excitation is applied through transmitter coils. The same coils can be

used to transmit and receive signals. After the RF excitation pulse is turned off, the spin system begins to return to equilibrium.

1.2.3 Relaxation

To restore the system to equilibrium, the protons in the high energy state must return to the low energy state by releasing the same amount of energy that it took for them to become excited. When this occurs, the magnitude of the net magnetization that was perpendicular to the main static magnetic field decreases and the magnetization along the direction of the main static field is restored. Due to the orientation of the coils that are used to detect the MRI signal, only magnetization that is perpendicular to the main magnetic field can be detected. The process whereby the hydrogen nuclei lose energy and return to equilibrium is called relaxation. The time it takes the protons to relax is characterized by two time constants called T_1 and T_2 relaxation.

T_1 relaxation, also known as spin-lattice relaxation, refers to the recovery of the longitudinal magnetization as the electromagnetic energy is released as thermal energy into the surrounding tissue (lattice). T_2 relaxation refers to the dephasing of the spins within the transverse plane. One mechanism that causes T_2 relaxation is spin-spin interactions, which cause some of the spins to precess at different speeds. T_1 and T_2 relaxation are two independent processes occurring simultaneously but at two different rates. In tissue, T_2 decay typically occurs 5-10 times more rapidly than T_1 recovery. T_1 relaxation describes recovery of magnetization along the direction of the main magnetic field (longitudinal magnetization) while T_2 relaxation describes the decay of magnetization in the transverse plane.

T_2* is another time constant used to describe relaxation (or decay) of the signal in the transverse plane. T_2* occurs due to local inhomogeneities of the magnetic field in addition to spin-spin interactions. Therefore, the T_2* time constant is shorter than the T_2 time constant. It is used to produce contrast in tissue in response to changes in local magnetic fields that occur during fMRI, as will be further discussed in the next section.

1.2.4 Contrasts

Different tissues and anatomical structures or pathologies can be identified based on their unique relaxation properties. By adjusting image parameters, such as the repetition time (TR) and the echo time (TE), images can be weighted to highlight one type of relaxation (e.g. T_1-weighted, T_2-weighted, and proton density (PD) weighted (Figure 1.5)). The TR is defined as the time between two successive RF (excitation) pulses. The TE is the time between the excitation RF pulse and the centre of a magnetization echo produced during measurement. Tissue differences in the rate of recovery of the longitudinal magnetization (T_1) can be emphasized by using a short TR and a short TE. Fat appears bright and fluid appears dark on T_1-weighted images. Similarly, tissue differences in the rate of dephasing of the transverse magnetization (T_2) can be emphasized with a long TR and a long TE. Fat appears mid-grey and fluid appears bright on T_2-weighted images. PD-weighted images are acquired with a long TR and short TE and show the relative water concentration in different tissue types.

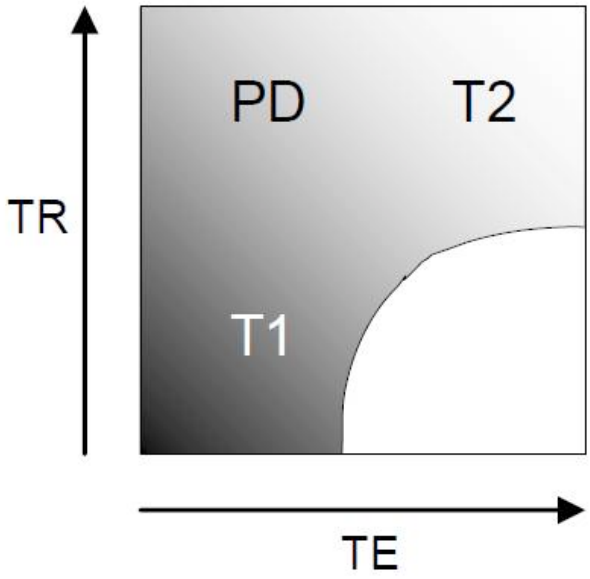

Figure 1.5: The diagram shows the relationship between TR (y-axis) and TE (x-axis). Different image contrasts can be created by adjusting these imaging parameters. Figure adapted from: *Huettel SA, McCarthy G, Song AW. Functional magnetic resonance imaging. 2nd ed. Sunderland, Mass.: Sinauer Associates; 2009.*

1.2.5 MRI in CSM and SCI

MRI is a very useful technique in diagnosing CSM as it provides excellent contrast in soft tissue, and great anatomical detail of the spinal cord structure. MRI can assess the size and shape of the spinal cord in the sagittal and axial plane. It is the preferred method of diagnosing CSM because it can be used to visualize soft tissue structures and determine the severity of the spinal cord compression, cord oedema, and intrinsic cord abnormalities through signal intensity changes.[22,44]

MRI is the preferred method of imaging for directing diagnosis and surgical management because anatomic and spinal cord anatomy can be easily measured and used to identify the presence of CSM. Normal cervical spinal canal diameter (C3-C7) ranges from 17 to 18 mm (with variation in sexes).[45] "Relative stenosis" is diagnosed when the cervical spinal canal diameter measures less than 13 mm and "absolute stenosis" with a diameter of less than 10 mm.[46-47] A congenitally small spinal canal of less than 13 mm is a predisposing factor for CSM.[48] Anatomic features that deform and narrow the spinal canal, such as osteophytes, loss of disc height, disc bulging, ligamentum flavum infolding and ossification of the posterior longitudinal ligament, can also be identified. In addition to anatomic characteristics, MRI is useful at determining cord properties indicative of CSM, specifically hyperintensity on T_2-weighted images or hypointensity on T_1-weighted images. Worse prognosis has been correlated with signal changes on T_2-weighted images, indicative of reversible changes in oedema and ischemia or irreversible changes, and/or T_1-weighted images, suggestive of necrosis, myelomalacia, and cavitation.[23-25]

Although these measurements and signal changes allow for a better identification of CSM, they are inconclusive in predicting surgical outcome. The debate remains: can canal measurements or cord characteristics differentiate the severity of symptoms in patients, and predict who will have a better prognosis following surgical intervention? A recent systematic review reported there are currently no anatomic factors that are associated with outcome.[44] The AOSpine International community confirmed these findings with a preliminary survey of 325 members where 87.66% members agreed MRI is a good prognostic tool and 83.33% members identified cord characteristics as more important than canal measurements.[44,49] Even though the cord properties are more important in diagnosing CSM, the accuracy of T_2 and/or T_1-weighted signal changes as a predictor of function are highly debated.[50-52] Two studies examined the prognostic value of high

signal intensity changes on T_2-weighted images.[50-51] In a prospective study of 70 CSM patients, Chibbaro *et al.* found a significant correlation between a hyperintense signal on T_2-weighted images and postoperative mJOA score.[50] They also found that a hypointense T_1-weighted image correlated with a lower post-operative mJOA score.[50] Setzer *et al.*, on the other hand, reported no predictive value of signal intensity changes on T_2-weighted imaging and the mJOA scores of an "improvement" and a "no-improvement" group following surgery.[51] Similarly, Nakashima *et al.* confirmed no significant associations between high signal intensity on T_2-weighted imaging and the JOA recovery rate or the lower limb function section of the JOA Cervical Myelopathy Evaluation Questionnaire (JOACMEQ-L) in a group of 101 CSM patients.[53] An important factor to keep in mind is that even though the presence of signal changes in T_1 or T_2 weighted images helps in the diagnosis of CSM, there is considerable patient heterogeneity. Patients can be asymptomatic but have signal changes on their MRI indicative of SCC. The discrepancy between the presentation of symptoms and the imaging markers makes it difficult to predict deterioration or success following intervention. New imaging techniques are available that may be more sensitive to spinal cord or cortical changes secondary to CSM. These techniques will be introduced and discussed in detail in the following sections.

1.3 Functional MRI

Functional MRI is a technique used to measure brain activity by detecting changes in the MRI signal as a consequence of changes in local blood flow and oxygenation. The fMRI technique is based on blood oxygen level-dependent (BOLD) contrast that is the result of the coupling between cerebral blood flow and neuronal activation.

1.3.1 Neurovascular Coupling

Neurovascular coupling refers to the relationship between neuronal activity and metabolism with cerebral blood flow. An increase in blood flow, due to increased neuronal activity, is called functional hyperaemia and involves the vascular, astroglial, and neuronal cells of the neurovascular unit. Neurons require adenosine triphosphate (ATP) during various processes. Neuronal ATP can be synthesized by two main mechanisms: glycolosis or oxidative metabolism of glucose. Glycolosis is an anaerobic process that produces a small amount of ATP (2 molecules) while oxidative metabolism is aerobic and produces large amounts of ATP (36 molecules). Cerebral metabolism is aerobic and thus requires a constant supply of glucose and oxygen, maintained by the cerebral blood flow. During neural activity, the consumption of glucose and oxygen triggers an increase in blood flow, which overcompensates for the amount of oxygen being extracted (Figure 1.6). The oversupply of the oxygen delivered provides the basis for the BOLD signal.[53-54]

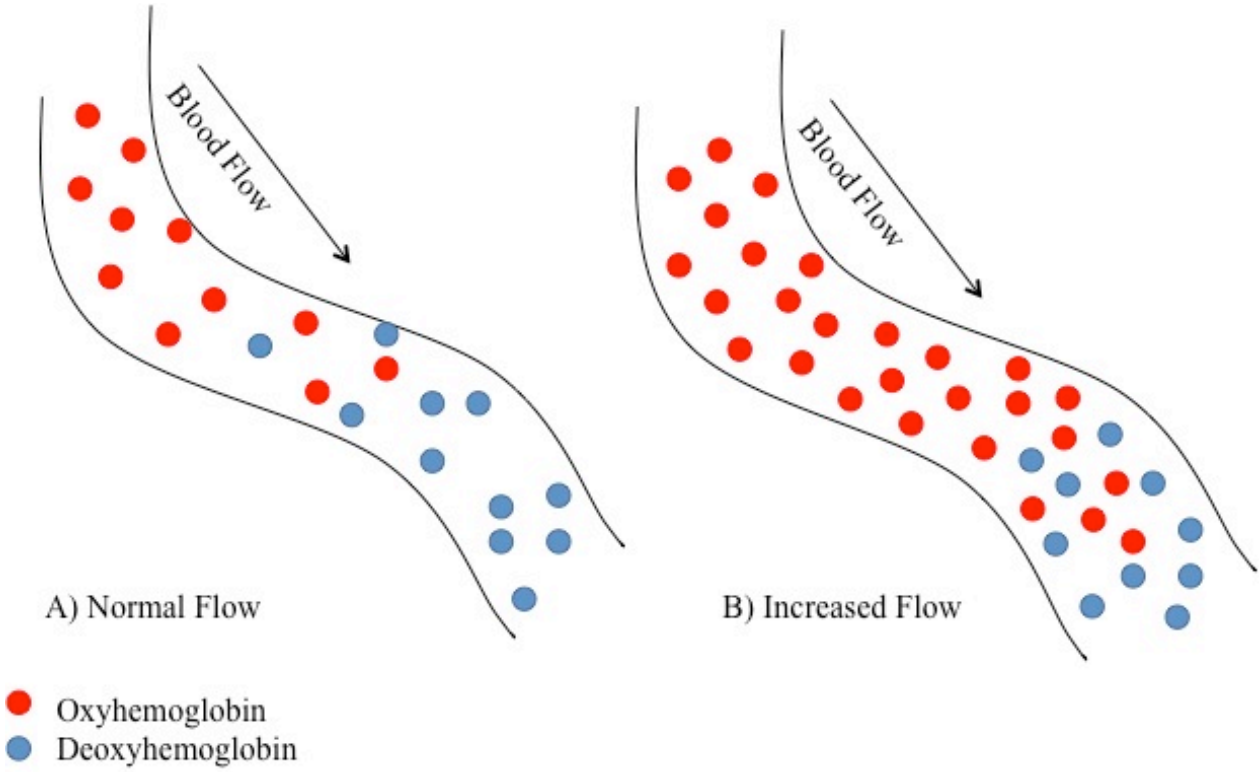

Figure 1.6: A) During normal blood flow, oxygen is extracted from the hemoglobin at a constant rate. B) During neural activity, the consumption of glucose and oxygen triggers an increase in blood flow, which overcompensates for the amount of oxygen being extracted. The oversupply of the oxygen delivered provides the basis for the BOLD signal.

Neural activity and oxygen metabolism are linked with blood flow, but the details of this coupling are still unknown. Several signalling pathways and mechanisms have been implicated. The first is a feedback mechanism by which changes to blood flow are directly mediated by energy demand.[55-57] The response is triggered by various concentrations of ions and metabolic by-products such as potassium (K+), nitric oxide (NO·), adenosine, carbon dioxide, low levels of oxygen, and arachidonic acid.[55-57] These ions and metabolic by-products directly or indirectly alter the blood flow by activating or inhibiting the vascular smooth muscle cells responsible for

vessel diameter.[55-57] The second possibility is a feedforward mechanism where neuronal signalling occurs through neurotransmitters. This requires astrocytes, glial cells that are ideally situated to act as the communication link between the neuronal and vascular systems, to play a large role. Astrocytes participate in glutamate uptake and recycling. Glutamate regulates cerebral blood flow by increasing intracellular calcium concentrations which in turn activate the arteriole smooth muscle cells to dilate or constrict. This mechanism relies on glial pathways as opposed to energy consumption. Lastly, the third mechanism involves the direct neuronal innervation of smooth muscle cells on the blood vessels themselves. It is likely that these three processes work in conjunction to mediate neurovascular coupling.[55-57]

1.3.2 Hemoglobin

Hemoglobin is the iron-containing protein molecule responsible for oxygen transport in red blood cells. In 1936, Linus Pauling and Charles Coryell discovered that hemoglobin has magnetic properties that depend on whether it is bound to oxygen or not.[58] Oxygenated hemoglobin (Hb) (oxygen molecules bound to hemoglobin) is diamagnetic. It has a magnetic moment of 0 and does not differ from other tissues or water when exposed to a magnetic field.[58] Deoxygenated hemoglobin (dHb), on the other hand, has no oxygen attached, which makes it paramagnetic.[58] In the presence of a magnetic field, dHb distorts the magnetic field locally by creating microscopic field gradients within and around the blood vessels, resulting in T_2* based signal loss.[57,59] Consequently, a decreased concentration of dHb leads to a more uniform local magnetic field and a longer period of time during which the precessing protons stay in phase. A tissue region with a decreased concentration of dHb would therefore have a higher MR signal on a T2* weighted image (brighter image pixels) relative to its normal resting state.[57,59] This mechanism by which dHb modulates MRI signal intensity was termed the BOLD effect.

1.3.3 BOLD Contrast

In the late 1980s, Ogawa and colleagues recognized that the different MRI signal intensities produced by the Hb and dHb could be used to measure brain physiology.[60] They manipulated blood oxygen levels in rats by adjusting the amount of oxygen and carbon monoxide the rats breathed.[60] They reported a uniform texture with structural differences but few blood vessels on T_2* contrast images in rats that breathed pure oxygen or carbon monoxide. When the rodents breathed normal air, there were areas of signal loss that corresponded to blood vessels. With increased levels of dHb (oxygen levels decreased to 0%), the blood vessels became more prominent in the T_2*-weighted MR images. The results showed that the presence of dHb decreased the MR signal on T_2* images compared to the presence of Hb. These experiments in the 1980s formed the basis for the BOLD contrast.[57,60-61]

1.3.4 BOLD Hemodynamic Response and Signal Generation

The hemodynamic response (HDR) refers to the MR signal changes on T_2* images triggered by neuronal activity.[57] Under normal conditions, the Hb is converted at a constant rate to dHb. The BOLD effect reflects an intricate relationship between the change in blood flow, blood volume and blood oxygenation. Figure 1.7 is a representation of the BOLD hemodynamic response described below.

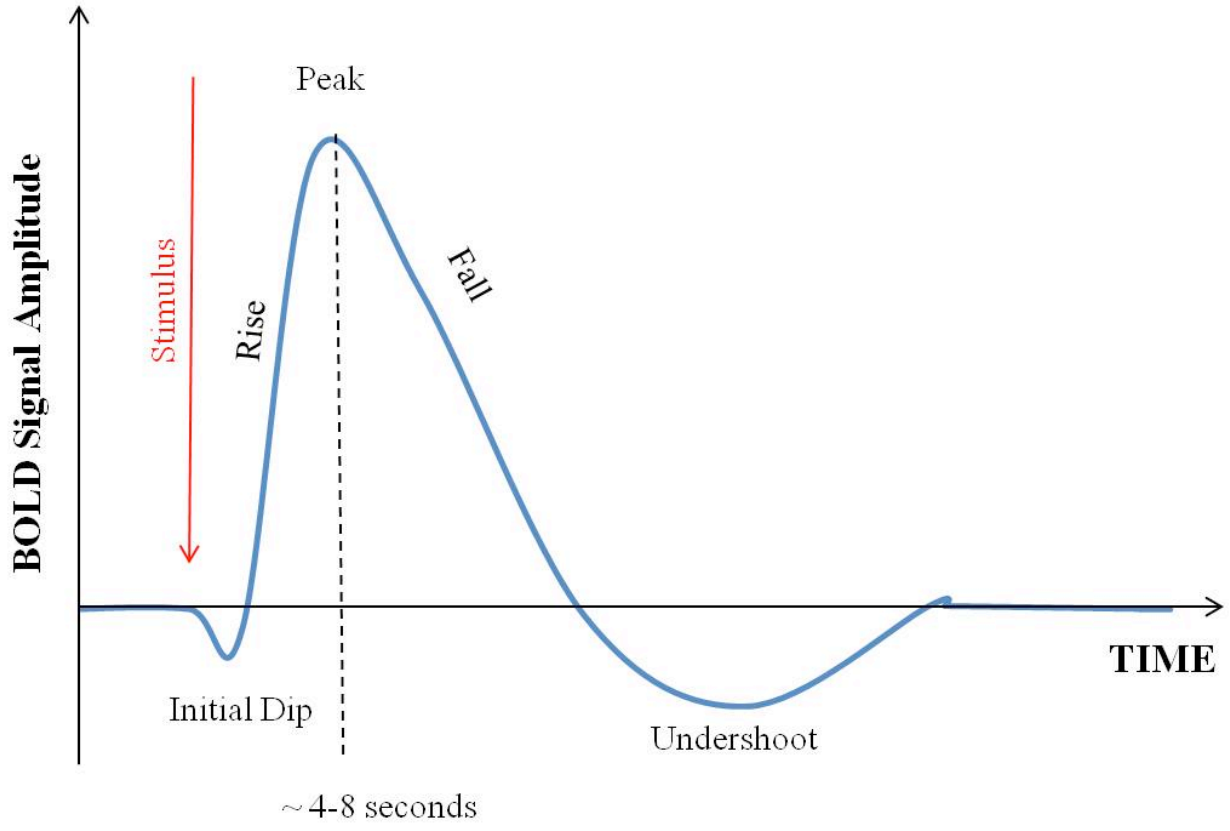

Figure 1.7: BOLD hemodynamic response. *Adapted from: Huettel SA, McCarthy G, Song AW. Functional magnetic resonance imaging. 2nd ed. Sunderland, Mass.: Sinauer Associates; 2009.*

An increase in neural activity requires increased blood flow to the selected brain region to meet oxygen and glucose demands. However, some studies have reported a momentary decrease in MR signal lasting 1-2 seconds immediately following the onset of neural activity, known as the "initial dip.[62]" This decrease was first reported by Menon and colleagues who suggested that the initial dip may reflect initial oxygen extraction localized to the capillaries resulting in a temporary increase in dHb.[62] This is followed by an increase in blood flow (and supply of Hb) and an overcompensatory response to meet the metabolic demands of increased neuronal activity. More oxygen is provided than used and this leads to a decrease in the amount of dHb in the

selected tissue region and consequently, a decrease in the signal loss due to T_2* effects. This corresponds to a BOLD signal increase about 2 seconds following the onset of neural activity to the peak of the HDR which occurs after about 5 seconds for a short-duration stimulus. During longer neuronal activity, the peak may spread into a plateau. Once the activity stops, the BOLD signal decreases below baseline in a phenomenon known as the poststimulus undershoot. The undershoot occurs because the blood flow decreases more rapidly than blood volume.

1.3.5 fMRI in CSM and SCI

In clinical applications, maps of cortical regions such as sensory and motor areas can be acquired based on the performance of simple tasks. Functional MRI can also be used to identify differences in activation between patient populations or to monitor the effects of a treatment/intervention in a single population.

The injured brain has the ability to reorganize itself following neuronal loss or axonal injury.[63] Previous fMRI studies have reported cortical reorganization and remodelling in CSM and SCC patients as a response to preserve neurological function.[42,64-65] Duggal *et al*. illustrated that reversible SCC leads to an increased activated volume within the primary motor cortex (M1) in comparison to controls.[42] Surgical decompression resulted in cortical reorganization that was accompanied by a significant return of clinical function.[42] Dong *et al*. demonstrated altered sensorimotor recruitment patterns during wrist and finger movements in 8 CSM patients that gained motor function following spinal decompression and recruitment maps similar to that of healthy controls.[64] Holly *et al*. reported that CSM patients undergo expanded cortical representation for the affected extremity following surgical decompression.[65] The exact mechanism by which cortical reorganization occurs is not completely understood; but it has been

suggested that it may happen due to modification of pre-existing connections and/or the development of new circuitry intended to preserve neurological functioning.[65] Henderson *et al.* suggested that reorganization may result from growth of new lateral connections, rather than just an unmasking of latent pre-existing connections.[66] The group studied 20 thoracic complete SCI patients and 23 controls while having their hands brushed with a plastic brush.[66] SCI resulted in medial displacement of auricular finger activation of >13 mm toward the lower body representation, the area of the sensory loss.[66] The greater the age of the patient and the longer the time since injury, the greater the medial displacement of the auricular finger activation.[66] Concomitant to the primary sensory cortex (S1) reorganization, there were associated physical changes in the cortical anatomy, suggesting such large movement may be due to growth of new connections.[66]

Freund *et al*. found similar results where movement of the impaired hand in cervical SCI patients showed activation not only in the expected hand area, but in the adjacent leg area.[67] The extent of activation was predicted by spinal cord atrophy where larger activations were found in patients with greater disability.[67] In a subsequent study on the same patients, the group hypothesized about what the shift represented and suggested two possibilities. The first, similar to past studies, that the brain has undergone reorganization where it innervated the neurons in the leg to represent inputs from the hand.[68] The second possibility suggests an uncontrolled "overflow" of activation to the leg area that is prevented in healthy individuals but is not inhibited in SCI because the leg has no movement.[68] Taken together, these results suggest that cortical plasticity influences functional recovery and rehabilitation in response to SCC.

Functional MRI has also been instrumental in discovering different adaptive strategies for functional compensation following SCI depending on the post-operative stage of recovery.[69] Nishimura *et al.* compared activation patterns in 20 macaque monkeys at early (1 month) and late (>3 months) recovery time points following SCI.[69] Based on a precision grip task, there was increased activity in the bilateral M1. During the late recovery stage, this activation was further increased in the contralesional M1 and extended into the bilateral pre-motor cortex.[69] This study suggests the brain uses pre-existing neural systems in the early stage by reducing inhibition and thus allowing larger activation.[69] By the late recovery stage, the brain undergoes plasticity by gradually enhancing the original systems or recruiting new ones for functional compensation.[69] It has also been suggested that an injury to newly developed pathways may be a possible explanation for the progressive deterioration observed in a subset of CSM patients.[63] But previous studies have not separately investigated the patterns of injury and recovery in the motor cortex of the mild and moderate CSM patient populations. Such studies could help optimize patient selection and aid in determining appropriate care, particularly in cases of early stage, mild CSM.

1.4 Diffusion Tensor Imaging

DTI measures the diffusion of water in tissue and can provide *in-vivo* information about tissue microstructure in healthy and neurodegenerative disease.

1.4.1 Diffusion Weighted Imaging

In 1827 a botanist named Robert Brown observed pollen grains in water through a microscope and found that the pollen particles moved through the water.[70] He called it Brownian motion but was unable to explain what caused the movement.[70] In 1905, Albert Einstein explained the theory

behind Brownian motion.[71] Brownian motion is the random motion of particles in a fluid due to the collisions with the molecules in the fluid.[71] Diffusion-weighted imaging (DWI) measures the Brownian motion, also known as diffusion, of water molecules due to thermal agitation. Magnetic field gradients are used to detect water motion. In DWI, two gradient pulses are applied. The first gradient produces a phase offset for each hydrogen nucleus in the sample that is dependent on its position. The second gradient pulse attempts to reverse the phase offset produced by the first gradient. Hydrogen nuclei within stationary water molecules will experience the exact same gradient amplitude both times. The result is that the effect of the two gradient pulses will cancel out and no signal attenuation will occur.[72] However, hydrogen nuclei in the water molecules that move will not be completely refocused after the second gradient pulse is applied. These hydrogen nuclei will have a phase offset that is dependent on how far they moved.[72] Since the MRI signal is equal to the sum of all magnetization components from all hydrogen nuclei, the moving water molecules will produce a lower signal than that produced by stationary molecules.[72] The time between the gradients is called the "diffusion time."[73]

1.4.2 Apparent Diffusion Coefficient

The changes that occur during the diffusion time result in signal attenuation that is proportional to the apparent diffusion coefficient (ADC).[74] ADC is the measure of water diffusion magnitude[74] or the "rate" of water diffusion.[73] It is called "apparent" because it is not possible to measure pure diffusion due to the overlaid capillary diffusion and the subject's gross motion.[73] ADC is also referred to as mean diffusivity (MD) and calculated from the raw diffusion-weighted images. In the body, water molecules diffuse farthest within the diffusion time in tissues with few boundaries. This results in greater signal loss, and a darker region on the diffusion weighted image.[73-74] These areas, such as within the cerebrospinal fluid, will have a higher ADC value and

appear hyperintense or bright on an ADC map because diffusion can occur in any direction without any interruption. Tissues with complex structures and boundaries, such as white matter fibers or tumors, appear bright on a DWI image because the water molecules are hindered in their movement, there is less diffusion, and consequently less signal loss.[73-74] These anisotropic areas have a lower ADC and will appear hypointense or darker on an ADC map.

1.4.3 Diffusion Tensor Imaging

DTI measures the magnitude and direction of water movement. The dephasing and rephasing gradient fields are applied as described above, but in at least 6 directions, so a diffusion tensor can be calculated. From the diffusion tensor, fractional anisotropy (FA) measures can be calculated that provide information about tissue microstructural integrity.[75-76]

1.4.4 Isotropic and Anisotropic Diffusion

Measures of FA range from a value of 0 representing isotropy to 1 representing anisotropy (unidirectional diffusion).[75-76] Isotropic diffusion occurs when water molecules are able to move freely in all directions without any boundaries, such as within cerebrospinal fluid (Figure 1.8A). Anisotropic diffusion describes water does not diffuse equally in all directions for example the movement of water along the long axis of the axon (Figure 1.8B).[73,75-76]

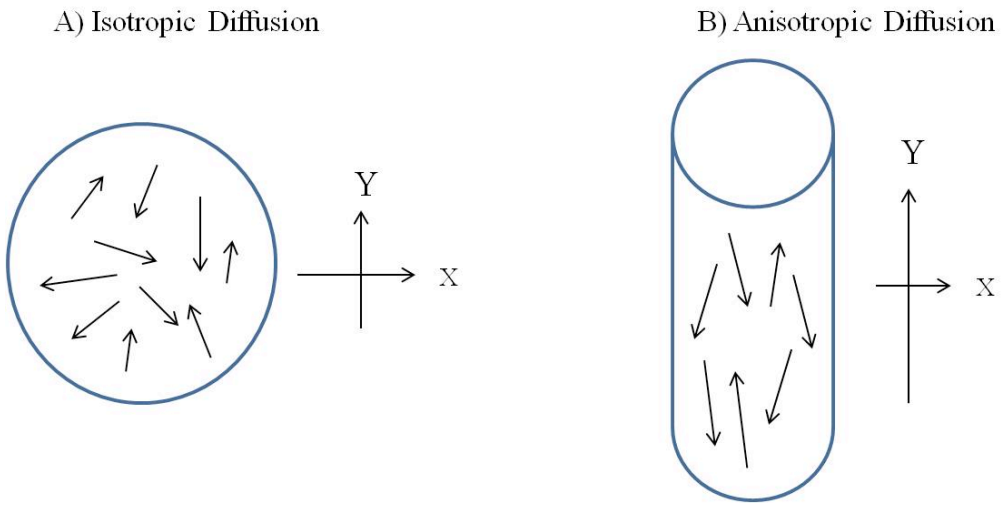

Figure 1.8: A) When motion is unconstrained, as in the large fluid–filled spaces deep in the brain (e.g. ventricles), diffusion is isotropic, which means that motion occurs equally and randomly in all directions. B) When motion is constrained, as in white–matter tracts, diffusion is anisotropic, meaning that motion is oriented more in one direction than another.

Diffusion in healthy white matter, whether in the brain or the spinal cord, is predominantly anisotropic. White matter consists of tightly packed fiber bundles oriented in a long parallel orientation surrounded by axon cellular membranes and myelin sheaths.[77] These membranes and sheaths act as barriers to water diffusion which forces water molecules to predominantly move in the preferred direction: parallel to the white matter fiber rather than perpendicular to it. Injured white matter lacks directional organization of the fibers and possibly decreased fiber tract density due to axon degeneration, myelin demyelination and/or ischemia (Figure 1.9).[74-76]

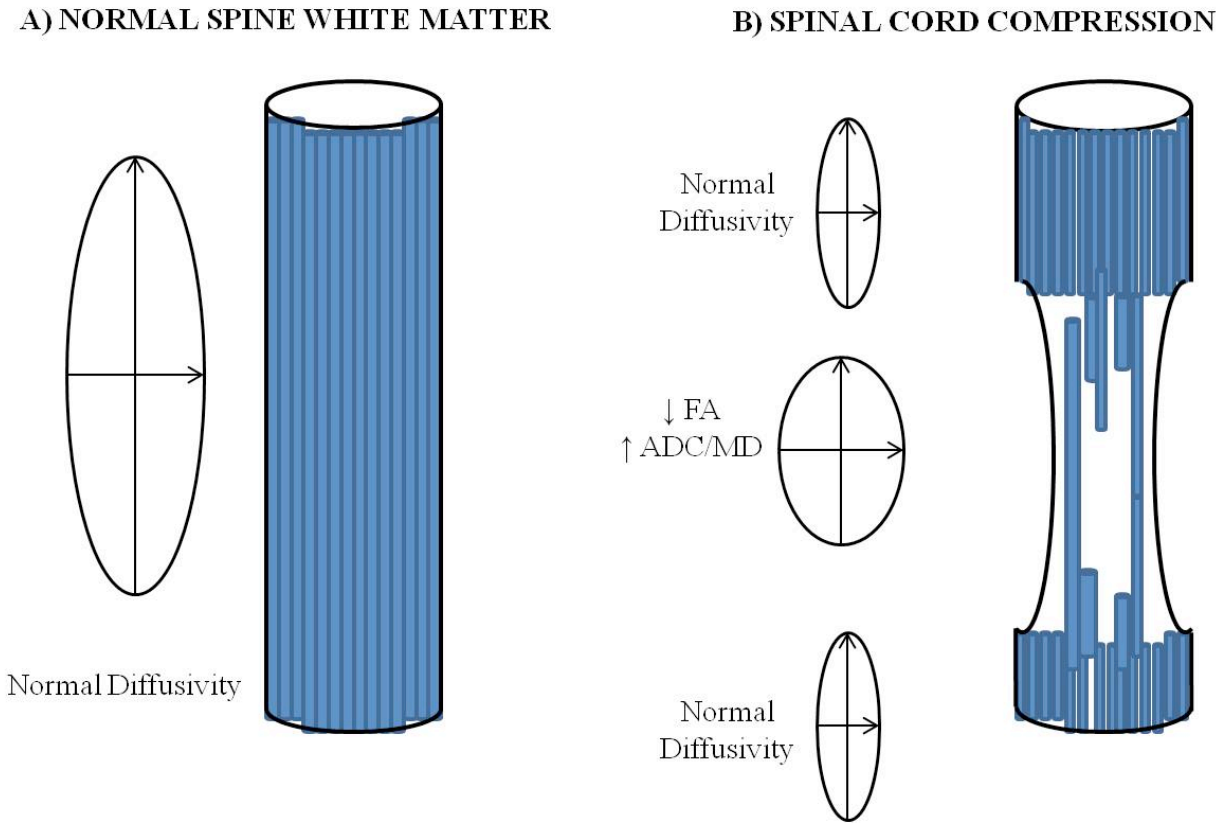

Figure 1.9: A) Healthy spinal white matter where the diffusion occurs along the long axis of the myelinated tract. B) After spinal cord compression, the white matter tracts in the injured area may degenerate and demyelinate, leading to functional impairment. Due to the decreased fiber tract density, the FA decreases and the ADC/MD increases. *Figure adapted from: Ellingson BM, Salamon N, Holly LT. Advances in MR imaging for cervical spondylotic myelopathy. Eur Spine J 2013 [Epub ahead of print]*.

1.4.5 DTI in CSM and SCI

DTI can be used to determine if white matter tracts have been disrupted or injured due to CSM. ADC maps have been shown to be more sensitive than conventional T_2-weighted imaging in detecting CSM in the spinal cord.[78-79] Demir *et al.* reported higher sensitivity rates of 80% in

ADC maps compared to 61% in T_2-weighted imaging in 26 CSM patients.[78] In some cases, studies have shown DTI measures are sensitive enough to detect changes in early stages of CSM where clinical symptoms are minor. Aota *et al.* showed ADC maps were able to detect abnormalities in early stages of CSM with higher sensitivity rates of 65% compared to 42% using T_2-weighted imaging.[79] Kara *et al.* used DTI for early detection of CSM in 16 patients without hyperintensity on T_2-weighted images.[80] They found decreased FA at the stenotic level prior to any signal intensity changes on the conventional T_2-weighted imaging.[80] Mamata *et al.* described a subset of CSM patients where slight ADC and FA abnormalities were found at the site of compression, in spite of few clinical symptoms present.[81]

There are also suggestions in the literature that focal changes in FA at the compression site in CSM patients may be a useful predictor of myelopathy.[82-83] Budzik *et al.* measured the FA and MD in 20 CSM patients at the C2-C3 and compressed level, and 15 controls at the C4-C7 level.[82] The FA was significantly lower at the compressed level in CSM patients and correlated to the patients' clinical scores, suggesting decreased FA may reflect the degree of microstructural disorganization of the spinal cord.[82] Consistent with this hypothesis, Jones *et al.* showed patients with a higher pre-operative FA at the stenotic level experienced more functional recovery when compared to patients with lower FA values.[83] These studies implicate FA as a useful biomarker for predicting successful outcome following surgery and determining the best surgical candidates.

The interconnectivity of the spinal cord with the cerebral cortex is important since CSM can lead to changes in the cortex. More recent SCI studies have acknowledged this intimate relationship and have shown that injury to the spinal cord prompts changes upstream in the cortical anatomy. Wrigley *et al.* used voxel based morphometry and DTI in SCI patients to identify structural

changes in cortical motor regions and descending motor tracts that may limit motor recovery following a SCI.[84] The FA was decreased in the cerebral cortex suggesting axonal degeneration and demyelination may occur due to growth of new (rewiring) or the unmasking of already existing connections.[66,85] Henderson *et al.* found that the greatest region of reorganization in the primary somatosensory cortex in thoracic SCI patients, correlated with FA changes.[66] The reorganization was attributed to changes in cortical anatomy, specifically the growth of new lateral connections, because reorganization from the unmasking of already existing connections would not change cortical anatomy.[66] Similarly, Freund *et al.* found dissociation between the task-related activations during handgrip motions and reduced FA in the M1 leg area of SCI patients and proposed subcortical rewiring as a possible mechanism.[85] Most importantly, these results suggest DTI metrics are able to detect changes upstream from the site of compression and may be used as biomarkers for monitoring disease progression or the effects of interventions targeting the injured spinal cord.

1.5 Magnetic Resonance Spectroscopy

MRS can provide metabolic information from different neural structures. An MR spectrum can be obtained using any nucleus with a magnetic moment such as phosphorus (^{31}P), fluorine (^{19}F), carbon (^{13}C), sodium (^{23}Na) and hydrogen (^{1}H). The most commonly used nucleus is the proton (^{1}H) due to its high sensitivity and abundance in the body. In theory, any molecule that contains ^{1}H may be detected by MRS. In practice, only molecules that are freely mobile (unrestricted) and present in high concentration (> 1 mM) can be observed in the brain. The spectrum produced by a specific molecule depends on its chemical structure which influences the chemical shift and J-coupling of the ^{1}H nuclei within the molecule. The concentration of the metabolite can be related to the signal intensity of its spectrum.

1.5.1 Chemical Shift

The chemical shift of the ^{1}H nuclei within a molecule determines the position of the peak representing the nucleus in the spectrum. As described earlier, when placed in a magnetic field, the hydrogen nucleus precesses at a specific frequency determined by the Larmor equation (Section 1.2.1). In molecules, the electron cloud surrounding the various hydrogen nuclei shield the nucleus and reduce the magnetic field it experiences.[86] The greater the density of the electron cloud, the greater the shielding experienced by the nucleus, and the greater the reduction in the Larmor frequency. The differences in resonance frequency for each hydrogen nucleus give information about its molecular group of origin, whether in different molecules or even for nuclei on the same molecule but in different positions. The shift in frequency is called the chemical shift and is expressed in a dimensionless number: parts per million (ppm). The chemical shift is dependent on the strength of the magnetic field and is measured in Hertz[87-88] Therefore an advantage of using high magnetic field strength is the distance between peaks in a spectrum (chemical shift dispersion) increases and allows for more accurate identification of metabolites.[87-88]

1.5.2 J-Coupling

Most metabolites contain multiple hydrogen nuclei and therefore produce multiple peaks in the spectrum. In some cases, a nucleus produces a single peak in the spectrum, but some peaks may be split into doublets, triplets or multiplets. The internal coupling of nuclei that are separated by three or less chemical bonds is called J-coupling or spin-spin coupling and is responsible for the peak splitting observed in a spectrum.[86,89] The splitting observed in a spectrum can help elucidate the molecular structure of a metabolite.[86,89] In the absence of coupling, each hydrogen nucleus

precesses at a frequency determined by the electronic shielding it experiences (Section 1.5.1). If coupled to a nearby hydrogen nucleus then the energy state of that nearby nucleus can modulate the electron cloud that is shielding the observed nucleus. This interaction occurs through the electron bonds creating a doublet (Figure 1.10).[86]

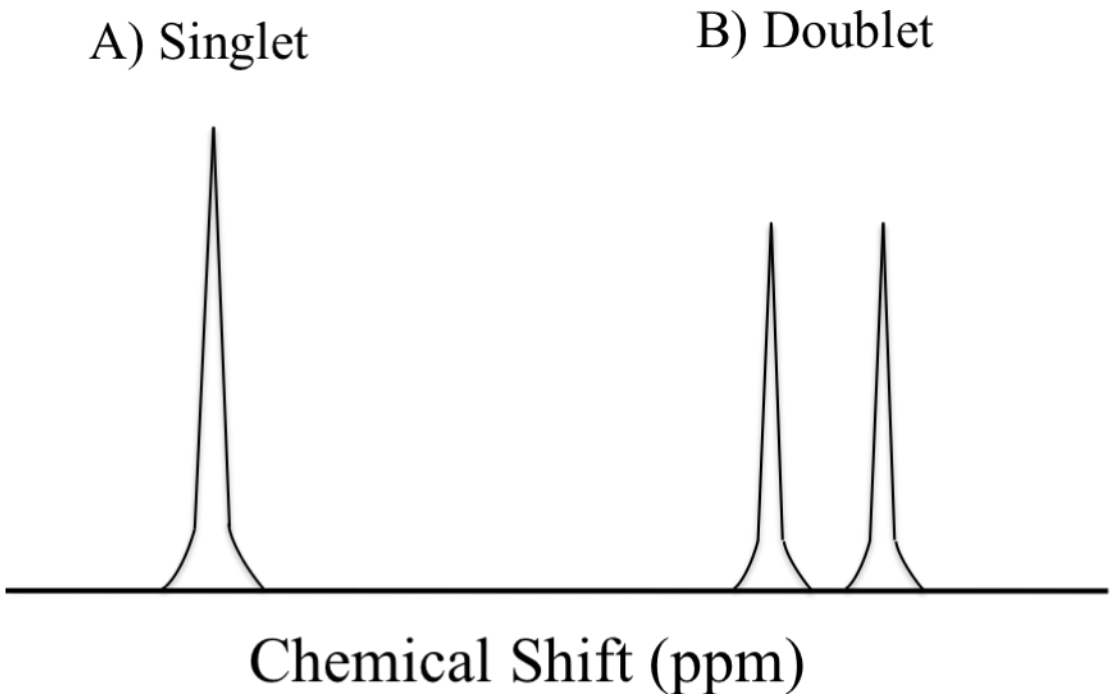

Figure 1.10: J-coupling occurs due to the interaction of different spins through the electron bonds. Uncoupled singlet (A) and coupled spectra with a peak splitting resulting in a doublet are shown (B).

Coupling is measured in Hertz and is independent of the external magnetic field strength. If a hydrogen nucleus is coupled to more than one other nucleus then triplets, quartets, and more complicated multiplets can be formed.

1.5.3 Data Acquisition

In spectroscopy, the signal is obtained from a predefined volume of interest called a voxel. This voxel is localized by exciting three orthogonal slices. The intersection of the orthogonal planes gives the selected volume of interest (VOI). The signal around the voxel can also be crushed to improve spatial selectivity.

Prior to data acquisition, magnetic field uniformity over the VOI is optimized; a process called shimming. Shimming corrects for the spatial inhomogeneity of the magnetic field. It is achieved by adjusting the current that is going through coils that are designed to produce magnetic fields that spatially vary according to specific predefined functions (spherical harmonics). These functions include linear and higher order terms. This step can be performed manually or automatically. Strong second-order shims correct inhomogeneities in small VOIs while first-order shim corrections are very effective across large volumes selected for multi-voxel MRS.

The water concentration is approximately 10,000:1 higher than most metabolites in the brain. The water signal overpowers the signals from metabolites. The water signal needs to be suppressed in order to see the metabolites clearly. A RF pulse designed to excite a narrow frequency band is applied. The band is centred at the water peak frequency (~4.7 ppm) so that other metabolites are not affected. The water magnetization is tipped into the transverse plane. A crusher gradient is then applied to dephase the selected water spins. This method effectively suppresses the water peak and the acquisition of the remaining metabolites begins.

1.5.4 Spectra

Each metabolite produces its own "fingerprint" spectral profile. The combination of these "fingerprints" results in a spectrum of overlapping peaks. A spectrum is a frequency decomposition or a Fourier transform of the acquired time-domain signal.[89] The spectrum of the resulting metabolites is shown on a graph (Figure 1.11). The x-axis corresponds to the metabolite frequency determined by the chemical shift relative to a reference standard (commonly sodium 3-trimethylsilyl-propionic acid (TSP)) at 0 ppm. For example, in-vivo, the water peak (H_2O) is centred at 4.7 ppm and the most prominent metabolite peak from *N*-acetylaspartate (NAA) is centred at 2.02 ppm. The y-axis corresponds to the signal magnitude of the metabolite. The height of each peak and the area under each peak is proportional to the number of protons contributing to the peak (metabolite concentration).[89-90]

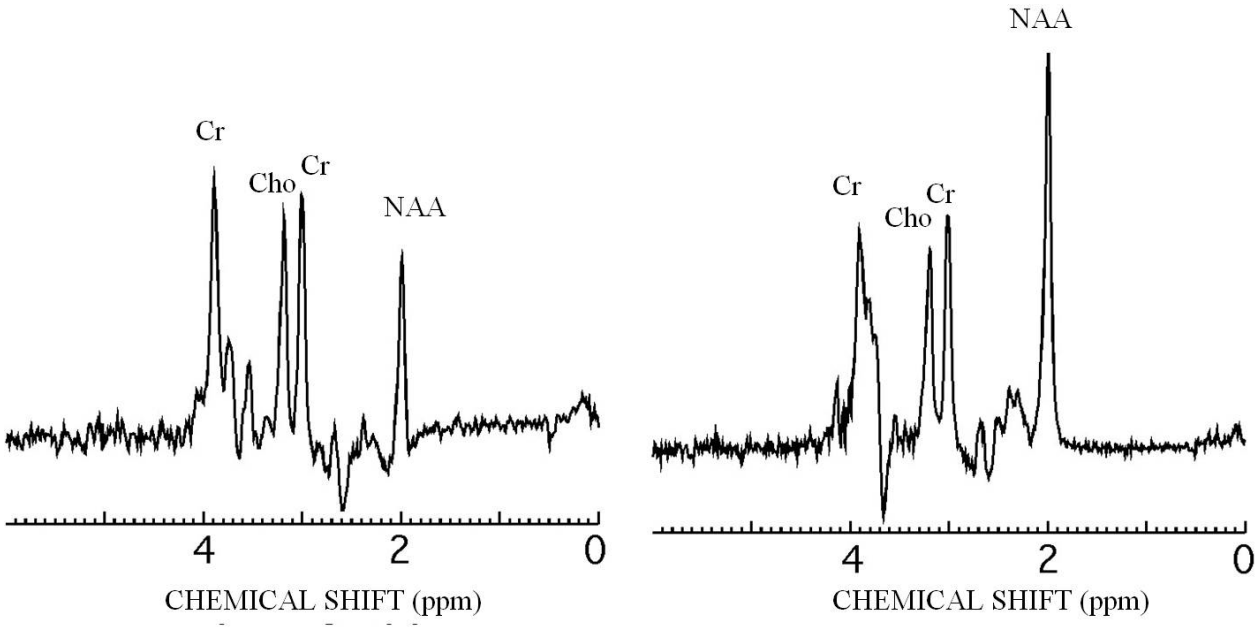

Figure 1.11: The x-axis represents the frequency or chemical shift measured in ppm and the amplitude of the peak is on the y-axis. Each peak represents a metabolite. The area under the peak is calculated to determine the concentration of the metabolite in the voxel. Two examples from a 20 mm isotropic voxel placed over the human primary motor cortex are presented that demonstrate large differences in NAA concentration (PRESS localization at 3 Tesla , TE=135).

1.5.5 High field MRI/MRS

There are several advantages of using a high static magnetic field strength (3.0 T and 7.0 T) for MR spectroscopy. First, signal-to-noise ratio (SNR) increases linearly with field strength.[87-88] An increased SNR allows for reduced acquisition time which is very beneficial in a clinical setting.[86,91] If the examination time is reduced, then several voxels of interest or larger brain volumes can be studied.[86,91] Second, spectral resolution is improved. This is important because it increases the distance between the peaks, making it easier to differentiate and measure the

metabolite concentrations.[86,91] There are also several disadvantages of high field MRS including increased magnetic field inhomogeneity and magnetic susceptibility distortions, particularly near air/bone interfaces, increased power deposition, and increased chemical shift artefacts during the voxel localization process.

1.5.6 Metabolites

1.5.6.1 *N*-Acetylaspartate

N-acetylaspartate (NAA) produces one of the strongest peaks in the in-vivo brain spectrum at 2.02 ppm.[92] The structure is shown in Figure 1.12. NAA has one of the highest concentrations of all free amino acids in the brain (~9.2 mmol/kg in brain tissue).[92] NAA is synthesized in neuronal mitochondria, then transported into neuronal cytoplasm along axons and broken down in oligodendrocytes.[86,89] Within a neuron, 75% of NAA is found in the cytosol, and 25% in the mitochondria.[93] It is found exclusively in neurons of the peripheral and central nervous systems in grey and white matter.

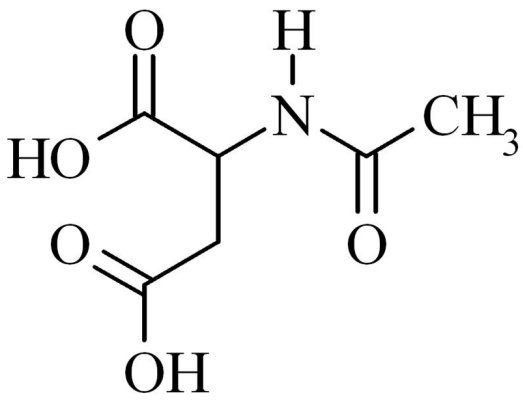

Figure 1.12: NAA Structure

The various functions of NAA are under investigation. It is primarily used as a marker of neuronal and axonal viability due to its location in the neurons.[94-95] NAA is a marker of cellular function because it is synthesized in neuronal mitochondria. It acts as a potential osmolyte because it is involved in fluid balance in the brain as a molecular water pump. It is a source of acetate for lipid and myelin synthesis in oligodendrocytes. Lastly, it is a precursor for the synthesis of the neuronal dipeptide neurotransmitter *N*-Acetylaspartylglutamate (NAAG).

Absent or reduced NAA may imply neuronal death or neurometabolic impairment.[94-95] White matter diseases, tumours, chronic stages of stroke, and multiple sclerosis results in decreased concentrations of NAA.[86] Increased NAA is fairly specific to Canavan disease.[86] Several *in-vivo* studies found that NAA levels can reversibly decline after treatment in neurological disorders such as epilepsy,[96] head trauma,[97] and multiple sclerosis.[98] Caution must be taken when using NAA as a marker of neuronal health because its concentration changes over a person's life. In developing newborns, the NAA is low despite the presence of neurons. The NAA concentration rapidly increases as the brain matures, peaking at about 10-15 years of age followed by a slow decline over time.[99]

1.5.6.2 Creatine

Creatine (Cr) produces two peaks in the in-vivo spectrum at 3.02 and 3.93 ppm. The term Cr in this thesis, represents contributions from free Cr and phosphocreatine (PCr) in roughly equal proportions. Cr and PCr are found in both gray and white matter, and in other brain cell types such as: neurons, astrocytes and oligodendrocytes.[100] Cr has an essential role in energy homeostasis and is a potential marker of the energy potential available in brain tissues.[100] In the

presence of ATP, Cr can be phosphorylated to PCr by the enzyme creatine kinase (CK). This reaction is reversible and Cr can replenish ATP though the CK reaction. Due to this reaction, Cr has been suggested to act as an energy buffer (and ATP reservoir). Some other suggested roles include acting as an energy shuttle. ADP and ATP cannot rapidly diffuse across subcellular regions whereas Cr/PCr can freely diffuse from energy producing (mitochondria) to energy utilizing (myofibril) areas.[101] A ratio of PCr and CR can be measured using phosphorus MRS in addition to proton MRS in order to acquire additional information about the energy metabolism and high-energy phosphate bonds.[100] However, we are unable to distinguish between free Cr and PCr using proton MRS alone. Total Cr (free Cr and PCr) concentration is indicative of brain tissue health and energy homeostasis.

Similarly to NAA, Cr is low in the newborn and then remains increased in adulthood.[99] Its concentration tends to remain stable in the normal brain due to the high metabolic needs of brain tissue cells. Due to its relatively constant concentration, total Cr is often used as an internal reference to normalize the signals from the other metabolites and calculate metabolite ratios. There are several advantages to calculating ratios. First, they provide a reproducible and sensitive measurement and are not prone to errors associated with absolute metabolite level measurements such as those attributed to measurement of tissue partial volume and scaling by tissue relaxation time constants. Tissue partial volume effects that arise from having different amounts of white/grey matter and CSF in selected voxels can be largely avoided with metabolite ratios.[102] Ratios can also be more sensitive in detecting metabolite changes when one metabolite in the ratio (e.g. the numerator) increases while another metabolite in the ratio (e.g. the denominator) decreases.

The main disadvantage of ratios normalized to Cr is that the Cr signal may alter due to pathological changes. Cr concentrations are decreased in brain tumors.[103] Cr increases have been described in gliosis and in MS, due to glial and astrocyte proliferation, respectively.[101,104] Systemic disease may also affect Cr levels in the brain because Cr and PCr are metabolized to creatinine which is then excreted by the kidneys.[103] If CSM patients with renal disease were included in the recruitment for this thesis, then the ratio of a metabolite relative to Cr would be altered. For example, a decreased NAA/Cr would normally be attributed to decreases in NAA and a stable Cr concentration. In CSM patients with renal disease, a decrease in NAA/Cr could represent a decrease in NAA at a faster rate than the decreases in Cr. For this reason, patients were excluded if they had any other disease or neurological disorders that could affect Cr, or any of the other metabolite concentrations.

1.5.6.3 Choline

Choline (Cho) has a peak at 3.22 ppm due to nine equivalent protons in three methyl groups. It also contains protons that resonate at 3.54 and 4.05 ppm as doublets. However, these have a lower intensity and overlap with other resonances making them difficult to detect *in-vivo*. Cho is comprised of: phosphorylated cholines, phosphocholine (PCho), and glycerophosphorylcholine (GPCho).[89] Cho-containing compounds are found in higher concentrations in myelin and cell membranes compared to PCho and GPCho.[105] However, Cho-containing compounds are not freely movable, are not measurable and do not contribute to the Cho resonance signal at 3.22 ppm.[100] Therefore the main Cho signal is made up of PCho and GPCho. PCho is a precursor for membrane synthesis.[100] Mainly GPCho and a smaller concentration of PCho are generated during

membrane degradation.[100] Measures of total Cho are interpreted as a marker of cellular membrane turnover.[89,100,105] Cho is also found to be a precursor to the neurotransmitter acetylcholine.

Elevated Cho can occur due to the accumulation of myelin breakdown products, as found in demyelination.[100] Cho has also been shown to correlate with the degree of malignancy in tumours.[86] Increases in Cho may be difficult to interpret because they cannot distinguish between the increases observed following infarction (gliosis or ischemic damage to myelin) and inflammation (glial proliferation).[86]

1.5.6.4 Myo-inositol

Myo-inositol (Myo) is a simple sugar and produces a doublet signal centered at 3.56 ppm. Myo is often considered a glial marker because it is synthesized in glial cells, specifically astrocytes.[106] Astrocytes provide neurons with energy, substrates for neurotransmission and are required for neuronal repair following injury.[107-109] Myo also functions as an osmolyte in astrocytes, which means it can efflux from (or enter into) brain cells to preserve the cell volume in response to hypotonic (or hypertonic) stress.[110-111] Myo is also reported to act as an intermediate in membrane and myelin phospholipids metabolism and may represent a product of myelin degradation.[86,100]

Elevated concentrations of Myo can be found elevated in cortical regions of gliosis, astrocytosis, and diseases such as Alzheimer's disease.[103] Increased Myo suggests proliferation of glial cells or inflammation.[103] Gliosis may be associated with neuronal atrophy and/or inflammation of neural tissue, thus increases in Myo are often accompanied by decreases in NAA.

1.5.6.5 Glutamine and Glutamate (Glx)

Glutamate (Glu) is the main excitatory neurotransmitter in the brain.[89] Glu is a structural component in proteins and also involved in energy metabolism.[86,89] It is a precursor for glutamine (Gln), gamma-aminobutyric acid (GABA) and glutathione.[112] Glu and Gln have overlapping peaks centered at 2.05 and 2.50 ppm. The discrimination between the two metabolites is reliable at 7T MRI but much more difficult at 3T MRI. Therefore, Glu and Gln are often presented as a complex called Glx. The Glx resonance signal reflects the total MRS-visible pool of Glu and Gln, and minor contributions from GABA, glutathione and other metabolites, available for synaptic and metabolic activity.[100]

Glu and Gln are found intracellularly (in neurons and glial cells) and extracellularly. Once Glu is released from neurons into the synaptic cleft, it is taken up by astrocytes.[112] Uptake by astrocytes prevents excitotoxic damage by maintaining low levels of extracellular Glu.[113] Neuronal uptake of released Glu is low, but may help sustain the neuronal Glu pool.[113] Once Glu is in astrocytes, it is degraded or converted to Gln. Gln is the major precursor for neuronal Glu and GABA. Gln is then released from astrocytes and is taken up by neurons and converted back to Glu. This process is called the Glu-Gln cycle.[112] The rate of the Glu-Gln cycle is moderated by neuronal and metabolic activity of the stimulated extrasynaptic Glu receptors.[112-113] The ratio of Glu in the metabolic versus the neurotransmitter pool is a subject of debate. Therefore the Glu concentrations measured by MRS, cannot be attributed directly to one specific function. It has been suggested, however, that the Glx measured by MRS is most likely related to glutamatergic

neurotransmission because Glu cannot pass through the blood-brain barrier (except in a few small areas that have fenestrated capillaries) and must therefore be synthesized in the central nervous system.[114] Furthermore, Glu and Gln are the building blocks of proteins, but once they are bound, they are not visible by MRS. Elevated levels of Gln and Glx have been found in hepatic encephalopathy and traumatic brain injury.[86,89]

1.5.7 MRS in CSM

MR spectroscopy can be applied to study many disorders as metabolite concentrations can be altered in the presence of structural damage (degenerative disorders, gliomas, etc), altered physiological conditions (ischemia, etc.) and biochemical or genetic problems.[89] MRS has been underutilized in the CSM population. One study detected lactate in one-third of their 21 patients with CSM and found a significantly lower NAA/Cr ratio at the C2 level of the spinal cord in the patient group compared to the control group suggesting axonal or neuronal loss in the spinal cord.[115] Salamon *et al.* also measured metabolite changes at the C2 level of 21 cervical spondylosis patients separated into two groups, those with and without T_2 signal changes, compared to 11 healthy controls.[116] An elevated Cho/NAA ratio was observed only in the spondylosis patients without T_2 signal changes while increased Cho/Cr was reported in spondylosis patients with and without T_2 signal changes.[116] These results suggest progression of cellular and microstructural changes in the spinal cord as patients progress from asymptomatic to severe neurological impairment.[116]

Only a few studies have focussed on cortical metabolite changes distal to the site of injury. Yabuki *et al*. demonstrated altered metabolite levels in the thalamus of lumbar spine disease.[117]

These patients presented with decreased NAA/Cr and NAA/Cho ratios on the side of the thalamus contralateral to the symptoms.[117] Similarly, Sharma and colleagues reported decreased NAA levels in the primary somatosensory cortex in patients with chronic low back pain suggesting altered neuronal-glial interactions that also correlate with the clinical characteristics of pain.[118]

1.6 Goal and Hypothesis

CSM is a devastating disorder where the spinal cord is compressed and the corticospinal tract is compromised. The pathways mediating the efferent and afferent flow of communication between the brain and spinal cord are disrupted and alterations within the neural circuits may occur. The pathologic changes occurring in the spinal cord due to CSM have been studied extensively, but remain relatively unexplored in the cortex. Remote injury of the sensorimotor cortex in patients with CSM could be a critical factor in recovery.

The overall goal of this research is to develop biomarkers to predict the outcome of spinal decompression surgery that would allow surgeons to optimize treatment plans, especially in early stage mild CSM. The goal of this thesis was to characterize the functional, metabolic, and structural changes in the primary motor cortex occurring in the CSM patient population using advanced MRI methods. We hypothesized that CSM patients who experienced the greatest clinical recovery will also demonstrate the greatest ability for cortical adaptation following surgery. The specific aims of this thesis are:

1) To compare metabolite concentrations, specifically *N*-Acetylaspartate, brain function, and white matter integrity in the motor cortex region of CSM patients with healthy controls;

2) To determine whether these measures change to normal healthy levels in the primary motor cortex following decompressive surgery;

3) To assess the role of pre-operative imaging biomarkers as potential predictors of surgical outcome by correlating them with neurological improvement; and

4) To characterize imaging differences between the mild and moderate CSM populations prior to and following decompressive surgery.

To answer these questions, a single cohort of 28 CSM patients and 11 healthy controls was recruited. Each chapter within this thesis presents results obtained from the same patient population using advanced MRI techniques. Each subject participated in two scanning sessions; one at baseline and a second session 6 months later. Each MRI session included the acquisition of anatomical images, MRS, DTI and fMRI data. CSM patients all underwent spinal decompression surgery after the baseline imaging scan.

1.7 References

1. Bernhardt M, Hynes RA, Blume HW, White AA 3rd. Cervical spondylotic myelopathy. *J Bone Joint Surg* 75(1):119-128, 1993.

2. Toledano M, Bartleson JD .Cervical Spondylotic Myelopathy. *Neurol Clin* 31(1):297-305, 2013.

3. Murray MT, Tay BBKB. Natural History of Cervical Myelopathy. *Seminars in Spine Surgery*. 222-227, 2004.

4. Northover JR, Wild JB, Braybrooke J, Blanco J. The epidemiology of cervical spondylotic myelopathy. *Skeletal Radiol* 41(12):1543-1546, 2012.

5. Kalsi-Ryan S, Karadimas SK, Fehlings MG. Cervical spondylotic myelopathy: The clinical phenomenon and the current pathobiology of an increasingly prevalent and devastating disorder. *Neuroscientist* 19(4):409-421, 2013.

6. Tracy JA, Bartleson JD. Cervical Spondylotic Myelopathy. *Neurologist* 16(3),176-187, 2010.

7. Young WF. Cervical spondylotic myelopathy: a common cause of spinal cord dysfunction in older adults. *Am Fam Physician* 62(5):1064-1070, 2000.

8. Fehlings MG, Skaf G. A review of the pathophysiology of cervical spondylotic myelopathy with insights for potential novel mechanisms drawn from traumatic spinal cord injury. *Spine* 23(4):2730-2734, 1998.

9. Mattei TA, Goulart CR, Milano JB, Dutra LP, Fasset DR. Cervical spondylotic myelopathy: Pathophysiology, diagnosis, and surgical techniques. *ISRN Neurol* 2011:463729, 2011.

10. Baptiste DC, Fehlings MG. Pathophysiology of cervical myelopathy. *Spine J* 6(6 Suppl):190S-197S, 2006.

11. Kim DH, Vaccaro AR, Henderson FC, Benzel EC. Molecular biology of cervical myelopathy and spinal cord injury: role of oligodendrocyte apoptosis. *Spine J* 3(6):510-519, 2003.

12. Tetreault LA, Karpova A, Fehlings MG. Predictors of outcome in patients with degenerative cervical spondylotic myelopathy undergoing surgical treatment: results of a systematic review. *Eur Spine J* 2013 [epub ahead of print].

13. Clarke E, Robinson PK. Cervical myelopathy: a complication of cervical spondylosis. *Brain* 79(3):483-510, 1956.

14. Epstein JA, Carras R, Epstein BS, Levine LS. Myelopathy in cervical spondylosis with vertebral subluxation and hypolordosis. *J Neurosurg* 32(4):421-426, 1970.

15. Matz PG, Anderson PA, Holly LT *et al*. The natural history of cervical spondylotic myelopathy. *J Neurosurg Spine* 11(2):104-111, 2009.

16. Yarbrough CK, Murphy RK, Ray WZ, Stewart TJ. The natural history and clinical presentation of cervical spondylotic myelopathy. *Adv Orthop* 2012:480643, 2012.

17. Journal of the Japanese Association. Criteria on the evaluation of the treatment of cervical myelopathy. *J Jpn Orthop Assoc* 50:5, 1976.

18. Benzel EC, Lancon J, Kesterson L, Hadden T. Cervical laminectomy and dentate ligament section for cervical spondylotic myelopathy. *J Spinal Disord* 4(3):286-295, 1991.

19. Revanappa KK, Rajshekhar V. Comparison of Nurick grading system and modified Japanese Orthopaedic Association scoring system in evaluation of patients with cervical spondylotic myelopathy. *Eur Spine J* 20(9):1545-1551, 2011.

20. Ware JE, Sherbourne CD. The MOS 36-item Short-Form Health Survey (SF-36) 1.Conceptual framework and item selection. *Med Care* 30(6):473-483, 1992.

21. Vernon H, Mior S. The Neck Disability Index: A study of reliability and validity. *J Manipulative Physiol Ther* 14(7):409-415, 1991.

22. Lebl DR, Hughes A, Cammisa FP Jr., O'Leary PF. Cervical spondylotic myelopathy: Pathophysiology, clinical presentation, and treatment. *HSS J* 7(2):170-178, 2011.

23. Morio Y, Teshima R, Nagashima H, Nawata K, Yamasaki D, Nanjo Y. Correlation between operative outcomes of cervical compression myelopathy and MRI of the spinal cord. *Spine* 26(11):1238-1245, 2001.

24. McCormick WE, Steinmetz MP, Benzel EC. Cervical spondylotic myelopathy: make the difficult diagnosis, then refer for surgery. *Cleve Clin J Med* 70(10):899-904, 2003.

25. Okada Y, Ikata T, Yamada H. Magnetic resonance imaging study on the results of surgery for cervical compression myelopathy. *Spine* 18(14):2024-2029, 1993.

26. Oshima Y, Seichi A, Takeshita K, *et al*. Natural course and prognostic factors in patients with mild cervical spondylotic myelopathy with increased signal intensity on T2-weighted magnetic resonance imaging. *Spine* 37(22):1909-1913, 2012.

27. Fager CA. Posterior surgical tactics for the neurological syndromes of cervical disc and spondylotic lesions. *Clin Neurosurg* 25:218-244, 1978.

28. Bishara SN. The posterior operation-treatment of cervical spondylosis with myelopathy: long-term follow-up study. *J Neurol Neurosurg Psychiatry* 34(4):393-395, 1971.

29. Fehlings MG, Wilson JR, Kopjar B, *et al*. Efficacy and safety of surgical decompression in patients with cervical spondylotic myelopathy: Results of the AOSpine North America Prospective Multi-Center Study. *J Bone Joint Surg Am* 95(18):1651-1658, 2013.

30. Bucciero A, Vizioli L, Tedeschi G. Cord diameters and their significance in prognostication and decisions about management of cervical spondylotic myelopathy. *J Neurosurg Sci* 37(4):223-228, 1993.

31. Fukushima T, Ikata T, Taoka Y, Takata S. Magnetic resonance imaging study on spinal cord plasticity in patients with cervical compression myelopathy. *Spine* 16(10Suppl):S534-S538, 1991.

32. Morio Y, Yamamoto K, Kuranobu K, Murata M, Tuda K. Does increased signal intensity of the spinal cord on MR images due to cervical myelopathy predict prognosis? *Arch Orthop Trauma Surg* 113(5):254-259, 1994.

33. Takahashi M, Yamashita Y, Sakamoto Y, Kojima R. Chronic cervical cord compression: Clinical significance of increased signal intensity on MR images. *Radiology* 173(1):219-224, 1989.

34. Waller A. Experiments on the section of glossopharyngeal and hypoglossal nerves of the frog and observations of the alternatives produced thereby in the structure of their primitive fibers. *Phil Trans R Soc Lond* 140:423, 1850.

35. Hains BC, Black JA, Waxman SG. Primary cortical motor neurons undergo apoptosis after axotomizing spinal cord injury. *J Comp Neurol* 462(3):328-341, 2003.

36. Wannier T, Schmidlin E, Bloch J, Rouiller EM. A unilateral section of the corticospinal tract at cervical level in primate does not lead to measureable cell loss in motor cortex. *J Neurotrauma* 22(6):703-717, 2005.

37. Kim BG, Dai HN, McAtee M, Vicini S, Bregman BS. Remodeling of synaptic structures in the motor cortex following spinal cord injury. *Exp Neurol* 198(2):401-415, 2006.

38. Jurkiewicz MT, Crawley AP, Verrier MC, Fehlings MG, Mikulis DJ. Somatosensory cortical atrophy after spinal cord injury: A voxel-based morphometry study. *Neurology* 66(5):762-764, 2006.

39. Dobkin BH. Spinal and supraspinal plasticity after incomplete spinal cord injury: correlations between functional magnetic resonance imaging and engaged locomotor networks. *Prog Brain Res* 128:99-111, 2000.

40. Raineteau O, Schwab ME. Plasticity of motor systems after incomplete spinal cord injury. *Nat Rev Neurosci* 2(4):263-273, 2001.

41. Kadanka Z, Bednarik J, Novotny O, Urbanek I, Dusek L. Cervical spondylotic myelopathy: conservative versus surgical treatment after 10 years. *Eur Spine J* 20(9):1533-1538, 2011.

42. Duggal N, Rabin D, Bartha R, *et al*. Brain reorganization in patients with spinal cord compression evaluated using fMRI. *Neurology* 74(13):1048-1054, 2010.

43. Berger A. How does it work? MRI. *BMJ* 324:35, 2002.

44. Tetreault LA, Dettori JR, Wilson JR, *et al*. Systematic review of magnetic resonance imaging characteristics that affect treatment decision making and predict clinical outcome in patients with cervical spondylotic myelopathy. *Spine* 38(22 Suppl 1):S89-110, 2013.

45. Matsunaga S, Sakou T, Taketomi E, Yamaguchi M, Okano T. The natural course of myelopathy caused by ossification of the posterior longitudinal ligament in the cervical spine. *Clin Orthop* 305:168-177, 1994.

46. Arnold JG Jr. The clinical manifestations of spondylochondrosis (spondylosis) of the cervical spine. *Ann Surg* 141(6):872-889, 1955.

47. Wolf BS, Khilnani M, Malis L. The sagittal diameter of the bony cervical spinal canal and its significance in cervical spondylosis. *J Mt Sinai Hosp N Y* 23(3):283-292, 1956.

48. Morishita Y, Naito M, Hymanson H, Miyazaki M, Wu G, Wang JC. The relationship between the cervical spinal canal diameter and the pathological changes in the cervical spine. *Eur Spine J* 18(6):877-883, 2009.

49. Tetreault LA, Nouri A, Singh A, Fawcett M, Fehlings MG. Predictor of outcome in patients with cervical spondylotic myelopathy undergoing surgical treatment: a survey of members from AOSpine International. *World Neurosurg* 81(3-4):623-633, 2014.

50. Chibbaro S, Benvenuti L, Carnesecchi S, *et al*. Anterior cervical corpectomy for cervical spondylotic myelopathy: Experience and surgical results in a series of 70 consecutive patients. *J Clin Neurosci* 13(2):233-238, 2006.

51. Setzer M, Vrionis FD, Hermann EJ, Seifert V, Marquardt G. Effect of apolipoprotein E genotype on the outcome after anterior cervical decompression and fusion in patients with cervical spondylotic myelopathy. *J Neurosurg Spine* 11(6):659-666, 2009.

52. Nakashima H, Yukawa Y, Ito K, *et al*. Prediction of lower limb functional recovery after laminoplasty for cervical myelopathy: focusing on the 10-s step test. *Eur Spine J* 21(7):1389-1395, 2012.

53. Fox PT, Raichle ME. Focal physiological uncoupling of cerebral blood flow and oxidative metabolism during somatosensory stimulation in human subjects. *Proc Natl Acad Sci USA* 83(4):1140-1144, 1986.

54. Fox PT, Raichle ME, Mintun MA, Dence C. Nonoxidative glucose consumption during focal physiologic neural activity. Science 241:462-464, 1988.

55. Heeger DJ, Ress D. What does fMRI tell us about neuronal activity? *Nat Rev Neurosci* 3(2):142-151, 2002.

56. Attwell D, Buchan M, Charpak S, Lauritzen M, Macvicar BA, Newman EA. Glial and neuronal control of brain blood flow. *Nature* 468(7321):232-243, 2010.

57. Huettel, Scott A, Allen W Song, and Gregory McCarthy. *Functional Magnetic Resonance Imaging*. Sunderland, MA: Sinauer Associates, 2004. Print.

58. Pauling L, Coryell CD. The magnetic properties and structure of hemoglobin , oxygenated hemoglobin, and carbonmonoxygenated hemoglobin. *Proc Natl Acad Sci USA* 22(4):210-236, 1986.

59. Buckner RL. Event-related fMRI and the hemodynamic response. *Hum Brain Mapp* 6(5-6):373-377, 1998.

60. Ogawa S, Lee TM, Kay AR, Tank DW. Brain magnetic resonance imaging with contrast dependent on blood oxygenation. *Proc Natl Acad Sci USA* 87(24):9868-9872, 1990.

61. Thulborn KR, Warterton CJ, Matthews PM, Radda GK. Oxygenation dependence of the transverse relaxation time of water protons in while blood at high field. *Biochim Biophys Acta* 714:216-270, 1982.

62. Menon RS, Ogawa S, Hu X, Strupp JP, Anderson P, Ugurbil K. BOLD based functional MRI at 4 Tesla includes a capillary bed contribution: echo-planar imaging correlates with previous optical imaging using intrinsic signals. *Magn Reson Med* 33(3):453-459, 1995.

63. Holly LT. Management of cervical spondylotic myelopathy with insights from metabolic imaging of the spinal cord and brain. *Curr Opin Neurol* 22(6):575-581, 2009.

64. Dong Y, Holly LT, Albistegui-DuBois R, *et al*. Compensatory cerebral adaptations before and evolving changes after surgical decompression in cervical spondylotic myelopathy. *J Neurosurg Spine* 9(6):538-551, 2008.

65. Holly LT, Dong Y, Albistegui-DuBois R, Marehbian J, Dobkin B. Cortical reorganization in patients with cervical spondylotic myelopathy. *J Neurosurg Spine* 6(6):544-551, 2007.

66. Henderson LA, Gustin SM, Macey PM, Wrigley PJ, Siddall PJ. Functional reorganization of the brain in humans following spinal cord injury: Evidence for underlying changes in cortical anatomy. *J Neurosci* 31(7):2630-2637, 2011.

67. Freund P, Weiskopf N, Ward NS, *et al*. Disability, atrophy and cortical reorganization following spinal cord injury. *Brain* 134(Pt 6):1610-1622, 2011.

68. Freund P, Rothwell J, Craggs M, Thompson AJ, Bestmann S. Corticomotor representation to a human forearm muscle changes following cervical spinal cord injury. *Eur J Neurosci* 34(11):1839-1846, 2011.

69. Nishimura Y, Onoe H, Morichika Y, Perfiliev S, Tsukada H, Isa T. Time-dependent compensatory mechanisms of finger dexterity after spinal cord injury. *Science* 318(5853):1150-1155, 2007.

70. Brown R. A brief account of microscopical observations made in the months of June, July and August, 1827, on the particles contained in the pollen of plants; and on the general existence of active molecules in organic and inorganic bodies. *Edinburgh new Philosophical J* 5:358-371, 1828.

71. Einstein A. Investigations on the theory of the Brownian movement. *Ann Physik* 17:549-560, 1905.

72. Alexander AL, Lee JE, Lazar M, Field AS. Diffusion tensor imaging of the brain. *Neurotherapeutics* 4(3):316-329, 2007.

73. Mori S, Zhang J. Principles of diffusion tensor imaging and its applications to basic neuroscience research. *Neuron* 51(5):527-539, 2006.

74. Ellingson BM, Salamon N, Holly LT. Advances in MR imaging for cervical spondylotic myelopathy. *Eur Spine J* 2013 [epub ahead of print].

75. Basser PJ, Pierpaoli C. Microstructural and physiological features of tissues elucidated by quantitative-diffusion-tensor MRI. *J Magn Reson B* 111(3):209-219, 1996.

76. Pierpaoli C, Jezzard P, Basser PJ, Barnett A, Di Chiro G. Diffusion tensor MR imaging of the human brain. *Radiology* 201(3):637-648, 1996.

77. Melhem ES, Mori S, Mukundan G, Kraut MA, Pomper MG, van Zijl PC. Diffusion tensor MR imaging of the brain and white matter tractography. *AJR Am J Roentgenol* 178(1):3-16, 2002.

78. Demir A, Ries M, Moonen CT, *et al*. Diffusion-weighted MR imaging with apparent diffusion coefficient and apparent diffusion tensor maps in cervical spondylotic myelopathy. *Radiology* 229(1):37-43, 2003.

79. Aota Y, Niwa T, Uesugi M, Yamashita T, Inoue T, Saito T. The correlation of diffusion-weighted magnetic resonance imaging in cervical compression myelopathy with neurologic and radiologic severity. *Spine* 33(7):814-820, 2008.

80. Kara B, Celik A, Karadereler S, *et al*. The role of DTI in early detection of cervical spondylotic myelopathy: a preliminary study with 3-T MRI. *Neuroradiology* 53(8):609-616, 2011.

81. Mamata H, Jolesz FA, Maier SE. Apparent diffusion coefficient and fractional anisotropy in spinal cord: Age and cervical spondylosis-related changes. *J Magn Reson Imaging* 22(1):38-43, 2005.

82. Budzik JF, Balbi V, Le Thuc V, Duhamel A, Assaker R, Cotten A. Diffusion tensor imaging and fibre tracking in cervical spondylotic myelopathy. *Eur Radiol* 21(2):426-433, 2011.

83. Jones JG, Cen SY, Lebel RM, Hsieh PC, Law M. DTI correlates with the clinical assessment of disease severity in cervical spondylotic myelopathy and predicts outcome following surgery. *AJNR Am J Neuroradiol* 34(2):471-478, 2012.

84. Wrigley PJ, Gustin SM, Macey PM, *et al*. Anatomical Changes in Human Motor Cortex and Motor Pathways Following Complete Thoracic Spinal Cord Injury. *Cereb Cortex* 19(1):224-232, 2009.

85. Freund P, Wheeler-Kingshott CA, Nagy Z, *et al*. Axonal integrity predicts cortical reorganisation following cervical injury. *J Neurol Neurosurg Psychiatry* 83(6):629-637, 2012.

86. Bertholdo D, Watcharakorn A, Castillo M. Brain proton magnetic resonance spectroscopy. *Neuroimaging Clinics* 23(3):359-380, 2013.

87. Boer VO, Siero JCW, Hoogduin H, van Gorp JS, Luijten PR, Klomp DW. High-field MRS of the human brain at short TE and TR. *NMR Biomed* 24(9):1081-1088, 2011.

88. Tkac I, Oz G, Adriany G, Ugurbil K, Gruetter R. In vivo 1H NMR spectroscopy of the human brain at high magnetic fields: Metabolite quantification at 4T vs 7T. *Magn Reson Med* 62(4):868-879, 2009.

89. Bluml, S. "Magnetic Resonance Spectroscopy: Physical Properties". *Functional neuroradiology: principles and clinical applications.* Eds: Faro SH, FB Mohamed and M Law. New York: Springer Science+Business Media, LLC, 2011. 141-154. Print.

90. Fayed N, Olmos S, Morales H, Modrego PJ. Physical basis of MRS and its application to CNS disease. *Am J Applied Sci* 3:1836-1845, 2006.

91. Bartha R, Drost DJ, Menon RS, Williamson PC. Comparison of the quantification precision of human short echo time (1)H spectroscopy at 1.5 and 4.0 Tesla. *Magn Reson Med* 44(2):185-192, 2000.

92. Pouwels PJ, Frahm J. Regional metabolite concentrations in human brain as determined by quantitative localized proton MRS. *Magn Reson Med* 39(1):53-60, 1998.

93. Birken DL, Oldendorf WH. N-acetyl-L-aspartic acid: a literature review of a compound prominent in 1H-NMR spectroscopic studies of brain. *Neurosci Biobehav Rev* 13(1):23-31, 1989.

94. De Stefano N, Matthers PM, Arnold DL. Reversible decreases in N-acetylaspartate after acute brain injury. *Magn Reson Med* 34(5):721-727, 1995.

95. Geurts JJG, van Horssen J. The brake on neurodegeneration: Increased mitochondrial metabolism in the injured MS spinal cord. *Neurology* 74(9):710-711, 2010.

96. Hugg JW, Kuzniecky RI, Gilliam FG, Morawetz RB, Fraught RE, Hetherington HP. Normalization of contralateral metabolic function following temporal lobectomy demonstrated by 1H magnetic resonance spectroscopic imaging. *Ann Neurol* 40(2):236-239, 1999.

97. Brooks WM, Stidley CA, Petropoulos H, *et al*. Metabolic and cognitive response to human traumatic brain injury: a quantitative proton magnetic resonance study. *J Neurotrauma* 17(8):629-640, 2000.

98. Khan O, Shen Y, Caon C, *et al*. Axonal metabolic recovery and potential neuroprotective effect of glatiramer acetate in relapsing-remitting multiple sclerosis. *Mult Scler* 11(6):646-651, 2005.

99. Kreis R, Ernst T, Ross BD. Development of the human brain: in vivo quantification of metabolite and water content with proton magnetic resonance spectroscopy. *Magn Reson Med* 30(4):424-437, 1993.

100. Maddock RJ, Buonocore MH. MR spectroscopic studies of the brain in psychiatric disorders. *Curr Topic Behav Neurosci* 2012 [epub ahead of print].

101. Andres RH, Ducray AD, Schlattner U, Wallimann T, Widmer HR. Functions and effects of creatine in the central nervous system. *Brain Res Bull* 76(4):329-343, 2008.

102. Jensen JFA, Backes WH, Nicolay K, Kooi ME. 1H MR spectroscopy of the brain: absolute quantification of metabolites. *Radiology* 240(2): 318-332, 2006.

103. Soares DP, Law M. Magnetic resonance spectroscopy of the brain: review of metabolites and clinical applications. *Clin Radiol* 64(1):12-21, 2009.

104. Caramanos Z, Narayanan S, Arnold DL. 1H-MRS quantification of tNA and tCr in patients with multiple sclerosis: a meta-analytic review. *Brain* 128(Pt 11):2483-2506, 2005.

105. Boulanger Y, Labelle M, Khiat A. Role of phospholipase A(2) on the variations of the choline signal intensity observed by 1H magnetic resonance spectroscopy in brain diseases. *Brain Res Brain Res Rev* 33(2-3):380-389, 2000.

106. Bitsch A, Bruhn H, Vougioukas V, *et al.* Inflammatory CNS demyelination: histopathologic correlation with in vivo quantitative proton MR spectroscopy. *AJNR Am J Neuroradiol* 20(9):1619-1627, 1999.

107. Allen NJ, Barres BA. Glia - more than just brain glue. *Nature* 457(7230):675-677, 2009.

108. Bains JS, Oliet SHR. Glia: they make -your memories stick! TRENDS in Neurosciences 30(8):417-424, 2007.

109. Barres BA. The Mystery and Magic of Glia: A Perspective on Their Role in Health and Disease. *Neuron* 60(3):430-440, 2008.

110. Lien YH, Shapiro JI, Chan L. Effects of hypernatremia on organic brain osmoles. *J Clin Invest* 85(5):1427-1436, 1990.

111. Videen JS. Human cerebral osmolytes during chronic hyponatremia. A proton magnetic resonance spectroscopy study. *J Clin Investig* 95(2):788-93, 1995.

112. Bak LK, Schousboe A, Waagepetersen HS. The glutamate/GABA-glutamine cycle: aspects of transport, neurotransmitter homeostasis and ammonia transfer. *J Neurochem* 98(3):641-653, 2006.

113. Schousboe A. Role of astrocytes in the maintenance and modulation of glutamatergic and GABAergic neurotransmission. *Neurochem Res* 28(2):347-352, 2003.

114. Hawkins RA. The blood-brain barrier and glutamate. *Am J Clin Nutr.* 90(3):867S-874S, 2009.

115. Holly LT, Freitas B, McArthur DL, Salamon N. Proton magnetic resonance spectroscopy to evaluate spinal cord axonal injury in cervical spondylotic myelopathy. *J Neurosurg Spine* 10(3):194-200, 2009.

116. Salamon N, Ellingson BM, Nagarajan R, Gebara N, Thomas A, Holly LT. Proton magnetic resonance spectroscopy of human cervical spondylosis at 3T. *Spinal Cord* 51(7):558-563, 2013.

117. Yabuki S, Konno S, Kikuchi S. Assessment of pain due to lumbar spine diseases using MR spectroscopy: a preliminary report. *J Orthop Sci* 18(3):363-368, 2013.

118. Sharma NK, McCarson K, Van Dillen K, Lentz A, Khan T, Cirstea CM. Primary somatosensory cortex in chronic low back pain - a H-MRS study. *J Pain Res* 4:143–150, 2011.

CHAPTER 2:

PROTON MAGNETIC RESONANCE SPECTROSCOPY OF THE MOTOR CORTEX IN CERVICAL SPONDYLOTIC MYELOPATHY

State of Publication: Published in: **Kowalczyk I**, Duggal N Bartha R. Proton Magnetic Resonance Spectroscopy of the Motor Cortex in Cervical Myelopathy. *Brain* 135(Pt 2):461-468, 2012.

2.1 Abstract:

Alterations in motor function in cervical spondylotic myelopathy (CSM) secondary to degenerative disease may be due to local effects of spinal compression or distal effects related to cortical reorganization. This prospective study characterizes differences in metabolite levels in the motor cortex, specifically *N*-acetylaspartate (NAA), creatine (Cr), choline (Cho), myo-inositol (Myo) and glutamate plus glutamine (Glx), due to alterations in cortical function in patients with reversible spinal cord compression (SCC) compared to healthy controls. We hypothesized that NAA/Cr levels would be decreased in the motor cortex of CSM patients due to reduced neuronal integrity/function and Myo/Cr levels would be increased due to reactive gliosis.

Twenty-four CSM patients and 11 age-matched healthy controls underwent proton-magnetic resonance spectroscopy (MRS) on a 3.0 Tesla Siemens Magnetom Tim Trio MRI (Erlangen, Germany). Areas of activation from functional magnetic resonance imaging (fMRI) scans of a finger-tapping paradigm were used to localize a voxel on the side of greater motor deficit in the myelopathy group (n=10 on right side and n=14 on left side of the brain) and on each side of the motor cortex in controls. Neurological function was measured with the Neck Disability Index (NDI), modified Japanese Orthopaedic Association (mJOA) and American Spinal Injury Association (ASIA) questionnaires. Metabolite levels were measured relative to total Cr within the voxel of interest.

No metabolite differences were detected between the right side and left side of the motor cortex in controls. The CSM patients had significantly decreased neurological function compared to the control group (NDI: $p<0.001$ and mJOA: $p<0.001$). There was a significant decrease in the NAA/Cr metabolite ratio in the motor cortex of the myelopathy group (1.21±0.07) compared to

the right (1.37±0.03; p=0.01) and left (1.38±0.03; p=0.007) motor cortex in controls suggesting neuronal death or dysfunction distal to the lesion in the spine. No difference was observed in levels of Myo/Cr.

Therefore, cortical levels of NAA/Cr may be a meaningful biomarker in CSM, indicative of neuronal death or dysfunction.

2.2 Key words:

cervical myelopathy, magnetic resonance spectroscopy, *N*-acetylaspartate, functional MRI, motor cortex.

2.3 Introduction:

Cervical spondylotic myelopathy secondary to degenerative disease (CSM) is the most common type of spinal cord dysfunction in people greater than 55 years of age,[1] yet its natural history continues to be poorly understood.[2] CSM is characterized by the narrowing of the spinal canal secondary to disc degeneration and herniation, the development of facet arthropathy and ligamentum flavum hypertrophy.[2,3] The natural history is typically a gradual deterioration in a stepwise pattern with clinical manifestations such as numbness, loss of dexterity, instability and bowel and bladder incontinence.[2,4] The majority of studies on spinal cord compression focus on the local changes in the spinal column or cord and neglect the intimate interconnection with the cerebral cortex.

Patients with spinal cord injury (SCI) have shown some degree of functional recovery through cortical reorganization and plasticity.[2,5-11] In previous work by our group, we demonstrated that CSM patients' had a greater volume of activation in the brain than control volunteers when performing a motor task.[11] Following decompression surgery, the volume of activation difference between the patients and controls increased, suggesting cortical reorganization and recruitment of surrounding cortex to perform the motor.[11] Similarly, Jurkiewicz *et al.* suggested the extent of movement related activation in the primary motor cortex is strongly associated with the return of movement in the upper limbs following SCI.[10] Based on these results, our goal was to determine if the initial deficits in neurological function experienced by CSM patients were also associated with measurable alterations in cortical metabolite levels.

Proton-magnetic resonance spectroscopy (^{1}H-MRS) is a non-invasive method that can repeatedly and directly measure levels of relevant metabolites such as *N*-acetylaspartate (NAA), creatine

(Cr), choline (Cho), myo-inositol (Myo) and glutamate plus glutamine (represented together as Glx) in the brain. NAA, a marker of neural integrity or viability, is localized to neurons and neuronal processes[12] and is decreased in several pathological conditions such as Alzheimer's disease, bipolar disease,[13] epilepsy,[14] post-traumatic stress disorder,[15] amyotrophic lateral sclerosis,[16] multiple sclerosis[17-18] and stroke.[19] Although the specific role of NAA is still unknown, it has been linked to the functional status of the mitochondria and is therefore considered a marker of cellular function.[20] As a functional indicator, the NAA/Cr ratio has been shown to increase in the motor cortex of patients with SCI who experienced functional recovery.[21]

Myo, a sugar primarily found in glial cells, has been associated with gliosis.[22] Neuronal loss or dysfunction is often accompanied by increased levels of Myo that reflect glial activation or proliferation. Zhu *et al.* reported increases of Myo and Myo/Cr ratio in the grey matter of the parietal lobe in Alzheimer's disease.[23] Many other studies have detected increased Myo levels in multiple sclerosis[24,25] and epilepsy[14] while decreased levels have been found in major depressive disorder[26] and low-grade hepatic encephalopathy.[27]

The purpose of this study was to determine whether altered metabolite levels are detectable in the brain distal to the site of injury in CSM patients using ^{1}H-MRS. We hypothesize that NAA levels would be decreased in CSM patients compared to healthy controls due to reduced neuronal integrity/function and Myo levels would be increased due to reactive gliosis.

2.4 Methods:

2.4.1 Patient Population

Twenty-four CSM patients secondary to cervical spondylosis disease were recruited with no other neurological disorder such as cerebral palsy, or a history of trauma. Fifty percent of patients (*n*=12/24) were treated for multilevel spondylotic disease and 50% (*n*=12/24) were treated for focal single-level cervical disc herniations causing myelopathy. Patients with CSM had symptoms manifesting no longer than a year prior to initial clinic visit. Exclusion criteria included any metal implants (aneurysm clips, etc), claustrophobia, pregnancy, nerve root symptoms or damage, or any other neurological disorders. CSM was supported by clinical MR imaging (Figure 2.1) in all patients. Subjects ranged in age from 32 to 71 years (mean ± standard error of the mean; 53 ± 2 years, 16 males, 22 right-handed). The youngest subjects had developmental canal stenosis and were carefully assessed prior to inclusion.

Figure 2.1: Sagittal cervical spine MR image obtained from a CSM patient with the red arrow pointing at the compression.

Eleven subjects of a similar age (46 ± 4 years, 7 males, 11 right-handed) with no previous clinical history of CSM or neurological disease were recruited as control subjects. Screening MRI of the brain and cervical spine was evaluated by one of the authors (ND) to confirm that there was no existing radiographic evidence of cerebral or spinal cord disease, including spinal cord compression. All participants gave written informed consent according to the Declaration of

Helsinki.[28] This study was approved by The University of Western Ontario's Human Subjects Research Ethics Board.

All CSM patients were assessed by the American Spinal Injury Association Impairment Classification (ASIA) scale. The maximum motor score is 100 (50 for upper and 50 for lower) and the maximum sensory light touch and pin prick was adjusted to test only levels between C2-T2 and L2-S2 for a total score of 60 for each parameter. All patients and controls completed the modified Japanese Orthopaedic Association (mJOA) score as well as patient derived functional assessments that include the disease specific Neck Disability Index (NDI).

2.4.2 MRI Acquisition

All MR data were acquired using a 3.0 T Siemens Magnetom Tim Trio MRI (Erlangen, Germany), using a twelve channel head coil with a neck and spine array. Each exam included the acquisition of sagittal T_1-weighted inversion prepared (T_i = 900 ms) 3D-MPRAGE anatomical images (192 slices, 1 mm isotropic resolution, TR/TE = 2300/3.42 ms) covering the entire brain to produce high gray matter/white matter contrast. Body coils integrated in the MR scanner were used for transmission, while a 12-channel head coil with spine array was used to receive signal. Functional MRI (fMRI) was used as a localization tool, to identify the specific region of the motor cortex for metabolite level measurement. Each functional brain volume was acquired using an interleaved echo-planar imaging pulse sequence (parallel imaging PAT=2, 240x240 acquisition matrix, 45 slices/volume, 3 mm isotropic resolution, TR/TE = 2500/30 ms, flip angle = 90^o). The total acquisition time was approximately 5 minutes and 30 seconds for 132 volumes.

2.4.3 Activation Paradigm

The motor pathway was activated during fMRI by instructing the participant to perform finger to thumb opposition ("duck quack") with the right hand followed by the left hand using a button box placed on the thumb. Participants were instructed to press the button simultaneously with all four fingers followed by an extension upwards to a box surrounding the button. This paradigm ensured all participants performed the finger extension to the same angle. The movement rate of the repetitive task is known to affect cerebral activation.[29-31] To control the frequency of the tapping, a block paradigm was designed in which participants received visual cues during alternating 30-second intervals of rest and activity. During the activity a visual cue instructed the participants to tap every 3 seconds for the 30-second interval. Participants received training prior to the fMRI session to reinforce the standardization and reduce learning effects during the imaging session.

2.4.4 MRS Acquisition and Analysis

The anatomical and functional images were used to guide the placement of a 20 mm isotropic voxel on the activated region near the "knob" area of the motor cortex.[32] Youstry *et al.* showed that neural elements involved in motor hand function are located in a characteristic 'precentral knob', which is a reliable landmark that identifies the precentral gyrus under normal and pathological conditions.[32] This landmark along with the location of hand activation in each subject was used to ensure consistent voxel placement in each participant. In the CSM group, the voxel was placed on the motor cortex contralateral to the side with greater functional deficits (n=11 on right side and n=13 on left side of the brain) while control data were acquired from two separate voxels placed on each side of the motor cortex. The greater functional deficit was

determined based on the objective ASIA score that differentiates between the left and right motor and sensory deficits, as well as simply asking the CSM patient which side was worse. Water suppressed spectroscopic data were localized using PRESS (TR/TE = 2000/135 ms, 192 averages, voxel size = 8 cm^3, BW = 1200 Hz, 1024 complex points). Any remaining unsuppressed water was removed from the spectrum using a Hankel singular value decomposition (HSVD) by subtracting resonances between 4.1 and 5.1 parts per million (ppm) (water ~4.7 ppm) as determined by the HSVD algorithm.[33]

Resultant metabolite spectra were fit in the time domain using a Levenberg-Marquardt minimization routine incorporating a template of prior knowledge of metabolic lineshapes. The analysis software (fitMAN) is incorporated into a graphical user interface written in our laboratory in the IDL (Version 5.4 Research Systems Inc, Boulder, CO, USA) programming language.[34] The acquisition of metabolite prior knowledge data has been previously described in detail.[33,34] Briefly, high-resolution *in vitro* spectra were acquired from solutions (pH adjusted to 7.04) of NAA, Cr, Cho, Myo, Glu and Gln using the same sequence that was used to acquire all *in vivo* data. Each metabolite solution contained sodium 3-trimethylsilyl-propionic acid (TSP) as a reference for chemical shift and Lorentzian damping (linewidth). The high resolution metabolite spectra were fitted to produce metabolite templates that were subsequently used to fit in-vivo spectra.

The metabolites NAA, Cr, Cho, Myo, and Glx (Glu + Gln) were examined based on previous studies that have implicated these metabolites in neurological disorders such as SCI and CSM,[21,35] and since these metabolites could be reliably measured. More specifically, metabolite ratios (NAA/Cr, Cho/Cr, Myo/Cr, and Glx/Cr) were calculated and compared between groups.

Metabolite ratios relative to Cr provide a reproducible and sensitive measurement and are not prone to errors associated with absolute metabolite level measurements such as those attributed to measurement of tissue partial volume and scaling by tissue relaxation time constants. Tissue partial volume effects that arise from having different amounts of white/grey matter and cerebral spinal fluid in selected voxels can be largely avoided with metabolite ratios.[36] Ratios can also be more sensitive in detecting metabolite changes when one metabolite in the ratio (e.g. the numerator) increases while the another metabolite in the ratio (e.g. the denominator) decreases.

2.4.5 Statistical Analysis

Metabolite ratios were compared between groups using a two-tailed Student's t-test with alpha error of 0.05. Post hoc analyses utilized the Tukey's test. The Pearson Product Moment Correlation Coefficient (r) was used to determine whether there were any correlations between metabolite ratios and clinical scores for each group. All statistical tests were two-sided, with significance set at the 0.05 level. Corrections for multiple comparisons were not performed because this was an exploratory study and we wanted to be sensitive to small metabolite changes. mJOA and NDI scores were compared between the CM group and controls using a two-tailed Student's t-test.

2.5 Results:

2.5.1 Clinical Data

Table 2.1 lists the demographics and clinical data of the study groups. The groups were not different with respect to age ($p = 0.158$) or sex ($p = 0.522$). Patients presented with loss of dexterity in the hands and gait dysfunction. CSM and control groups had significantly different NDI, mJOA and ASIA scores. NDI scores were significantly higher in patients compared to

controls (15.8 ± 1.6 and 1.7 ± 0.8, respectively, $p < 0.0001$). Since a score of 5 or greater is required to achieve a classification of mild disability on the NDI scale, the control group in the current study was considered to have no disability based on the mean NDI score of 1.7. The non-zero NDI score of 1.7 in the control group was attributed to minor neck pain. The motor upper and lower, sensory upper and sphincter dysfunction segments as well as the mean overall mJOA scores were significantly lower in patients compared to controls ($p < 0.001$). All controls recorded a perfect score of 18 on the mJOA questionnaire. As expected, patients had lower ASIA scores. There was no significant asymmetry between the right and left side in the motor upper or lower scores or in the sensory light touch and pin prick scores. Healthy controls were considered to have perfect ASIA scores as no disability was described.

Table 2.1: Demographic data and clinical outcome scores for the CSM patient group and healthy controls.

SUBJECT	CSM GROUP	CONTROLS	p-VALUE
N	24	11	n/a
Age	53 ± 2	46 ± 4	p=0.158
Sex (Male/Female)	16M/8F	7M/4F	p=0.522
Handedness (Right/Left)	22R/2L	11R/0L	p=0.083
NDI			
Score	15.8 ± 1.6	1.7 ± 0.8	p<0.0001
mJOA Scores			
Total Score	12.9 ± 0.6	18 ± 0	p<0.0001
Motor Upper	3.4 ± 0.3	5 ± 0	p<0.0001
Motor Lower	5.1 ± 0.2	7 ± 0	p<0.0001
Sensory Upper	1.8 ± 0.2	3 ± 0	p<0.0001
Sphincter Dysfunction	2.6 ± 0.1	3 ± 0	p=0.0011
ASIA Scores	**Right**	**Left**	
Upper Motor	23.2 ± 0.3	23.4 ± 0.6	n/a	n/a
Lower Motor	23.9 ± 0.4	24.1 ± 0.3	n/a	n/a
Light Touch	26.2 ± 1.2	26.7 ± 1.1	n/a	n/a
Pin Prick	25.2 ± 1.2	25.9 ± 1.1	n/a	n/a

n/a - not applicable; CSM – cervical spondylotic myelopathy; NDI – Neck Disability Index; mJOA – modified Japanese Orthopaedic Association; ASIA – American Spinal Injury Association Impairment Classification

2.5.2 Magnetic Resonance Spectroscopy

Magnetic resonance spectra were successfully acquired in all patients and controls. The positioning of the MRS voxel is shown as a white box on the motor cortex in Figure 2.2.

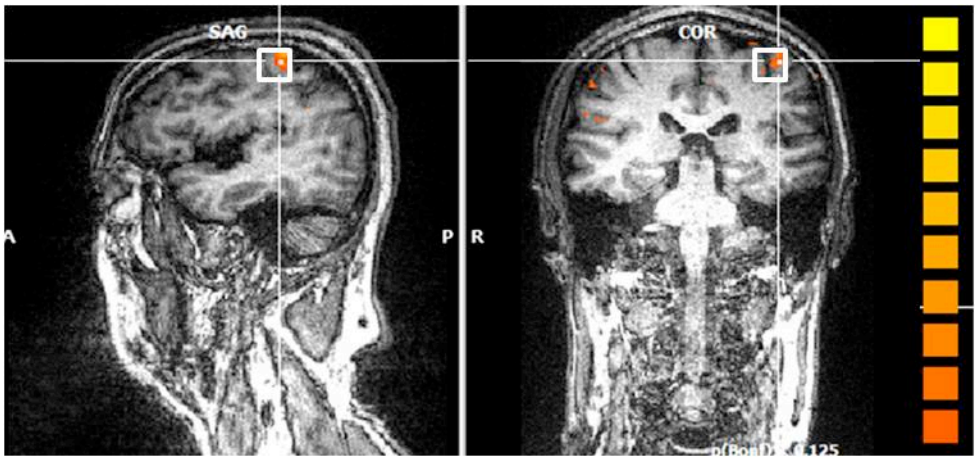

Figure 2.2: The spectroscopy voxel is outlined in white on coronal (*left*) and sagittal (*right*) images. The voxel is placed in the motor cortex over the site of finger tapping activation.

Figure 2.3 shows the spectrum acquired in one patient along with the fitted result and the residual (the difference between the fit and the spectrum). The individual metabolite components for NAA, Cho, Cr, Myo, Glu and Gln are also provided in Figure 2.3.

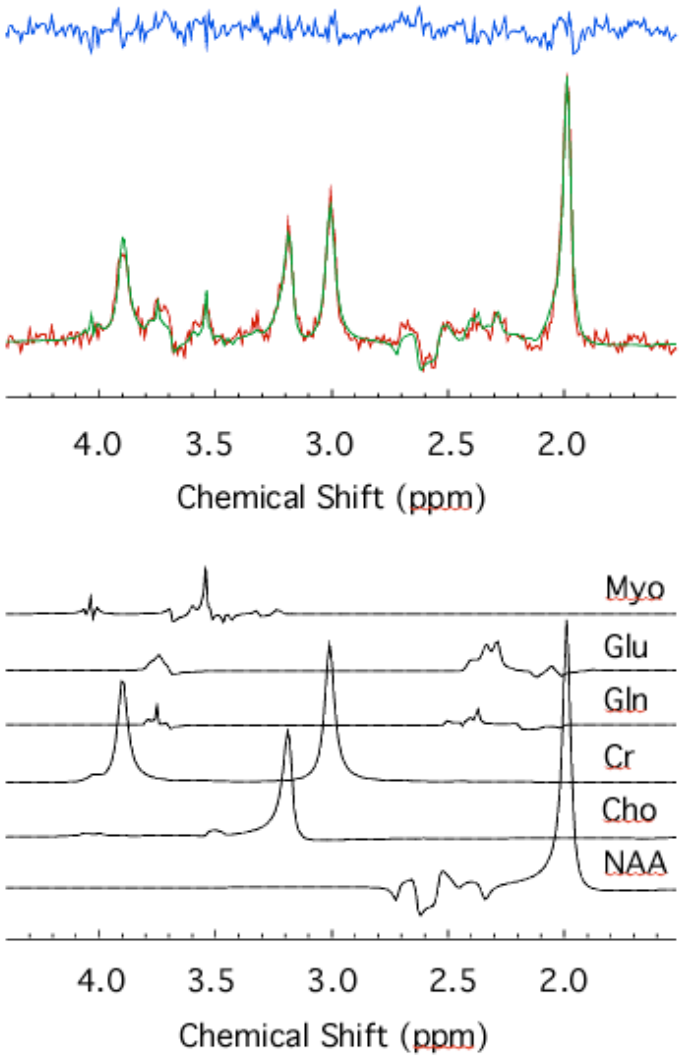

Figure 2.3: *Top:* The result of fitting (green line) is superimposed on the spectrum (red line) below the residual line (blue line). *Bottom:* Individual metabolite components.

No differences in any metabolite ratios were detected between the right side (RS) and left side (LS) of the motor cortex in the control subjects ($p>0.05$). Since there were no lateralized differences in controls, it was reasonable that metabolite data were combined for all CSM patients (10 right side, 14 left side). The average metabolite ratios are shown in figure 2.4 for all study groups. There was a significant decrease in the NAA/Cr metabolite ratio in the CSM group (1.16 ± 0.07) compared to RS (1.37 ± 0.03; $p=0.01$) and LS controls (1.38 ± 0.03; $p=0.007$) in the motor cortex. There was no significant difference in the Myo/Cr metabolite ratio in the CSM group (0.30 ± 0.02) compared to RS (0.28 ± 0.02; $p=0.50$) and LS controls (0.31 ± 0.02; $p=0.73$) in the motor cortex. No other metabolite ratio differences were observed.

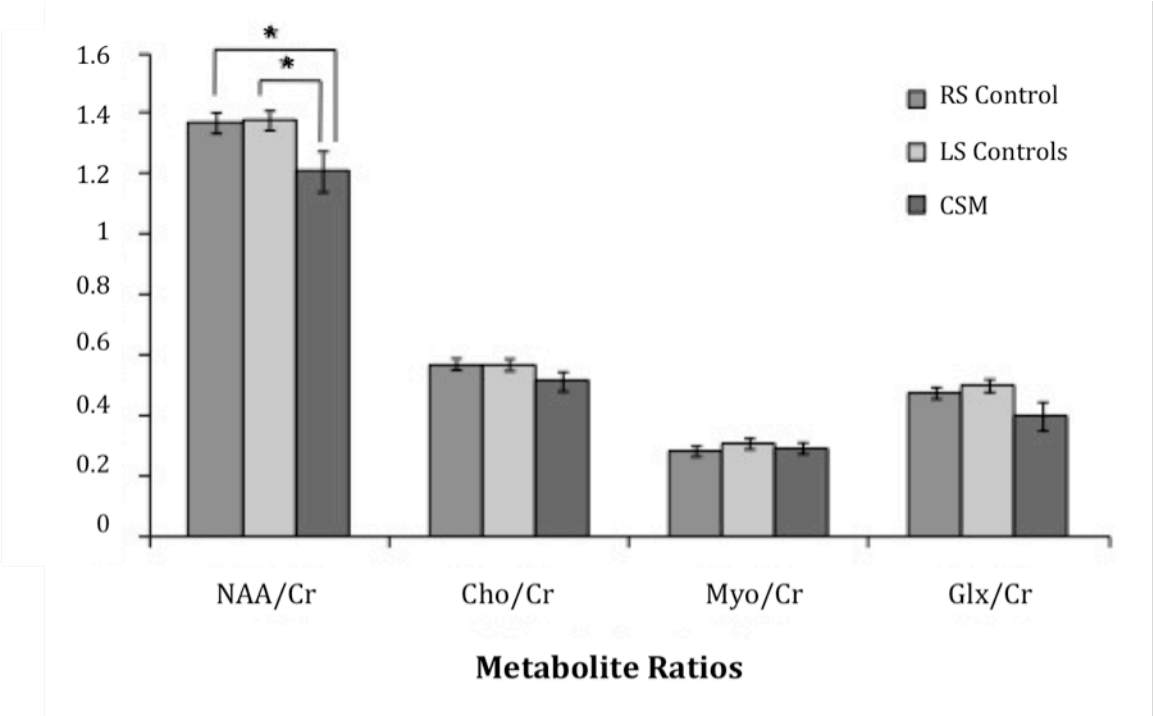

Figure 2.4: Average metabolite ratios of control and CSM groups. The error bars represent the standard error of the mean and asterisks (*) represents significant differences between the specified groups with $p<0.05$.

Tukey's post hoc analysis was completed in our exploratory study between CSM patient and control groups to determine patterns that were not specified *a priori*. The patient group was divided into two groups based on the side of the brain that was studied. There were no differences in metabolite ratios between 13 CSM patients and controls when comparing the left side directly. There was a significant decrease in the NAA/Cr ($p=0.008$), ratio in the 11 CSM patients who had the voxel placed on the right side of the motor cortex compared to the RS controls.

2.5.3 Correlations

There were no significant correlations between any of the metabolite ratio and questionnaire scores ($p<0.05$). There was also no correlation between the duration of symptoms (7.5 ± 1.4 months) in the CSM group and the NAA/Cr ratio ($r=0.008$ $p=0.48$). The presence of spinal cord signal change was found in 87.5% (21/24) of the CSM patient group and did not correlate with the NAA/Cr ratio ($r=0.05$, $p=0.40$).

2.6 Discussion:

The overall goal of this study was to investigate the effects of cervical spondylotic myelopathy on the neuronal metabolism and activity of the motor cortex, specifically, to characterize the metabolic correlates of spinal cord compression in the brain. This pilot study is the first to perform MRS in the motor cortex to evaluate metabolite levels in patients with reversible spinal cord compression. Our findings demonstrated a decrease in the NAA/Cr ratio in the hand area of the primary motor cortex in CSM patients compared to healthy controls. Although previous studies[9,37] have examined local metabolite changes in the spinal cord, our study demonstrated altered metabolite levels remote to the site of injury. Remote injury of the sensorimotor cortex in

CSM patients could be a critical factor underlying recovery.

Given that cortical synaptic plasticity has been shown in a variety of neurological disorders, we focussed our efforts on the metabolite changes in the hand region of the motor cortex instead of local changes occurring in the cervical spinal cord. Recent studies have described changes in cortical activation during sensory and/or motor tasks in CSM and SCI patients.[9-11,38-41] Our group has previously reported an increased volume of activation within the primary motor cortex and a decreased volume of activation within the primary sensory cortex in CSM patients followed by cortical reorganization after decompressive surgery on the spinal cord.[11] Based on these results, we hypothesized that cortical metabolic changes, particularly changes in NAA/Cr and Myo/Cr, may result from spinal cord compression.

The current study found significant decreases in NAA/Cr ratio in the motor cortex of CSM patients. Studies into the physiological relationship between NAA and neuronal cells have suggested that NAA/Cr is a marker of neuronal density and/or viability.[12,20] Reduced NAA/Cr may imply neuronal death or neurometabolic impairment.[12,20] Additional support for NAA/Cr as a neuronal health marker comes from several *in vivo* studies that found NAA/Cr levels can reversibly decline after treatment in neurological disorders such as acute brain injury[12] and amyotrophic lateral sclerosis.[16] The metabolic abnormalities of NAA/Cr detected using MRS may precede anatomic degeneration found using structural MRI.

Our results of a decreased NAA/Cr ratio are consistent with a previous study by Holly *et al.* who found CSM patients (n = 21) had a significantly lower average NAA/Cr ratio than healthy controls at the C2 level of the spinal cord.[35] Decreases in NAA/Cr are more likely to be attributed to decreases in NAA than increases in Cr, suggesting axonal or neuronal damage/loss. It remains controversial whether neuronal damage, as suggested by NAA levels, is permanent or reversible in the setting of incomplete injury secondary to degenerative spinal cord compression. Puri *et al*. performed ^{1}H-MRS on the motor cortex of the dominant hand/cortical hemisphere unless motor function was lateralised, in which case the weaker side was assessed, in 6 patients recovering from incomplete SCI and 5 healthy controls.[21] They found the NAA/Cr ratio was higher in the motor cortex of recovering patients than of the motor cortical area in controls.[21] These results have clinical implications in determining the role of potential surgery. If it is confirmed that increases in NAA/Cr accompany recovery in CSM patients after the initial decrease as observed in our study, MRS could provide a non-invasive method for prognosis and monitoring of CSM patients.

We found no significant change in the Myo/Cr ratio. Myo regulates osmotic pressure in neuroglial cells and is found specifically in astrocytes.[42-44] It has been shown to increase in neurodegenerative diseases such as Alzheimer's disease[45] and multiple sclerosis[24,25] and is considered a glial marker. Astrocytes provide neurons with energy, substrates for neurotransmission and are required for neuronal repair following injury.[42-44] However they can also suppress repair[43,44] by forming a scar and producing molecules that inhibit re-growth of damaged or severed axons.[44] In SCI, a glial scar may act as a local barrier to the regeneration of damaged axons.[43,44,46] Lebrun-Julien *et al.* disrupted the signalling events surrounding retinal

glial cells and found they could protect the majority of neurons and confirmed that glial cell events play a key role in death triggered by glutamate.[47] The lack of any changes with Myo may indicate that reversible spinal cord compression does not trigger glial activation and proliferation in the motor cortex. Glial activation and scarring may only occur in the setting of irreversible neuronal cell death.

Past research has found more than 60% of CSM patients have a T2 signal change in the spinal cord on MR imaging.[48,49] Spinal cord signal change is most commonly found in the more severe CSM and can be associated with changes such as myelomalacia.[50] The presence of signal intensity changes on MRI has been suggested as a possible criterion for surgery.[51,52] Even though the presence of spinal cord change was found in 87.5% of the CSM subjects in this study, there was no correlation with the decrease in NAA/Cr. The lack of correlation could be suggestive of a disconnect between significant spinal cord injury and the neuronal integrity or viability in the motor cortex.

We hypothesized that there may be correlations between changes in the NAA/Cr and Myo/Cr metabolite ratios and the neurological functional scores. However no significant correlations were observed between any metabolite ratios and the NDI, mJOA or ASIA questionnaires. Since the NAA/Cr ratio was significantly decreased in the patient group and the clinical scores were also found to be significantly worse in the patient group, the lack of a correlation between the metabolite ratio and clinical scores suggests that functional changes may be dominated by the local insult to the cord, not damage to the cortex. Future work will determine whether alterations in the cortex correlate with or limit functional recovery following spinal decompression surgery.

2.6.1 Limitations

Stringent inclusion criteria, along with rigorous acquisition and post-processing methods are required to reduce data variance. Our pilot study included a sample size of 24 patients, with an attempt to select a homogenous population of patients with a similar clinical history. We performed high magnetic field MRS at 3.0 T, which provides greater signal-to-noise ratio and greater spectral separation of multiplets that tend to overlap at lower field strength.[53,54] A larger cohort will be necessary to determine whether MRS findings have prognostic significance. Prospective studies should include patients with both short and long term pathology to determine how cortical metabolite levels are altered during the course of CSM. Other regions of the motor cortex may also be of interest. A limitation of our study was that spectra were acquired only from the contralateral motor cortex of the weaker side in CSM patients rather than on both sides as done in the control subjects. Spectroscopy data were only acquired from a single side in patients due to time constraints as patients could not tolerate the long scan times required to obtain spectroscopy data from both sides. The pooling of spectroscopy data in the patient group from the side of the motor cortex with the greatest functional deficit as previously described[21] was a reasonable approach as lateralized spectroscopy measurements in the control group did not show metabolite level differences. However, future studies would benefit from lateralized spectroscopy measurements in CSM patients to evaluate potential heterogeneity, and correlation of metabolite level changes in the cortex with findings on cervical MRI.

2.7 Conclusion:

This study demonstrates decreased NAA/Cr in the motor cortex of patients with CSM, indicating the presence of neurological damage or dysfunction likely caused by neuronal and/or axonal injury.

2.8 References:

1. Simeone FA, and Rothman RH. In: Rothman RH, Simeone FA, editors. *Cervical disc disease: The Spine* (ed2). Philadelphia: WB Saunders, 1982, p. 440-476. Print.

2. Bernhardt M, Hynes RA, Blume HW, White III AA. Cervical spondylotic myelopathy. *J Bone Joint Surg Am* 75(1):119-128, 1993.

3. Matz PG, Anderson PA, Holly LT, *et al*. The natural history of cervical spondylotic myelopathy. *J Neurosurg Spine* 11(2):104-111, 2009.

4. Emery SE. Cervical Spondylotic Myelopathy: Diagnosis and Treatment. *J Am Acad Orthop Surg* 9(6):376-388, 2001.

5. Levy WJ, Amassian VE, Traad M, Cadwell J. Focal magnetic coil stimulation reveals motor cortical systems reorganized in humans after traumatic quadriplegia. *Brain* 510(1):130-134, 1990.

6. Topka H, Cohen LG, Cole RA, Hallett M. Reorganization of corticospinal pathways following spinal cord injury. *Neurology* 41(8):1276-1283, 1991.

7. Bruehlmeier M, Dietz V, Leenders KL, Roelcke U, Missimer J, Curt A. How does the human brain deal with a spinal cord injury? *Eur J Neurosci* 10(12):3918-3922, 1998.

8. Sabbah P, de SS, Leveque C, Gay S, *et al*. Sensorimotor cortical activity in patients with complete spinal cord injury: a functional magnetic resonance imaging study. *J Neurotrauma* 19(1):53-60, 2002.

9. Holly LT, Dong Y, Albistegui-DuBois R, Marehbian J, Dobkin B. Cortical reorganization in patients with cervical spondylotic myelopathy. *J Neurosurg Spine* 6(6):544-551, 2007.

10. Jurkiewicz MT, Mikulis DJ, McIlroy WE, Fehlings MG, Verrier MC. Sensorimotor cortical plasticity during recovery following spinal cord injury: a longitudinal fMRI study. *Neurorehabil Neural Repair* 21(6):527-538, 2007.

11. Duggal N, Rabin D, Bartha R, *et al*. Brain reorganization in patients with spinal cord compression evaluated using fMRI. *Neurology* 74(13):1048-1054, 2010.

12. De Stefano N, Matthews PM, Arnold DL. Reversible decreases in N-acetylaspartate after acute brain injury. *Magn Reson Med* 34(5):721-727, 1995.

13. Molina V, Sanche J, Sanz J, *et al*. Dorsolateral prefrontal N-acetylaspartate concentration in male patients with chronic schizophrenia and with chronic bipolar disorder. *Eur Psychiatry* 22(8):505-512, 2007.

14. Simister RJ, McLean MA, Barker GJ, Duncan JS. Proton magnetic resonance spectroscopy of malformations of cortical development causing epilepsy. *Epilepsy Res* 74(2-3):107-115, 2007.

15. Ham BJ, Chey J, Yoon SJ, *et al*. Decreased N-acetyl-aspartate levels in anterior cingulate and hippocampus in subjects with post-traumatic stress disorder: a proton magnetic resonance spectroscopy study. *Eur J Neurosci* 25(1):324-329, 2007.

16. Rooney WD, Miller RG, Gelinas D, Schuff N, Maudsley AA, Weiner MW. Decreased NAA in motor cortex and corticospinal tract in ALS. *Neurology* 50(6):1800-1805, 1998.

17. Arnold DL, Matthews PM, Francis G, Antel J. Proton magnetic resonance spectroscopy of the human brain *in vivo* in the evaluation of multiple sclerosis: assessment of the load of disease. *Magn Reson Med* 14(1):154-159, 1990.

18. Husted CA, Matson GB, Adams DA, Goodin DS, Weiner MW. In vivo detection of myelin phospholipids in multiple sclerosis with phosphorus magnetic resonance spectroscopic imaging. *Ann Neurol* 36(2):239-241, 1994.

19. Gideon P, Henriksen O. In vivo relaxation of N-acetyl-aspartate, creatine plus phosphocreatine, and choline containing compounds during the course of brain infarction: a proton MRS study. *Magn Reson Imaging* 10(6):983-988, 1992.

20. Geurts JJ, van Horssen J. The brake on neurodegeneration: Increased mitochondrial metabolism in the injured MS spinal cord. *Neurology* 74(9):710-711, 2010.

21. Puri BK, Smith HC, Cox IJ, *et al*. The human motor cortex after incomplete spinal cord injury: an investigation using proton magnetic resonance spectroscopy. *J Neurol Neurosurg Psychiatry* 65(5):748-754, 1998.

22. Ross BD, Bluml S, Cowan R, Danielson E, Farrow N, Tan J. In vivo MR spectroscopy of human dementia. *Neuroimaging Clin N Am* 8(4):809-822, 1998.

23. Zhu X, Schuff N, Kornak J, *et al*. Effects of Alzheimer disease on fronto-parietal brain N-acetyl aspartate and myo-inositol using magnetic resonance spectroscopic imaging. *Alzheimer Dis Assoc Disord* 20(2):77-85, 2006.

24. Fernando KT, McLean MA, Chard DT, *et al*. Elevated white matter myo-inositol in clinically isolated syndromes suggestive of multiple sclerosis. *Brain* 127(Pt6):1361-1369, 2004.

25. Vrenken H, Barkhof F, Uitdehaag BM, Castelijns JA, Polman CH, Pouwels PJ. MR spectroscopic evidence for glial increase but not for neuro-axonal damage in MS normal-appearing white matter. *Magn Reson Med* 53(2):256-266, 2005.

26. Coupland NJ, Ogilvie CJ, Hegadoren KM, Seres P, Hanstock CC, Allen PS. Decreased prefrontal Myo-inositol in major depressive disorder. *Biol Psychiatry* 57(12):1526-1534, 2005.

27. Haussinger D, Laubenberger J, vom Dahl S, *et al*. Proton magnetic resonance spectroscopy studies on human brain myo-inositol in hypo-osmolarity and hepatic encephalopathy. *Gastroenterology* 107(5):1475-1480, 1994.

28. World Medical Association. Declaration of Helsinki [document on the Internet] Seoul: The Association; 2008. [updated 2008 Oct 22]. Available from: http://www.wma.net/en/30publications/10policies/b3/index.html (16 February 2011, date last accessed).

29. Blinkenberg M, Bonde C, Holm S, *et al*. Rate dependence of regional cerebral activation during performance of a repetitive motor task: a PET study. *J Cereb Blood Flow Metab* 16(5):794-803, 1996.

30. Rao SM, Bandettini PA, Binder JR, *et al*. Relationship between finger movement rate and functional magnetic resonance signal change in human primary motor cortex. *J Cereb Blood Flow Metab* 16(6):1250-1254, 1996.

31. Schlaug G, Sanes JN, Thangaraj V, *et al*. Cerebral activation covaries with movement rate. *Neuroreport* 7(4):879-883, 1996.

32. Youstry TA, Schmid UD, Alkadhi H, *et al*. Localization of the motor hand area to a knob on the precentral gyrus: A new landmark. *Brain* 120(Pt1):141-157, 1997.

33. Kassem MN, Bartha R. Quantitative proton short-echo time LASER spectroscopy of normal human white matter and hippocampus at 4 Tesla incorporating macromolecule subtraction. *Magn Reson Med* 49(5):918-927, 2003.

34. Bartha R, Drost DJ, Williamson PC. Factors affecting the quantification of short echo in-vivo 1H MR spectra: prior knowledge, peak elimination and filtering. *NMR Biomed* 12(4):205-216, 1999.

35. Holly LT, Freitas B, McArthur DL, Salamon N. Proton magnetic resonance spectroscopy to evaluate spinal cord axonal injury in cervical spondylotic myelopathy. *J Neurosurg Spine* 10(3):194-200, 2009.

36. Jensen JF, Backes WH, Nicolay K, Kooi ME. 1H MR spectroscopy of the brain: absolute quantification of metabolites. *Radiology* 240(2):318-332, 2006.

37. Nagashima H, Morio Y, Meshitsuka S, Yamane K, Nanjo Y, Teshima R. High-resolution nuclear magnetic resonance spectroscopic study of metabolites in the cerebrospinal fluid of patients with cervical myelopathy and lumbar radiculopathy. *Eur Spine J* 19(8):1363-1368, 2010.

38. Curt A, Bruehlmeier M, Leenders KL, Roelcke U, Dietz V. Differential effect of spinal cord injury and functional impairment on human brain activation. *J Neurotrauma* 19(1):43-51, 2002.

39. Curt A, Alkadhi H, Crelier GR, Boendermaker SH, Hepp-Reymond MC, Kollias SS. Changes of non-affected upper limb cortical representation in paraplegic patients as assessed by fMRI. *Brain* 125(Pt11):2567-2578, 2002.

40. Dong Y, Holly LT, Albistegui-Dubois R, *et al*. Compensatory cerebral adaptations before and evolving changes after surgical decompression in cervical spondylotic myelopathy. *J Neurosurg Spine* 9(6):538-551, 2008.

41. Tam S, Barry RL, Bartha R, Duggal N. Changes in fMRI cortical activation after decompression of cervical spondylosis: a case report. *Neurosurgery* 67(3):E863-E864, 2010.

42. Bains JS, Oliet SHR. Glia: they make your memories stick! *TRENDS Neurosci* 30(8):417-424, 2007.

43. Barres BA. The mystery and magic of glia: a perspective on their role in health and disease. *Neuron* 60(3):430-440, 2008.

44. Allen NJ, Barres BA. Neuroscience: Glia - more than just brain glue. *Nature* 457(7230):675-677, 2009.

45. Chen SQ, Wang PJ, Ten GJ, Zhan W, Li MH, Zang FC. Role of myo-inositol by magnetic resonance spectroscopy in early diagnosis of Alzheimer's disease in APP/PS1 transgenic mice. *Dement Geriatr Cogn Disord* 28(6):558-566, 2009.

46. Silver J, Miller JH. Regeneration beyond the glial scar. *Nat Rev Neurosci* 5(2):146-156, 2004.

47. Lebrun-Julien F, Duplan L, Pernet V, *et al*. Excitotoxic death of retinal neurons in vivo occurs via a non-cell-autonomous mechanism. *J Neurosci* 29(17):5536-5545, 2009.

48. Matsumoto M, Toyama Y, Ishikawa M, Chiba K, Suzuki N, Fujimura Y. Increased signal intensity of the spinal cord on magnetic resonance images in cervical myelopathy. Does it predict the outcome in conservative treatment? *Spine* 25(6):677-682, 2000.

49. Suri A, Chabbra RP, Mehta VS, Gaikwad S, Pandey RM. Effect of intramedullary signal changes on the surgical outcome of patients with cervical spondylotic myelopathy. *Spine J* 3(1):33-45, 2003.

50. Wada E, Ohmura M, Yonenobu K. Intramedullary changes of the spinal cord in cervical spondylotic myelopathy. *Spine* 20(20):2226-2232, 1995.

51. Morio Y, Teshima R, Nagashima H, Nawata K, Yamasaki D, Nanjo Y. Correlation between operative outcomes of cervical compression myelopathy and MRI of the spinal cord. *Spine* 26(11):1238-1245, 2001.

52. Naderi S, Ozgen S, Pamir MN, Ozek MM, Erzen C. Cervical spondylotic myelopathy: surgical results and factors affecting prognosis. *Neurosurgery* 43(1):43-49, 1998.

53. Gonen O, Gruber S, Li BS, Mlynarik V, Moser E. Multivoxel 3D proton spectroscopy in the brain at 1.5 versus 3.0 T: Signal-to-noise ratio and resolution comparison. *AJNR Am J Neuroradiol* 22(9):1727-1731, 2001.

54. Bartha R, Drost DJ, Menon RS, Williamson PC. Comparison of the quantification precision of human short echo time (1)H spectroscopy at 1.5 and 4.0 Tesla. *Magn Reson Med* 44(2):185-192, 2000.

CHAPTER 3:

METABOLITE CHANGES IN THE PRIMARY MOTOR CORTEX AFTER SURGERY IN CERVICAL SPONDYLOTIC MYELOPATHY

State of Publication: **Aleksanderek I**, McGregor SM, Stevens TK, Goncalves S, Bartha R, Duggal N. Metabolite Changes in the Primary Motor Cortex After Surgery in Cervical Spondylotic Myelopathy. In preparation for submission.

3.1 Abstract:

N–Acetylaspartate (NAA), an indicator of neuronal mitochondrial function, is decreased in the motor cortex of patients with cervical spondylotic myelopathy (CSM). This decline may impact response to therapy. The goals of this study were to characterize longitudinal metabolite alterations in the motor cortex following decompression of the spinal cord using ^{1}H magnetic resonance spectroscopy (MRS) and evaluate white matter (WM) integrity with diffusion tensor imaging (DTI).

Twenty–eight CSM patients had two separate 3.0 Tesla MRI scans before and six months following surgery. Ten healthy controls underwent two MRI scans six months apart. Metabolite levels normalized to creatine (Cr) were measured from the motor cortex contralateral to the greater functional deficit side in the patient group and on both sides in controls. Fractional anisotropy (FA) and mean diffusivity (MD) were measured by DTI in the WM adjacent to the motor and sensory cortices of the hand and the entire cerebral WM.

In CSM patients, NAA/Cr levels were significantly lower six months following surgery (1.48±0.08; $p<0.03$) compared to pre-operative levels (1.73±0.09), despite significant clinical improvement in questionnaire scores. The FA and MD were the same between the patient and control groups in all measured regions at all time points, suggesting WM integrity is unaffected.

NAA/Cr levels decreased in the motor cortex in CSM patients six months following successful surgery. Intact WM integrity with decreased NAA/Cr levels suggests mitochondrial metabolic dysfunction persists following surgery.

3.2 Key words:

cervical spondylotic myelopathy; *N*-Acetylaspartate; primary motor cortex; magnetic resonance spectroscopy; diffusion tensor imaging; spinal cord compression

3.3 Introduction:

Cervical spondylotic myelopathy (CSM) represents a common and unique model of incomplete spinal cord injury (SCI) that is potentially reversible, providing an opportunity to examine the mechanisms involved in injury, recovery, and neuronal plasticity. Surgical intervention in CSM patients does not always provide consistent results, as patients may improve, remain static or even deteriorate after surgery.[1-3] Recently, our group employed functional magnetic resonance imaging (fMRI) to demonstrate cortical reorganization in the sensorimotor cortices in spinal cord compressed (SCC) patients prior to and after spinal decompression surgery.[4] To understand why recruitment of adjacent cortex was necessary post surgery in the setting of clinical improvement, we utilized proton magnetic resonance spectroscopy (^{1}H–MRS) in a second study to examine the metabolic alterations occurring in the primary motor cortex of CSM patients compared to controls.[5] CSM patients had lower *N*-acetylaspartate (NAA) to creatine (Cr) ratio, suggesting significant neuronal dysfunction upstream of injury site.[5] Functional decline in CSM may also involve alterations in white matter (WM) tract integrity measured by diffusion tensor imaging (DTI). However, until now, the potential for remote changes in the WM integrity of the brain have not been considered.

The goal was of this study was to follow the CSM patient population longitudinally to assess how metabolic changes and fibre tract integrity of the primary motor cortices correlate to clinical outcomes in the context of recovering neurological function following surgery.

3.4 Methods:

3.4.1 Patient Population

Twenty-eight patients (age 51 ± 2 years, 21 males, 26 right–handed) with a clinical history of CSM of less than or equal to one year and no other neurological disorders were recruited and participated in two 3.0 Tesla MR imaging sessions. Pre–operative clinical assessment involved patient history, neurological examination and radiological studies with x–rays and MRI. Surgery for the treatment of symptomatic CSM was considered when there was a history of progressive neurologic deficits (motor weakness, numbness, gait dysfunction, bowel and bladder dysfunction), concordant imaging with evidence of SCC, and limited or no response to appropriate conservative measures. CSM patients underwent a baseline research MRI scan, surgical decompression surgery, and then a second research MRI scan six months post–surgery. Ten subjects of similar age (48 ± 4 years, 5 males, 10 right–handed) with no previous evidence of SCC and no history of neurological disease were recruited as controls. Control subjects had two MRI sessions six months apart without surgical intervention. Informed written consent was obtained for all procedures and the study was approved by the Western University Human Subjects Research Ethics Board. All patients and controls completed validated instruments for assessing disability resulting from myelopathy such as the modified Japanese Orthopaedic Association (mJOA) outcome measure, in addition to the American Spinal Injury Association Impairment Scale (ASIA), and the Neck Disability Index (NDI).

3.4.2 MRI Acquisition

All MR data were acquired using a 3.0 T Siemens Magnetom Tim Trio MRI (Erlangen, Germany), using a twelve channel head coil with a neck and spine array. Before imaging, an

automated global shimming procedure using first- and second-order shims optimized the magnetic field over the brain. The imaging exam, which lasted between 80-90 minutes in total, included the acquisition of sagittal T_1-weighted inversion prepared (TI=900 ms) 3D-MPRAGE anatomical images (192 slices, 1 mm isotropic resolution, TR/TE=2300/3.42 ms) that covered the entire brain and produced high contrast between gray and white matter.

3.4.3 MR Spectroscopy Acquisition and Analysis

The anatomic images were used to guide the placement of a 20 mm isotropic voxel near the "precentral knob" area of the primary motor cortex (Figure 3.1).[6] The "knob" area is a reliable landmark that identifies the neural elements associated with motor hand function.[6] The voxel was placed on the motor cortex contralateral to the side with greater functional deficits in the CSM patient group (n=12 on right side and n=16 on left side) while controls had a separate voxel placed on each side of the motor cortex.

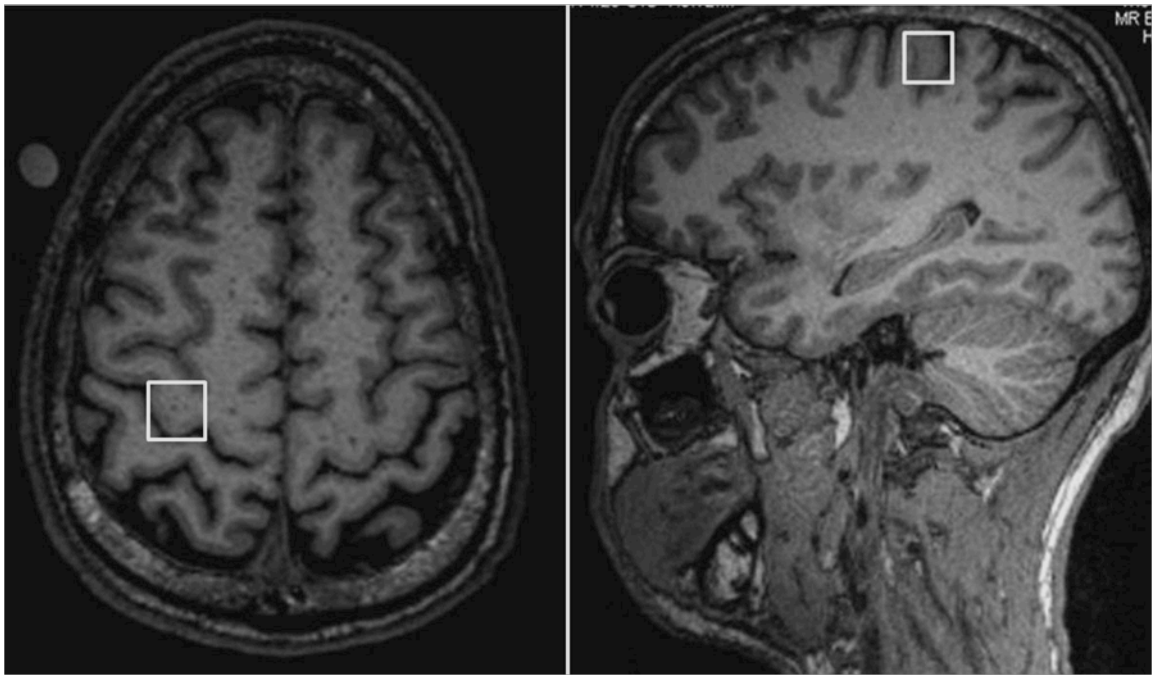

Figure 3.1: The spectroscopy voxel is outlined in white on anatomical images.

Water suppressed and unsuppressed spectroscopic data were acquired using the Point-Resolved Spectroscopy sequence (PRESS, TR/TE=2000/135 ms, suppressed: 192 acquisitions; unsuppressed: 8 acquisitions; voxel size=8 cm^3). Spectra were processed and fitted using custom built in-house software called fitMAN.[7] The analysis software (fitMAN) is incorporated into a graphical user interface written in our laboratory in the IDL programming language (Version 5.4 Research Systems Inc, Boulder, CO, USA). Initial post-processing involved combined QUALITY deconvolution to restore the Lorentzian lineshape and eddy current correction.[7-9] Following lineshape correction, any remaining unsuppressed water signal was removed from the spectrum using a Hankel singular value decomposition (HSVD) that required no prior knowledge. All unsuppressed water signal was removed by subtracting resonances between 4.1 and 5.1 parts per million (ppm, water ~4.7 ppm) as determined by the HSVD algorithm.[9]

Resultant metabolite spectra were fitted in the time domain using a Levenberg-Marquardt minimization routine that utilized prior knowledge templates of metabolic lineshapes. The acquisition of metabolite prior knowledge data has been previously described in detail.[7,9] The metabolites NAA, Cr, choline (Cho), myo-inositol (Myo), and glutamine plus glutamate (Glx) were examined based on previous studies that have implicated these metabolites in neurological disorders such as SCI and CSM.[10,11] More specifically, metabolite ratios (NAA/Cr, Cho/Cr, Myo/Cr, and Glx/Cr) were calculated and compared as this approach removes the potential for tissue partial volume errors and may be more sensitive to metabolite changes.

3.4.4 DTI Acquisition and Analysis

Diffusion weighted scans of the brain were acquired using a spin-echo echo-planar imaging (EPI) sequence (75 slices, iPAT=3, TR/TE=10000/83 ms, b-value=0 s/mm^2 and 1000 s/mm^2) incorporating 30 diffusion encoding directions. Diffusion data were analyzed using Brain Voyager QX v2.2. A diffusion-weighted magnetic resonance image and a volumetric magnetic resonance image were defined for each subject.[12] The volumetric magnetic resonance image was used to strip the skull and create a mask of the brain to avoid processing background noise. The diffusion-weighted magnetic resonance image was then co-registered with the volumetric magnetic resonance image. A volume diffusion weighted image was generated and subsequently used, along with the previously created mask, to calculate the FA and MD for each pixel. Regions of interest (ROI) were defined for each subject in the WM adjacent to the motor and sensory cortices of the hand in both right and left cerebral hemispheres (RM, LM, RS, LS; Figure 3.2). A new ROI was defined for each patients and control at each visit.

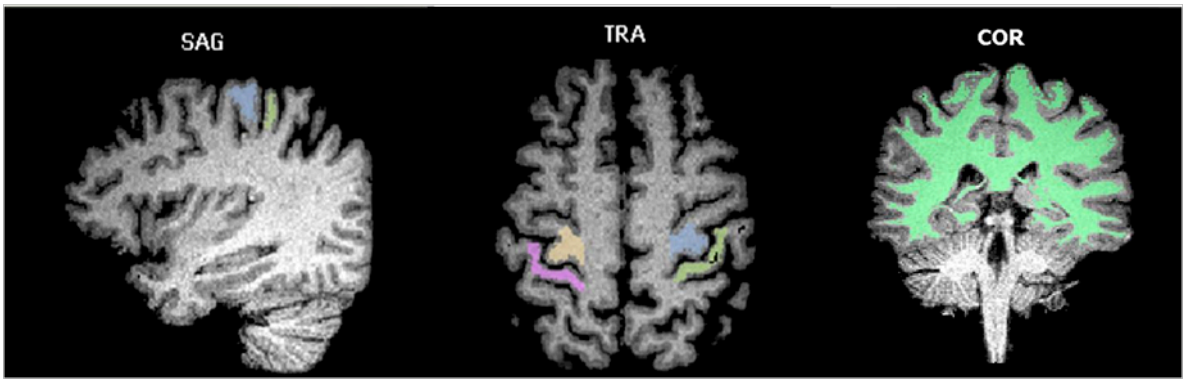

Figure 3.2: Regions of interest used for DTI analysis. Yellow and blue regions depict WM adjacent to the left and right primary motor cortices, respectively. Pink and green regions depict the WM adjacent to the left and right primary sensory cortices, respectively. The darker green is shown to indicate the boundaries of the cerebrum WM region.

The motor cortex was identified by the "precentral knob" area as documented by Youstry *et al.* to ensure consistent ROI placement in each participant.[6] The WM immediately adjacent to this portion of the neocortex was included (Figure 3.2). For the motor cortex, the "knob" was identified on axial images and the location was confirmed with the omega or horizontal epsilon sign location moving from the inferior to the superior slice. The entire omega sign was highlighted and extended up to the grey matter of the precentral sulcus. Medially, the motor cortex ROI extended in a straight line connecting the medial aspects of the precentral and central sulci, and extended equal distances laterally. The sensory cortex was demarcated as the gyrus directly posterior and surrounding the 'precentral knob' and ROIs were selected below the neocortex of that gyrus. The WM was selected on the VMR images. The cerebellum and spinal cord were not included when examining the entire cerebral WM.

3.4.5 Statistical Analysis

All data are presented as the group mean followed by the standard error of the mean. An *unpaired* Student's t-test was used for cross-sectional comparisons of imaging and functional measures between the CSM patients and controls at each time point. In the CSM patients, the pre- and post-surgery metabolite concentrations, FA and MD values, and questionnaire scores were compared using a *paired* Student's t-test. Paired t-tests were also used to evaluate measurement reproducibility in the control group. All statistical testes were two-sided, with significance set at an alpha level of 0.05.

3.5 Results:

3.5.1 Clinical Data

The patient and control groups were not different with respect to age, sex or hand dominance ($p>0.05$; Table 3.1). Nineteen of 28 CSM patients (68%) underwent 1–level surgery and 9 (32%) had 2–level surgery. From initial scan, the average follow-up time was 194 days (± 9) for CSM patients and 176 days (± 15) for the controls. The mean overall modified Japanese Orthopaedic Association (mJOA) score improved in the CSM patient group following surgery (13.0 ± 0.5 pre–operatively compared to 15.9 ± 0.3 following surgery; $p<0.0001$). Six months following surgery, CSM patients exhibited higher ASIA scores and less neck pain, demonstrated by lower NDI scores (Table 3.1). All controls recorded a perfect mJOA score of 18 and no disability captured by the ASIA and NDI scores during both visits ($p<0.05$).

Table 3.1: Demographic and clinical data for the CSM patient group and healthy controls (mean ± standard error of the mean).

Subject	CSM	Controls	p-value
N	28	10	--
Age (years)	51 ± 2	48 ± 4	0.45
Sex (Male/Female)	21M/7F	5M/5F	0.22
Hand Dominance (Right/Left)	26R/2L	10R/0L	0.08
Side of Worst Symptoms (Right/Left)	12R/16L	--	--
Surgery			
1 level	19 (68%)	--	--
2 level	9 (32%)	--	--
Follow-up time (days)			
Surgery (CSM) or baseline (controls) and 6 month scan	194 ± 9	176 ± 15	0.28
mJOA Score			
Pre-op	13.0 ± 0.5	18 ± 0	p<0.0001
Post-op	15.9 ± 0.3	18 ± 0	p<0.0001

CSM Patients	Pre-op Score	Post-op Score	p-value
mJOA Score – Total	13.0 ± 0.5	15.9 ± 0.3	p<0.0001
Motor Upper Extremity	3.4 ± 0.3	4.6 ± 0.1	0.0001
Motor Lower Extremity	5.2 ± 0.2	6.1 ± 0.2	0.0002
Sensory Upper Extremity	1.7 ± 0.1	2.3 ± 0.1	p<0.0001
Sphincter Dysfunction	2.6 ± 0.1	2.8 ± 0.1	0.09
ASIA Impairment Score	196.0 ± 4.4	213.5 ± 2.0	0.0009
NDI Score	16.7 ± 1.6	9.3 ± 1.4	0.0001

CSM – cervical spondylotic myelopathy; mJOA – modified Japanese Orthopaedic Association; ASIA – American Spinal Injury Association Impairment Scale; NDI – Neck Disability Index

3.5.2 Magnetic Resonance Spectroscopy

Magnetic resonance spectra were successfully acquired in all CSM patients and controls. No differences in any metabolite ratios were detected between the right side and left side of the motor cortex in the control subjects ($p>0.05$) at either time point. Since there were no lateralized differences in controls, we combined the metabolite data for all CSM patients (12 right side, 16 left side).[5,10] Control metabolite ratios have been described previously.[5] There were no changes in any of the metabolite ratios in the control group over time ($p>0.05$).

Following spinal decompression surgery, the NAA/Cr ratio significantly decreased in the CSM patients (1.73 ± 0.09 pre-operatively compared to 1.48 ± 0.08 post-operatively; $p=0.03$; Figure 3.3). There was no change in the Choline/Creatine (Cho/Cr), Myo-inositol/Cr (Myo/Cr) or Glutamine plus Glutamate/Cr (Glx/Cr) ratios over time (Figure 3.3).

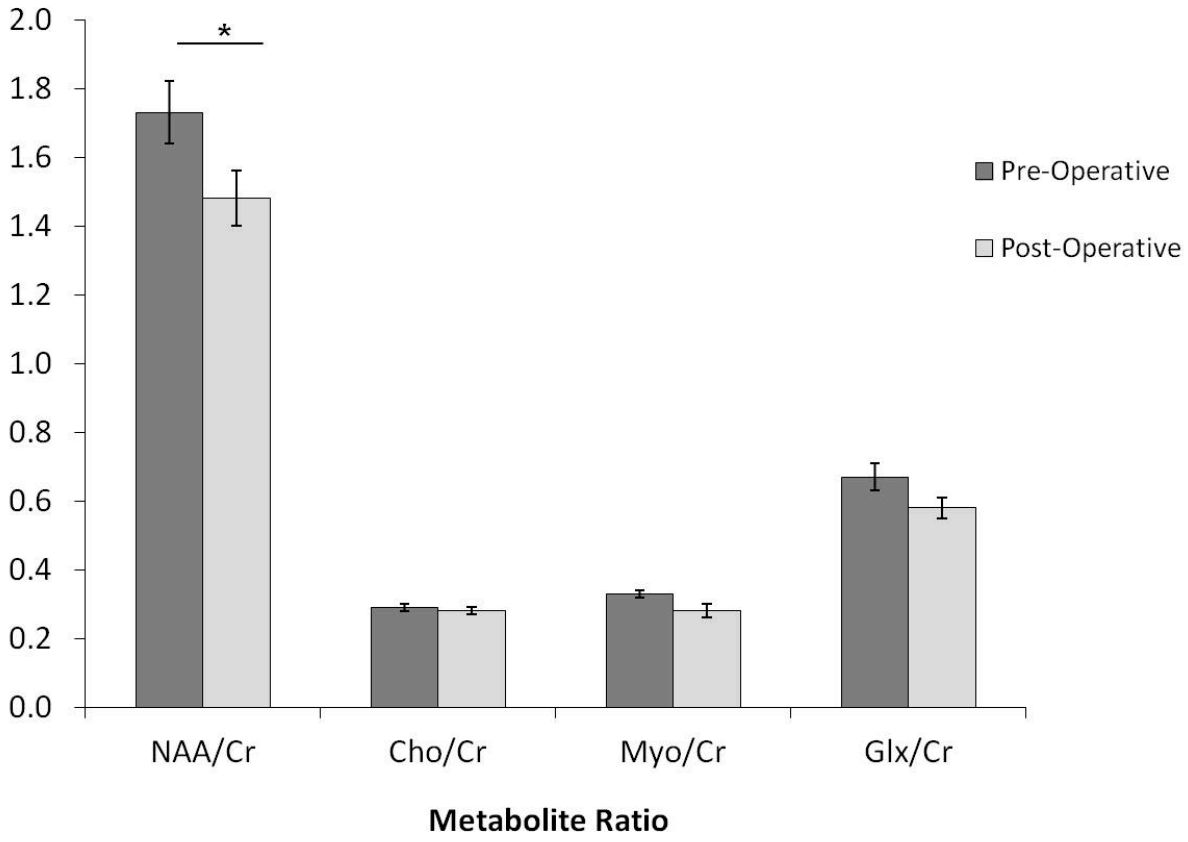

Figure 3.3: Average metabolite ratios for the CSM patients at pre and post-operative time points (asterisks represent significance differences). Error bars represent standard error of the mean.

3.5.3 Diffusion Tensor Imaging

Sixteen CSM patients and eight healthy controls were included in the DTI analysis. Subjects were excluded due to incomplete DTI acquisition (n=3) related to patient discomfort, misalignment of the diffusion tensor data on the anatomical images due to motion (n=3) or when no DTI scan was performed (n=8). CSM patient and control results are reported in Table 3.2. Pre-operatively, the FA and MD measurements were not statistically different between the CSM and control groups in any motor or sensory regions studied ($p>0.05$). There were also no significant

differences in FA or MD in any regions including the entire cerebrum following surgery ($p>0.05$) in CSM patients (Table 3.2).

Table 3.2: Average FA and MD (± standard error of the mean) data for the CSM patient and control groups in the specified regions of interest. (* indicates significant difference between groups or following surgery, $p<0.05$).

	Right Motor	**Left Motor**	**Right Sensory**	**Left Sensory**	**Entire Cerebrum**
Baseline FA					
CSM	0.40 ± 0.01	0.41 ± 0.01	0.31 ± 0.01	0.32 ± 0.01	0.43 ± 0.01
Controls	0.38 ± 0.02	0.39 ± 0.02	0.31 ± 0.01	0.32 ± 0.02	0.43 ± 0.01
Follow-up FA					
CSM	0.40 ± 0.004	0.41 ± 0.004	0.30 ± 0.01	0.32 ± 0.01	0.42 ± 0.01
Controls	0.39 ± 0.01	0.40 ± 0.01	0.29 ± 0.01	0.30 ± 0.02	0.41 ± 0.01
Baseline MD					
CSM	0.23 ± 0.01	0.23 ± 0.01	0.28 ± 0.01	0.27 ± 0.01	0.23 ± 0.01
Controls	0.24 ± 0.01	0.24 ± 0.01	0.27 ± 0.02	0.27 ± 0.02	0.23 ± 0.002
Follow-up MD					
CSM	0.23 ± 0.004	0.23 ± 0.004	0.29 ± 0.01	0.27 ± 0.01	0.23 ± 0.003
Controls	0.23 ± 0.001	0.23 ± 0.01	0.28 ± 0.01	0.28 ± 0.01	0.24 ± 0.003

CSM – cervical spondylotic myelopathy; FA – fractional anisotropy; MD – mean diffusivity

3.6 Discussion:

This study is the first to perform longitudinal MRS and DTI in the brain to determine whether metabolite concentrations and water diffusion characteristics in CSM patients are associated with

functional improvement following surgery. Six months following surgery, a decrease in NAA/Cr concentration was observed in the hand area of the primary motor cortex, despite a significant improvement in neurological function. There was no change detected in the water diffusion characteristics within the surrounding WM. Intact WM integrity with decreased NAA/Cr concentration suggests mitochondrial metabolic dysfunction rather than axonal damage occurs in the primary motor cortex. Therefore the functional improvement observed after six months may result from brain reorganization and recruitment of surrounding cortex as suggested by previous studies, rather than the reversal of cellular metabolic abnormalities.

The most striking finding in the current study was that NAA/Cr concentrations decreased in the motor cortex even though CSM patients experienced clinical recovery after surgery. NAA is an amino acid that is present at very high concentrations in the brain and has one of the strongest signals in the magnetic resonance spectrum at 2.02 ppm.[13,14] NAA is synthesized in the mitochondria of neurons, transported into the cytoplasm and then along the course of the axons.[14] Since it is found exclusively in neurons, it has become an important marker of neuronal density, integrity,[13,14] and mitochondrial dysfunction.[13] A decrease in NAA/Cr does not necessarily imply irreversible neuronal injury or death.[15] The results of the current study suggest that despite neurological recovery following surgical intervention a further decrease in NAA/Cr in the motor cortex also occurs. Metabolite levels did not recover as expected in concordance with reversible SCC and functional improvement.

Neuronal repair may occur by resolution of inflammation, remyelination and possibly cortical adaptation.[16] Duggal *et al.* has shown that the motor cortex recruits adjacent cortex in response to surgical intervention in SCC patients.[4] Dong *et al*. reported similar adaptations in sensorimotor

cortices that accompany clinical deterioration and a significant return of clinical function following surgery.[17] Freund *et al.* demonstrated increases in the BOLD response during a repetitive handgrip task, not only in the hand area, but also in the leg area of the primary motor cortex.[18] The primary motor cortex may have limited capacity for metabolic recovery and may provide functional recovery by brain reorganization as a compensatory mechanism. If this is the case, strategies to improve clinical outcomes should be targeted equally to the recruited adjacent cortex in addition to the recovery of the primary motor cortices.

The potential role of axonal injury in mediating decreased NAA/Cr concentration in the motor cortex following surgical intervention was evaluated by diffusion tensor imaging. Axonal integrity is one factor that can be inferred by FA and MD measurements.[19] An increase in FA suggests an increase in density, more coherent organization, or greater myelination of fibers;[12] while a decrease indicates Wallerian degeneration, local extracellular edema, smaller number of fibers, or axonal loss.[20,21] In contrast, MD is a measure of the ease of water movement and declines with increasing tissue barriers and increases in structural lesions, demyelination, and axonal loss.[22,23] The preservation of FA and MD values has been interpreted as protection or maintenance of axonal integrity.[24,25] Previous studies have demonstrated that retrograde Wallerian degeneration and the disruption of WM tracts, specifically the corticospinal tract, was less evident as the distance increased from the site of injury in the cervical spine.[26,27] Our DTI results suggest intact cortical connectivity with complete preservation of axonal integrity in the brain. Similar results were found in the setting of irreversible SCI where James *et al*. identified a population of axons that survived but remained chronically unable to function under normal

physiological conditions.[28] Our results suggest dysfunction of neuronal mitochondria in the motor cortex, and provide a potential target for future therapeutic interventions.

3.6.1 Limitations

Our study included stringent inclusion criteria, along with rigorous acquisition and post-processing methods to reduce data variance. We performed high magnetic field MRS at 3.0 T, which provides greater signal-to-noise ratio and greater spectral separation of multiplets that tend to overlap at lower field strength.[29,30] One limitation of our study was that spectra were acquired only from the contralateral motor cortex of the weaker side in CSM patients rather than on both sides as was performed in the control subjects. Spectroscopy data were only acquired from a single side in CSM patients due to time constraints as patients could not tolerate the long scan times (80-90 minutes) required to obtain spectroscopy data from both sides in addition to other imaging parameters. The pooling of spectroscopy data in the patient group from the side of the motor cortex with the greatest functional deficit as previously described[5,10] was an acceptable approach as lateralized spectroscopy measurements in the control group did not show metabolite level differences. Future studies would benefit from lateralized spectroscopy measurements in CSM patients to evaluate potential heterogeneity, and correlation of metabolite level changes in the cortex with findings on cervical MRI.

3.7 Conclusion:

NAA/Cr ratios were decreased in CSM patients 6 months following surgical intervention. Together with constant FA and MD values indicating maintenance of axonal integrity, the

decreases in NAA/Cr suggest neuronal mitochondrial impairment. Our findings of a clear neurological improvement in CSM patients following surgery support the hypothesis that neurological recovery may necessitate the recruitment of surrounding cortex, given that focal recovery in the motor cortex may be metabolically unattainable. Future studies will investigate the possible role for NAA as a predictive marker for clinical improvement during pre-operative screening.

3.8 References:

1. Kadanka Z, Bednarik J, Novotny O, Urbanek I, Dusek L. Cervical spondylotic myelopathy: conservative versus surgical treatment after 10 years. *Eur Spine J* 20(9):1533-1538, 2011.

2. Kadanka Z, Mares M, Bednanik J, *et al*. Approaches to spondylotic cervical myelopathy Conservative *versus* surgical results in a 3-year follow-up study. *Spine* 27(20):2205-2211, 2002.

3. Fehlings MG, Wilson JR, Kopjar B, *et al*. Efficacy and safety of surgical decompression in patients with cervical spondylotic myelopathy: Results of the AOSpine North America Prospective Multi-Center Study. *J Bone Joint Surg Am* 95(18):1651-1658, 2013.

4. Duggal N, Rabin D, Bartha R, *et al*. Brain reorganization in patients with spinal cord compression evaluated using fMRI. *Neurology* 74(13):1048-1054, 2010.

5. Kowalczyk I, Duggal N, Bartha R. Proton magnetic resonance spectroscopy of the motor cortex in cervical myelopathy. *Brain* 135(Pt2):461-468, 2012.

6. Youstry TA, Schmid UD, Alkadhi H, *et al*. Localization of the motor hand area to a knob on the precentral gyrus. A new landmark. *Brain* 120(Pt1):141-157, 1997.

7. Bartha R, Drost DJ, Williamson PC. Factors affecting the quantification of short echo in vivo 1H MR spectra: prior knowledge, peak elimination and filtering. *NMR Biomed* 12(4):205-216, 1999.

8. Bartha R, Drost DJ, Menon RS, Williamson PC. Spectroscopic lineshape correction by QUECC: combined QUALITY deconvolution and eddy current correction. *Magn Reson Med* 44(4):641-645, 2000.

9. Kassem MN, Bartha R. Quantitative proton short-echo time LASER spectroscopy of normal human white matter and hippocampus at 4 Tesla incorporating macromolecule subtraction. *Magn Reson Med* 49(5):918-927, 2003.

10. Puri BK, Smith HC, Cox IJ, *et al*. The human motor cortex after incomplete spinal cord injury: an investigation using proton magnetic resonance spectroscopy. *J Neurol Neurosurg Psychiatry* 65(5):748-754, 1998.

11. Holly LT, Freitas B, McArthur DL, Salamon N. Proton magnetic resonance spectroscopy to evaluate spinal cord axonal injury in cervical spondylotic myelopathy. *J Neurosurg Spine* 10(3):194-200, 2009.

12. Mori S, Zhang J. Principles of diffusion tensor imaging and its applications to basic neuroscience research. *Neuron* 51(5):527-539, 2006.

13. Bates TE, Strangward M, Keelan J, Davey GP, Munro PM, Clark JB. Inhibition of N-acetylaspartate production: implications for 1H MRS studies in vivo. *Neuroreport* 7(8):1397-1400, 1996.

14. Moffet JR, Ross B, Arun P, Madhavarao CN, Namboodiri AM. N-Acetylaspartate in the CNS: from neurodiagnostics to neurobiology. *Prog Neurobiol* 81(2):89-131, 2007.

15. De Stefano N, Matthers PM, Arnold DL. Reversible decreases in N-acetylaspartate after acute brain injury. *Magn Reson Med* 34(5):721-727, 1995.

16. van Horssen J, Witte ME, Ciccarelli O. The role of mitochondria in axonal degeneration and tissue repair in MS. *Mult Scler* 18(8):1058-1067, 2012.

17. Dong Y, Holly LT, Albistegui-Dubois R, *et al*. Compensatory cerebral adaptations before and evolving changes after surgical decompression in cervical spondylotic myelopathy. *J Neurosurg Spine* 9(6):538-551, 2008.

18. Freund P, Weiskopf N, Ward NS, *et al*. Disability, atrophy and cortical reorganization following spinal cord injury. *Brain* 134(Pt6):1610-1622, 2011.

19. Ciccarelli O, Toosy AT, De Stefano N, Wheeler-Kingshott CA, Miller DH, Thompson AJ. Assessing neuronal metabolism in vivo by modeling imaging measures. *J Neurosci* 30(45):15030-15033, 2010.

20. Budzik JF, Balbi V, Le Thuc V, Duhamel A, Assaker R, Cotten A. Diffusion tensor imaging and fibre tracking in cervical spondylotic myelopathy. *Eur Radiol* 21(2):426-433, 2011.

21. Beaulieu, C. The basis of anisotropic water diffusion in the nervous system – a technical review. *NMR Biomed* 15(7-8):435-455, 2002.

22. Basser PJ, Pierpaoli C. Microstructural and physiological features of tissues elucidated by quantitative-diffusion-tensor MRI. *J Magn Reson B* 111(3):209-219, 1996.

23. Pierpaoli C, Jezzard P, Basser PJ, Barnett A, Di Chiro G. Diffusion tensor MR imaging of the human brain. *Radiology* 201(3):637-648, 1996.

24. Song SK, Sun SW, Ramsbottom MJ, Chang C, Russell J, Cross AH. Dysmyelination revealed through MRI as increased radial (but unchanged axial) diffusion of water. *Neuroimage* 17(3):1429-1436, 2002.

25. Kang MM, Anderer EG, Elliott RE, *et al*. Diffusion tensor imaging of the spondylotic cervical spinal cord: a preliminary study of quantifiable markers in the evaluation for surgical decompression. *Internet J Head Neck Surg* 5(1):1-25, 2011.

26. Guleria S, Gupta RK, Saksena S, *et al*. Retrograde Wallerian degeneration of cranial corticospinal tracts in cervical spinal cord injury patients using diffusion tensor imaging. *J Neurosci Res* 86(10):2271-2280, 2008.

27. Roser F, Ebner FH, Maier G, Tatagiba M, Nagele T, Klose U. Fractional anisotropy levels derived from diffusion tensor imaging in cervical syringomyelia. *Neurosurgery* 67(4):901-905, 2010.

28. James ND, Bartus K, Grist J, Bennett D, McMahon SB, Bradbury EJ. Conduction failure following spinal cord injury: functional and anatomical changes from acute to chronic stages. *J Neurosci* 31(50):18543-18555, 2011.

29. Gonen O, Gruber S, Li BS, Mlynarik V, Moser E. Multivoxel 3D proton spectroscopy in the brain at 1.5 versus 3.0 T: signal-to-noise ratio and resolution comparison. *AJNR Am J Neuroradiol* 22(9):1727-1731, 2001.

30. Bartha R, Drost DJ, Menon RS, Williamson PC. Comparison of the quantification precision of human short echo time (1)H spectroscopy at 1.5 and 4.0 Tesla. *Magn Reson Med* 44(2):185-192, 2002.

CHAPTER 4:

MILD AND MODERATE CERVICAL SPONDYLOTIC MYELOPATHY: ARE THEY METABOLICALLY AND FUNCTIONALLY DIFFERENT?

State of Publication: **Aleksanderek I**, Stevens TK, Goncalves S, Bartha R, Duggal N. Mild and moderate cervical spondylotic myelopathy: Are they metabolically and functionally different? In preparation for submission.

4.1 Abstract:

The ideal timing of surgical intervention for CSM patients with early, mild symptoms, remains particularly controversial since select patients can stabilize clinically without operative intervention. Proton magnetic resonance spectroscopy (MRS) has demonstrated altered metabolite levels in the primary motor cortex of CSM patients suggesting mitochondrial impairment. In addition, functional MRI (fMRI) studies have demonstrated cortical reorganization in response to spinal cord compression and surgery. The goal of this study was to compare the recovery of neuronal metabolism and functional reorganization in the primary motor cortex between people with mild and moderate CSM following surgical intervention.

Twenty-eight CSM patients had two separate 3 Tesla MRI scans that included MRS and fMRI before and six months following surgery. The classification of CSM was based on neurological and functional disability measured using the modified Japanese Orthopaedic Association (mJOA) questionnaire. Specifically, mild CSM was defined by a mJOA score of >12 out of 18 (n=15) and moderate CSM by a score of 9-12 (n=13). Ten healthy controls underwent two MRI scans six months apart. Metabolite levels were measured in the motor cortex on the greater deficit side in the patients and on both sides in the control subjects. Motor function was assessed in patients and controls using a right finger-tapping paradigm. Significant differences in metabolite ratios and functional activation between the control, mild CSM, and moderate CSM groups at pre- and post-operative time points were identified. Paired t-test was used to detect the effects of surgery on the CSM group.

Mild CSM patients had a lower pre-operative *N*-acetylaspartate to creatine (NAA/Cr) ratio, suggesting mitochondrial dysfunction, compared to moderate CSM patients. Following surgery, NAA/Cr in the moderate CSM group decreased to the levels observed in the mild CSM group. The mild group had a larger functional volume of activation (VOA) in the primary motor cortex than moderate CSM group prior to surgery. Following surgery, the VOAs were comparable between the mild and moderate CSM groups and had shifted towards the primary sensory cortex.

NAA/Cr levels and the size of the VOA in the motor cortex can be used to discriminate between mild and moderate CSM. Following surgery, the metabolic profile of the motor cortex did not recover in either group, despite significant clinical improvement. We propose metabolic impairment in the motor cortex necessitates recruitment of healthy cortex to achieve functional recovery.

4.2 Key words:

cervical spondylotic myelopathy, functional MRI, magnetic resonance spectroscopy, *N*-Acetylaspartate, brain plasticity

4.3 Introduction:

The ideal timing of surgical intervention for patients with mild cervical spondylotic myelopathy (CSM) remains controversial. CSM occurs secondary to degenerative changes in the cervical spine resulting in compression of the spinal cord.[1-3] CSM can present abruptly with severe symptoms of neurological impairment or insidiously with a slow, stepwise deterioration.[1,4] Natural history studies have shown that these symptoms can improve, decline or stay stable with conservative treatment.[5,6] Surgical intervention is recommended for patients who fail to respond to conservative treatment and continue to deteriorate. However, the benefits of surgery in CSM patients with mild symptoms are controversial as some studies suggest that these patients can also stabilize if treated conservatively.[7-11] In contrast, recent reports suggest that surgery results in improved functional, disability-related, and quality-of-life outcomes at 1 year in symptomatic CSM, even when the disease was mild.[12]

Recent work by our group has demonstrated that CSM produces metabolic and functional changes in the brain.[13,14] Specifically, decreased *N*-acetylaspartate (NAA) to creatine (Cr) ratio was observed in the primary motor cortex of CSM patients suggesting mitochondrial impairment. Functional MRI studies have also demonstrated cortical reorganization in response to spinal cord compression and surgery.[14] This collective evidence reveals that the brain, distal to the site of injury, adapts and compensates for the compression of the cervical spinal cord.

Biomarkers must be developed to help optimize the selection of CSM patients for surgical treatment, particularly in cases of early stage, mild CSM, where it has been shown that a prolonged duration of symptoms may be associated with a poor surgical outcome.[15] Previous studies have not compared the patterns of injury and recovery in the motor cortex of mild and

moderate CSM patient populations. MRI changes within the spinal cord, including the presence of high-signal intensity changes on T_2-weighted images, do not reliably correlate with neurological function or predict post surgical outcomes.[9,16-19] Therefore, the goal of this longitudinal study was to compare the distinct metabolite and functional profiles in the primary motor cortex (M1) of mild and moderate CSM patients before and after decompressive surgery. We hypothesized that the reduction of NAA/Cr levels and functional impairment in M1 would be greater in moderate CSM compared to mild CSM, and the that moderate CSM would show the greatest change following surgery.

4.4 Methods:

4.4.1 Patient Population:

Twenty-eight patients with CSM were recruited. Each patient participated in two 3.0 Tesla MR imaging sessions, pre-operatively and 6 months following decompressive surgery. Ten healthy subjects with no history of neurological disorders were also recruited and underwent two MRI scans, six months apart. Participants were not excluded based on the use of any medications. Informed written consent was obtained and the study was approved by The University of Western Ontario Human Subjects Research Ethics Board. Each patient and control completed the disease specific modified Japanese Orthopaedic Association scale (mJOA) at each visit. The mJOA scale ranges from 0 to 18 points (with 18 representing the maximum score) and identifies upper and lower motor, upper sensory, and sphincter function.[20] Mild CSM (n=15) was defined as having a mJOA score of >12, while moderate CSM (n=13) patients presented with a mJOA score between 9 and 12 at the initial visit.[21] There were no severe CSM cases recruited in this study (mJOA <9).[21]

4.4.2 Anatomical Data Acquisition:

All MR data were acquired using a 3.0 T Siemens Magnetom Tim Trio MRI (Erlangen, Germany), using a twelve channel head coil with a neck and spine array. Each exam included the acquisition of sagittal T_1-weighted inversion prepared (TI = 900 ms) 3D-MPRAGE anatomical images (192 slices, 1 mm isotropic resolution, TR/TE = 2300/3.42 ms) that covered the entire brain and produced high gray matter/white matter contrast.

4.4.3 MRS Data Acquisition and Analysis:

Before imaging, an automated global shimming procedure using first- and second-order shims was performed to optimize the magnetic field over the imaging volume of interest. The hand area of the motor cortex was identified by the "knob" as described by Youstry *et al.* to guide the placement of a 20 mm isotropic voxel.[22] This "precentral knob" area is a reliable landmark that identifies the motor hand function in the precentral gyrus under normal and pathological conditions.[22] The voxel was placed on the motor cortex contralateral to the greater deficit side in the CSM patient group (n=12 on right side and n=16 on left side) while controls had a separate voxel placed on each side of the motor cortex.

Spectroscopic data were acquired using the Point-Resolved Spectroscopy (PRESS) acquisition sequence (TR/TE =2000/135 ms, suppressed: 192 averages; unsuppressed: 8 averages; voxel size = 8 cm^3) and post-processed by combined QUALITY deconvolution[23] to restore the Lorentzian lineshape and eddy current correction.[24-27] Following lineshape correction, any remaining unsuppressed water was removed from the spectrum using a Hankel singular value decomposition (HSVD) that required no prior knowledge. All unsuppressed water signal was

removed by subtracting resonances between 4.1 and 5.1 parts per million (ppm) (water ~4.7 ppm) as determined by the HSVD algorithm.[26]

A Levenberg-Marquardt minimization routine incorporating a template of prior knowledge of metabolite lineshapes was used to fit the resultant metabolite spectra in the time domain. The analysis software (fitMAN) is incorporated into a graphical user interface written in our laboratory in the IDL programming language (Version 5.4 Research Systems Inc, Boulder, CO, USA).[24] The acquisition of metabolite prior knowledge data has been previously described in detail.[25,26] The metabolites NAA, Cr, choline (Cho), myo-inositol (Myo), and Glutamine plus Glutamate (Glx) were examined based on previous studies that have implicated these metabolites in neurological disorders such as spinal cord injury (SCI) and CSM.[13,28,29] Ratios (NAA/Cr, Cho/Cr, Myo/Cr, and Glx/Cr) were calculated and compared between groups. Metabolite level ratios were measured relative to Cr because this removes the potential for tissue partial volume errors and may be more sensitive in detecting metabolite changes.

4.4.4 Functional MRI Data Acquisition and Analysis:

Each functional brain volume was acquired using an interleaved echo-planar imaging pulse sequence (parallel imaging iPAT=2, FOV = 240x240 mm, 80x80 acquisition matrix, 45 slices/volume, 3 mm isotropic resolution, TR/TE = 2500/30 ms, flip angle = 90^{o}).

The motor pathway was tested during fMRI by instructing the participants to perform finger to thumb opposition ("duck quack") in the right hand. Briefly, participants were instructed to press a button placed on their thumb simultaneously with all four fingers followed by an extension upwards to a box surrounding the button. The box ensured each participant lifted their fingers at

the same angle by touching the top of the box prior to the next tap. The movement rate of the repetitive task is known to affect cerebral activation,[30-32] therefore a standard block design was used in which participants received visual cues during alternating 30-second intervals of rest and activity. During the activity a visual cue instructed the participants to tap every 3 seconds for the 30-second interval. Participants received training prior to the fMRI session to reinforce the standardization and reduce learning effects during the imaging session.

Image analysis was completed using BrainVoyager QX (Brain Innovation B.V., Maastricht, The Netherlands, http://www.brainvoyager.com). Anatomic images were transformed to Talairach space for group analysis.[33] Preprocessing of functional images included 3D motion correction using trilinear/sinc interpolation where only data images with small motion-related effects (< 2 mm movement) were included. To improve signal-to-noise and reduce the effect of intersubject structural differences, spatial smoothing was performed by convolving each slice with a 6 mm FWHM Gaussian filter. Next, slice scan time correction and linear trend removal were completed. Functional data were then registered to the anatomical images in Talairach space and a 4D volume time course file was created for each subject.

A general linear model (GLM) and random-effects analysis (RFX) were used to create individual and group statistical parametric maps of brain activation and set to a threshold of $p<0.05$. A boxcar function coincident with the paradigm with a double-Gamma hemodynamic response function was used as a predictor of the fMRI response to the motor task. ANOVA tests were used to identify significant clusters of activation between groups at each time point (controls versus mild CSM versus moderate CSM). ANOVA tests were set to a threshold using a corrected value of $p<0.001$ for multiple comparisons using the False Discovery Rate (FDR). For all contrasts, a

VOA, corrected *p*-value, and Talairach coordinates of the center of gravity (COG) of the activation were examined. Talairach Daemon Client 2.0 (University of Texas Health Science Center, SAN Anotnio, TX) was used to convert the Talairach coordinates to their corresponding Brodmann areas.

4.4.5 Statistical Analysis:

All data are presented as the group mean followed by the standard error of the mean (SE). The mJOA scores were compared between mild and moderate groups using a two-tailed Student's t-test at both time points. The Student's t-test was also used to identify the significant differences in metabolite ratios between the controls, mild CSM, and moderate CSM groups at pre- and post-operative time points. Next, a paired t-test was used to detect the effects of surgery on the CSM group.

The Pearson Product Moment Correlation Coefficient (r) was used to determine whether metabolite ratios were correlated with clinical scores, and whether the change in metabolite ratios were correlated with the change in the clinical scores in each group. In this pilot study no corrections were made for multiple comparisons. The change in a parameter value was calculated by subtracting the pre-operative value from the post-operative value. All statistical tests were two-sided, with significance set at an alpha level of 0.05.

4.5 RESULTS:

4.5.1 Clinical Data:

We recruited fifteen mild CSM patients with a mean age of 50.1 (± 3 years; 13 males) and thirteen moderate CSM patients with a mean age of 53.0 (± 2 years; 8 males). Ten healthy

controls of similar age were recruited (48 ± 4 years, 5 males). The average follow-up times were 188 ± 16 days, 201 ± 18 days and 176 ± 15 days for the mild CSM, moderate CSM, and controls, respectively. The three groups did not differ with respect to age, sex or follow-up time (Table 1). The mild and moderate CSM groups did not differ in their duration of self-reported symptoms or the presence of signal change at the site of compression on T_2-weighted images (Table 1).

Table 4.1: Demographic and clinical data for the CSM patient group and healthy controls (mean ± SE).

Subject	Mild CSM	Moderate CSM	Controls
N	15	13	10
Age (years)	50.1 ± 3	53.0 ± 2	48 ± 4
Sex (Male/Female)	13M/2F	8M/5F	5M/5F
Hand Dominance (Right/Left)	13R/2L	13R/0L	10R/0L
Duration of symptoms (months)	7.9 ± 2.1	8.6 ± 1.5	--
Signal change on T_2-weighted image at site of compression	14/15	10/13	
Surgery			
1 level	12 (80%)	7 (54%)	--
2 level	3 (20%)	6 (46%)	--
Follow-up time (days)			
Surgery (CSM) or baseline (controls) and 6 month scan	188 ± 16	201 ± 18	176 ± 15
mJOA Score			
Pre-op	15.1 ± 0.3	10.6 ± 0.1	18 ± 0
Post-op	16.3 ± 0.3	15.4 ± 0.5	18 ± 0

CSM – cervical spondylotic myelopathy; mJOA – modified Japanese Orthopaedic Association

In the 6 months following surgery, the mJOA scores increased for all CSM patients except one who had a decrease of 1 point. Mild CSM patients with an average pre-operative mJOA score of 15.1 ± 0.3 improved to 16.3 ± 0.3 post-operatively ($p=0.002$). The moderate CSM group increased their average mJOA scores from 10.6 ± 0.4 pre-operatively to 15.4 ± 0.5 post-operatively ($p<0.0001$). The mild and moderate CSM groups were significantly different pre-operatively ($p<0.0001$) but recovered to the same post-operative score ($p=0.14$) (Figure 1). All controls recorded a perfect mJOA score of 18 at both visits.

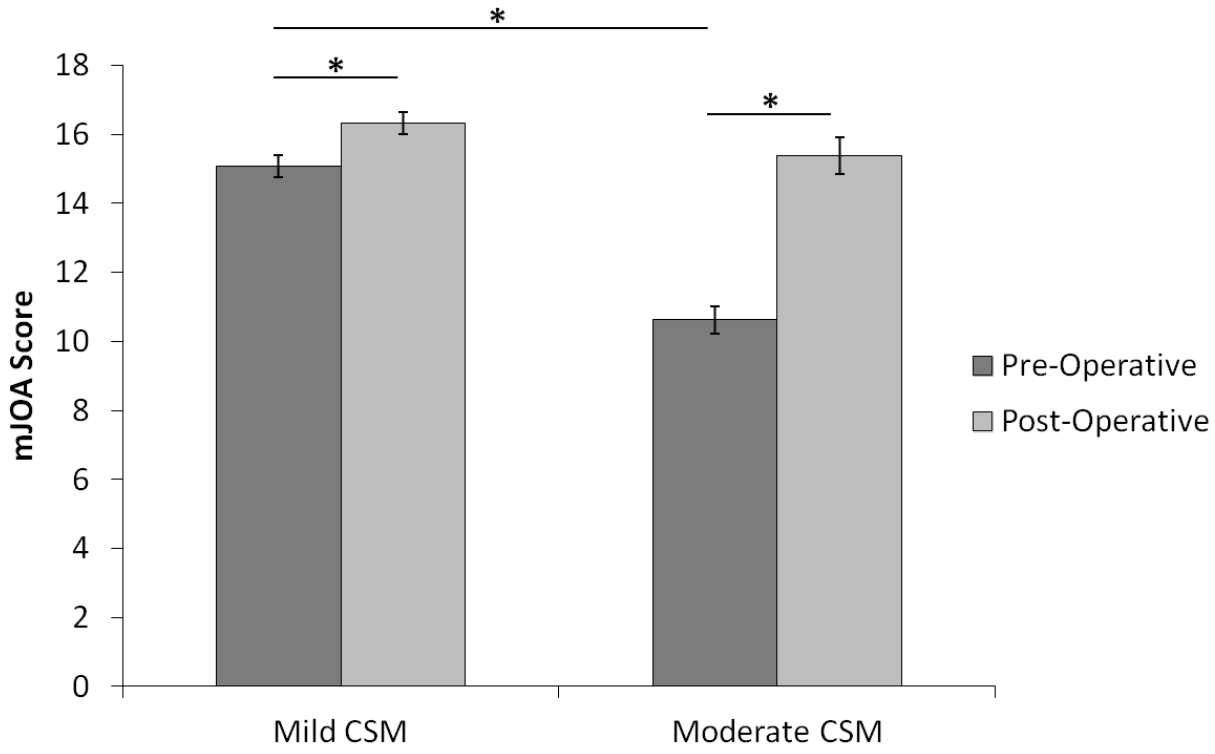

Figure 4.1: Mean pre- and post-operative mJOA questionnaire scores for the mild and moderate CSM patient groups. A perfect score of 18 represents no dysfunction. (Error bars represent the SE, * represents significance $p<0.05$).

4.5.2 Control Metabolic Profile:

The control group presented with no changes in any of the metabolite ratios over time: NAA/Cr (baseline 1.91 ± 0.04, follow-up 1.90 ± 0.07; p=0.89), Cho/Cr (baseline 0.31 ± 0.01, follow-up 0.32 ± 0.01; p=0.66), Myo/Cr (baseline 0.30 ± 0.01, follow-up 0.29 ± 0.02; p=0.79), and Glx/Cr (baseline 0.59 ± 0.02, follow-up 0.62 ± 0.04; p=0.58).

4.5.3 Mild CSM Metabolic Profile:

The pre-operative NAA/Cr ratio of 1.55 ± 0.13 did not change following surgery (1.44 ± 0.09; p=0.50), but was significantly decreased compared to the controls at pre (p=0.02) and post-operative (p=0.0004) time points (Figure 2). The pre-operative Cho/Cr ratio of 0.27 ± 0.01 did not change following surgery (0.27 ± 0.01; p=0.97), but was significantly decreased compared to the controls at pre (p=0.01) and post-operative (p=0.03) time points (Figure 3). Mild CSM has a pre-operative Myo/Cr ratio of 0.35 ± 0.03 which significantly dropped following surgery to 0.23 ± 0.03 (p=0.006, Figure 4). The post-operative Myo/Cr was significantly lower in mild CSM compared to controls (p=0.049, Figure 4). The remaining ratio of Glx/Cr did not change six months post-operatively and was not different from control values.

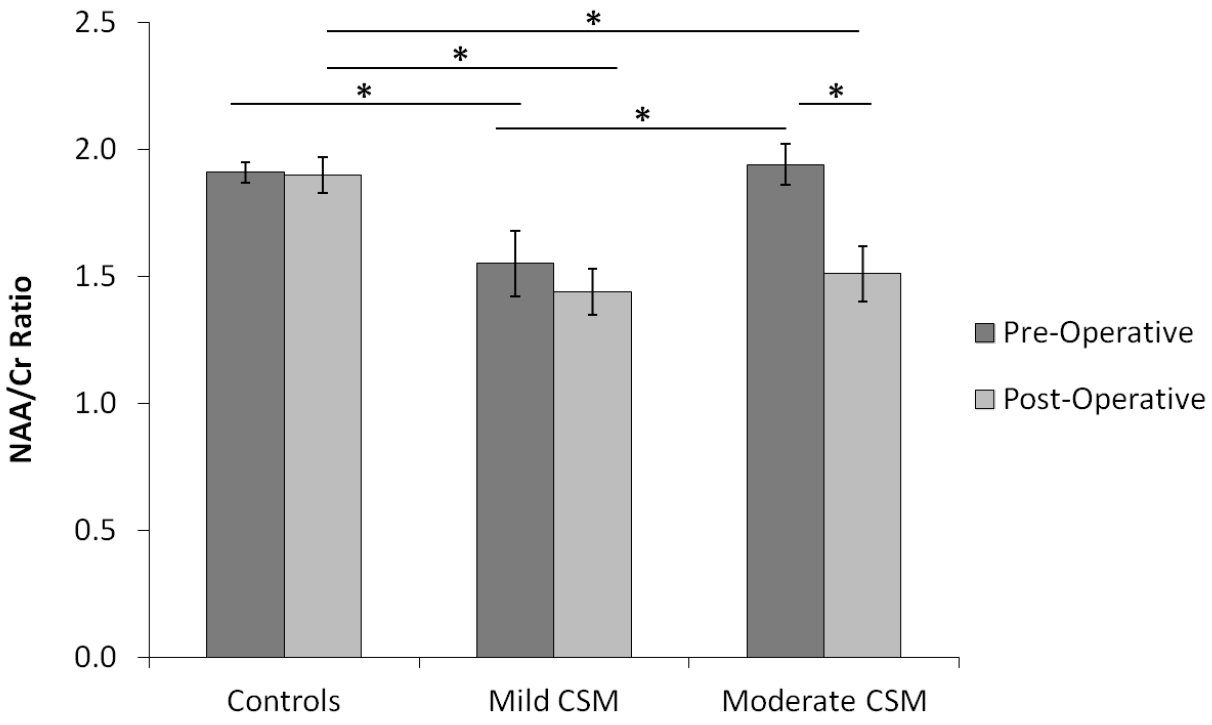

Figure 4.2: Average NAA/Cr metabolite concentrations in the controls at baseline and 6-month follow-up, and mild CSM, and moderate CSM groups prior to and following surgery (error bars represent the SE; * represents significance $p<0.05$).

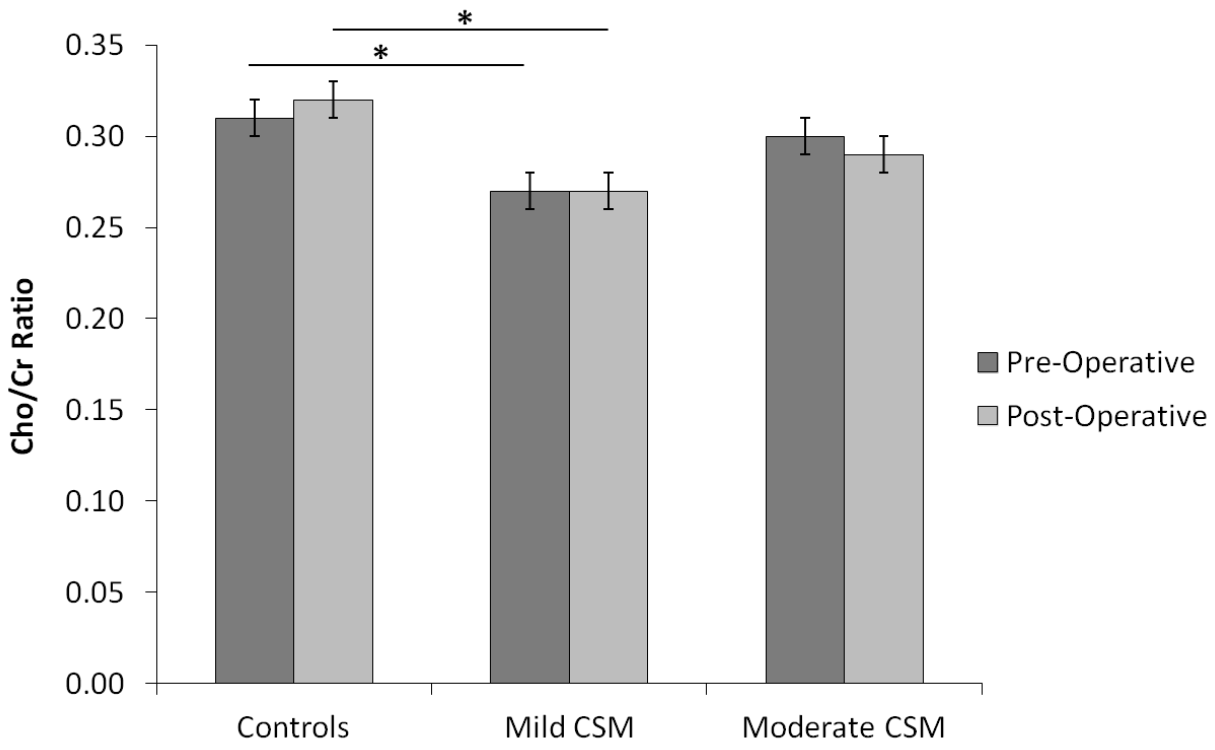

Figure 4.3: Average Cho/Cr metabolite concentrations in the controls at baseline and 6-month follow-up, and mild CSM, and moderate CSM groups prior to and following surgery (error bars represent the SE; * represents significance $p<0.05$).

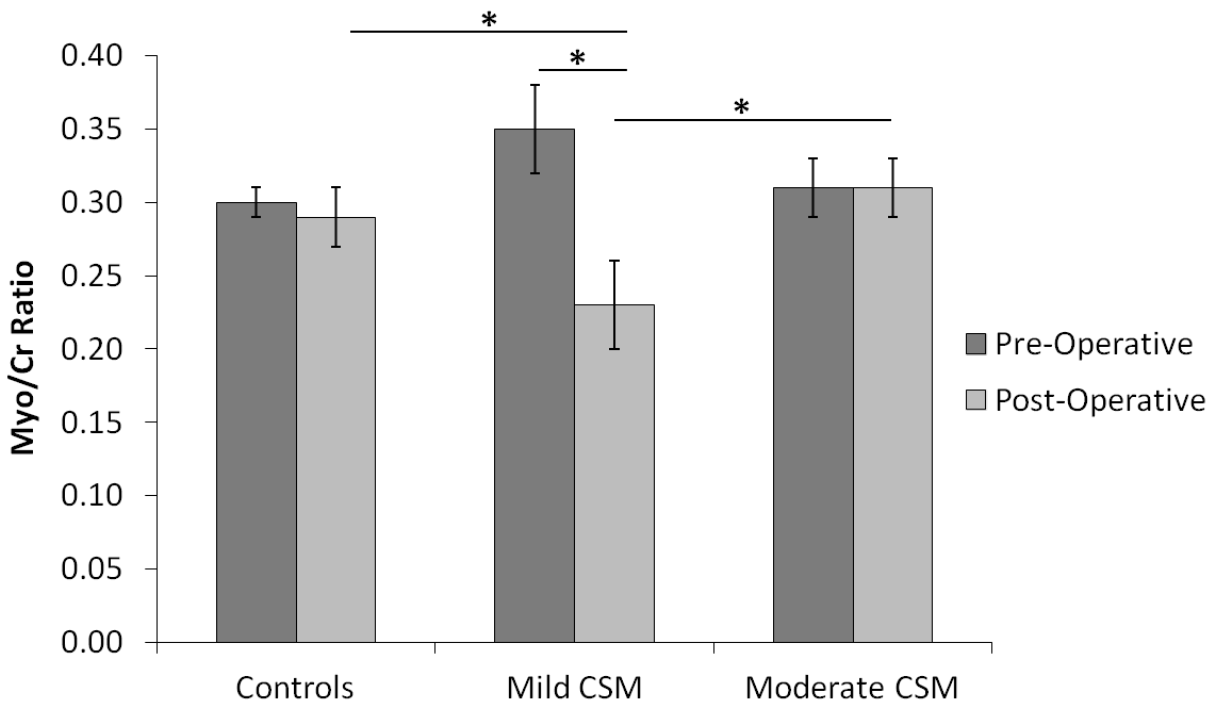

Figure 4.4: Average Myo/Cr metabolite concentrations in the controls at baseline and 6-month follow-up, and mild CSM, and moderate CSM groups prior to and following surgery (error bars represent the SE; * represents significance $p<0.05$).

4.5.4 Moderate CSM Metabolic Profile:

Moderate CSM patients presented with a pre-operative NAA/Cr ratio of 1.94 ± 0.08 which significantly decreased to 1.51 ± 0.11 ($p=0.03$) post-operatively (Figure 2). The post-operative NAA/Cr was significantly lower in moderate CSM compared to controls ($p=0.01$, Figure 2). The remaining ratios of Cho/Cr, Myo/Cr and Glx/Cr did not change six months post-operatively and were not significantly different from the control values (Figures 3 and 4).

4.5.5 Mild CSM versus Moderate CSM:

There are two important distinctions between mild and moderate CSM patients. First, mild CSM

presented with a much lower pre-operative NAA/Cr ratio compared to moderate CSM (p=0.02, Figure 2). Following surgery, the NAA/Cr ratio in moderate CSM decreased such that the mild and moderate CSM patients had a similar NAA/Cr ratio (Figure 2). Second, mild and moderate CSM had a similar pre-operative Myo/Cr ratio. Post-operatively, the Myo/Cr ratio significantly decreased in the mild group and became lower than that observed in moderate CSM (p=0.02), and in controls (Figure 4).

4.5.6 Metabolite Ratio Correlations to Clinical Function:

There were no significant correlations between any metabolite ratios and clinical questionnaires in mild and moderate CSM.

4.5.7 Motor Function Assessed by fMRI:

Pre-operatively, mild CSM patients had a larger VOA (Figure 5) compared to moderate CSM (p=0.05; min cluster size=118; COG (27, -42, 58), left parietal lobe, postcentral gyrus, BA 5). Following surgery, the VOAs centered around BA 3 in mild and moderate CSM did not differ significantly (mild CSM: FDR<0.001; p<0.000014; COG (38, -30, 53); left parietal lobe, postcentral gyrus, BA 3 and moderate CSM: FDR<0.001; p<0.000006; COG (37, -28, 54); left parietal lobe, postcentral gyrus, BA 3). There was an increase in the VOA in moderate CSM following surgery using an uncorrected p-value, however the change did not reach the threshold for significance after FDR correction (Figure 5). The controls did not significantly differ between the two visits in the VOA and location (p>0.05).

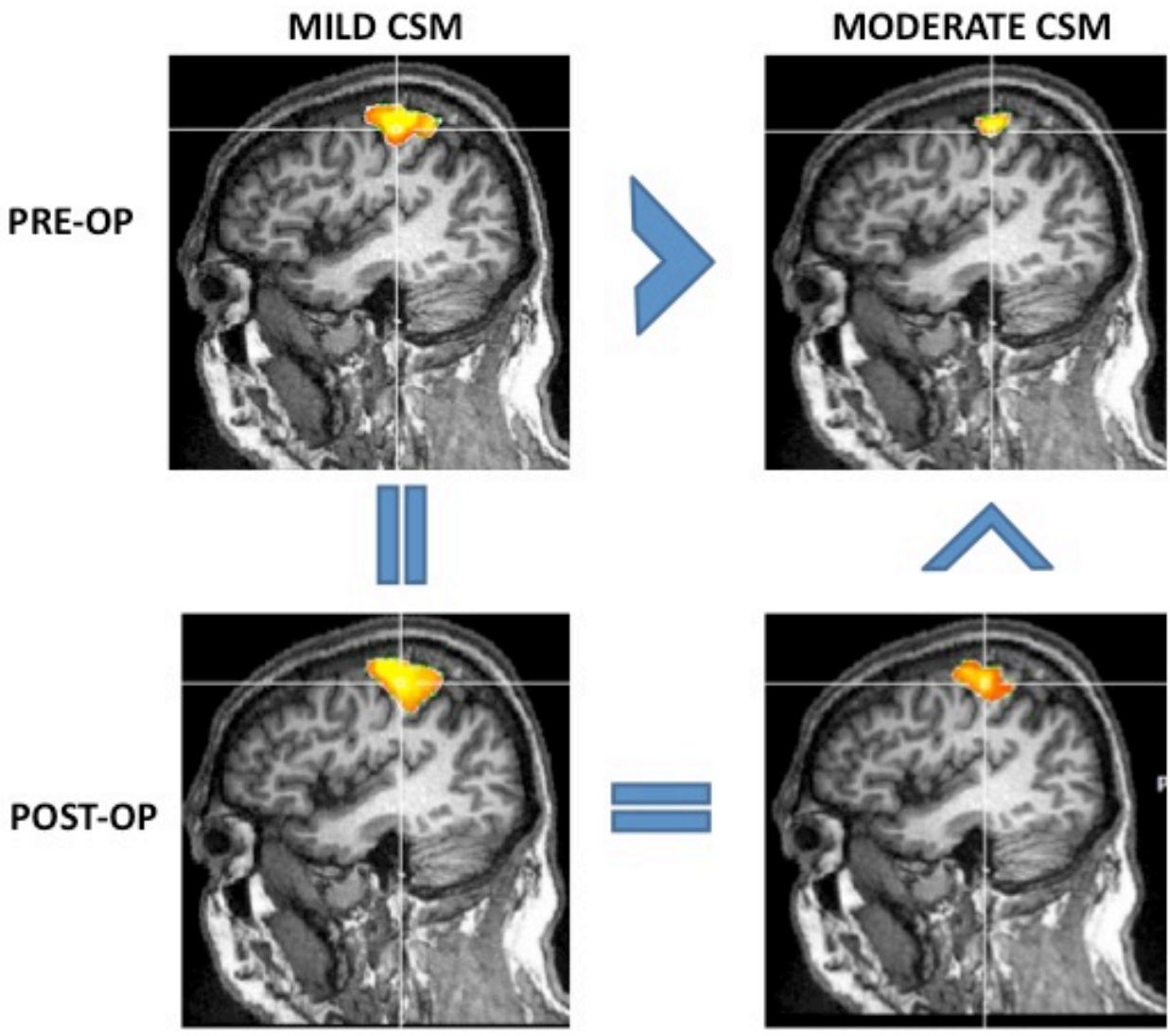

Figure 4.5: The corrected volume of activation for the mild CSM (left) and the moderate CSM (right) patients groups are shown. The pre-operative activation is displayed in the top row showing the mild CSM group had significantly larger activation near the primary motor cortex compared to the moderate CSM group. Following surgery, both groups had equal activation volume shifted towards BA 3, the primary somatosensory cortex. The moderate CSM patients showed an increase in the VOA after surgery using an uncorrected p-value, however this increase did not remain significant following FDR correction.

4.6 Discussion:

The overall goal of this study was to compare and contrast the effects of mild and moderate CSM on the neuronal metabolism and functional activity of M1. The need for surgical intervention for patients with clinical evidence of mild CSM has become increasingly controversial. Our findings demonstrated a lower NAA/Cr ratio in the hand area of M1 in mild CSM patients compared to healthy controls and moderate CSM patients. Following successful surgery and despite clinical improvement, NAA/Cr levels did not recover in mild CSM. The moderate CSM patients, which had significantly worse pre-operative mJOA scores and demonstrated the largest interval improvement following surgery, demonstrated a *decline* in NAA/Cr levels following surgery.

In conjunction with evaluation of tissue metabolism, functional MRI was used to evaluate motor cortex function prior to and following surgery. Prior to surgery, in the setting of low NAA/Cr levels in the mild CSM group, but normal NAA/Cr levels in the moderate CSM group, we found a larger VOA within the sensorimotor cortex of mild CSM compared to moderate CSM. Consistent with a previous study showing greater M1 activation in CSM patients compared to controls,[14] our fMRI findings suggest that the mild CSM group has recruited surrounding cortex to enhance motor task performance prior to surgery. In the moderate CSM group following surgery, functional improvement was accompanied by decreased NAA/Cr while the fMRI measured VOA equalized to that observed in the mild CSM group. These distinct patterns of remote injury of the sensorimotor cortex in mild and moderate CSM patients could underlie the natural history of the disease and be used to determine the timing and need for intervention. These results also suggest that therapies designed to enhance brain plasticity could provide functional benefits to CSM patients both prior to and following surgery.[34-37]

This study is the first to describe a clear distinction between mild and moderate CSM with respect to pre-operative NAA/Cr concentrations in the motor cortex. NAA has one of the highest concentrations of all free amino acids in the brain and is found primarily in the neurons of the central nervous system.[38,39] It is considered to be a marker of neuronal density and/or viability.[40,41] Reduced levels of NAA/Cr imply neuronal loss or metabolic impairment in the neuronal mitochondria.[39] We previously reported decreased NAA/Cr levels in the motor cortex of CSM patients compared to healthy controls.[13] Holly *et al.* also found a decreased NAA/Cr ratio at the C2 level of the spinal cord in CSM patients suggesting axonal or neuronal loss.[29] In the current study, the measured NAA/Cr levels were lower in mild CSM compared to moderate CSM, suggesting that metabolic impairment in the neuronal mitochondria may be a feature associated with mild functional impairment. Previous work has shown that decreased mitochondrial function can lead to synaptic dysfunction[42-44] that may in turn trigger cortical reorganization and recruitment of healthy regions in the primary sensory cortex (S1).[44] This process could explain why neurological function was better preserved in the mild CSM group at baseline; these patients were able to recruit adjacent cortex as indicated by a larger VOA at baseline compared to the moderate CSM patients. This result is also consistent with a previous study that found that patients with SCC had an increased VOA within the motor cortex in comparison to controls.[14] In contrast, the moderate CSM group, which had normal NAA/Cr levels, but profound neurological deficits pre-operatively, demonstrated small VOAs. This evidence suggests that the moderate CSM group had a limited compensatory ability for reorganization, accounting for the poor neurological scores prior to surgery.

Following surgery, both the mild and moderate CSM patients demonstrated interval functional improvement. However, a larger improvement was observed in moderate CSM, where six

months following surgery, both groups had a mJOA score reflecting mild neurological disability. Surgical intervention did not reverse the low NAA/Cr levels in the mild CSM group, nor did it preserve the normal levels of NAA/Cr in the moderate CSM group. Interestingly, the Myo/Cr ratio decreased significantly in the mild CSM group following surgery suggesting reduced glial activity, altered glial metabolism, or a loss of astrocytes.[45] Decreased Myo/Cr levels have previously been associated with decreased gliosis in major depression.[46-48] The Cho/Cr ratio remained low in mild CSM compared to controls following surgery suggesting continued abnormal membrane metabolism.[49]

In light of the low NAA/Cr ratio in mild CSM and the decrease in the NAA/Cr ratio observed in moderate CSM six months after surgery, adaptive plasticity in response to mitochondrial and synaptic dysfunction is a possible explanation for the observed neurological recovery. The observed increase in the VOA in moderate CSM (prior to FDR correction) is consistent with this notion. Prior studies have also shown that neurological recovery following surgical decompression is associated with cortical reorganization.[14,34,35] Specifically, surgery for spinal cord compression resulted in cortical reorganization that was accompanied by a significant return of clinical function.[14] Dong *et al*. also demonstrated altered sensorimotor recruitment patterns during wrist and finger movements in eight CSM patients that gained motor function following spinal decompression and recruitment maps similar to that of healthy controls.[35] Similarly, Holly *et al*. reported that CSM patients undergo expanded cortical representation for the affected extremity following surgical decompression.[34] The exact mechanism by which cortical reorganization occurs is not completely understood, but it has been suggested that it may occur by modification of pre-existing connections and/or the development of new circuitry intended to preserve neurological functioning.[34] Stroke patients have also presented with spontaneous

recovery that occurs due to cortical plasticity with the best recovery resulting from reorganization in the damaged hemisphere.[36,50-51] In the current study, one possible explanation for the posterior shift in activation is that the corticospinal axons originating in S1 are preserved since they are less vulnerable to injury than the axons originating in M1. This advantage exists because the S1 fibres run more medial and posterior in the spinal cord.[35,52] Future studies should include metabolite level measurements in both the M1 and S1 cortices to evaluate potential changes in NAA due to the reorganization.

4.7 Conclusion:

CSM is a unique condition of reversible spinal cord injury that can be exploited to understand the link between brain metabolic dysfunction and synaptic activity and remodelling. The current study found distinct metabolic and functional profiles in the motor cortex that discriminate between mild and moderate CSM patients prior to surgery. Following surgery, the NAA/Cr ratio in the motor cortex decreased significantly in moderate CSM but was accompanied by neurological improvement and a brain activation volume that equalled that observed in mild CSM patients. We propose mitochondrial dysfunction, indicated by low levels of NAA/Cr, is the primary trigger for cortical reorganization and recruitment leading to functional improvement.

4.8 References:

1. Fehlings MG, Skaf G. A review of the pathophysiology of cervical spondylotic myelopathy with insights for potential novel mechanisms drawn from traumatic spinal cord injury. *Spine* 23(24):2730-2737, 1998.

2. Ono K, Ota H, Tada K, Yamamoto T. Cervical myelopathy secondary to multiple spondylotic protrusions: A clinicopathologic study. *Spine* 2(2):109-125, 1977.

3. Ogino H, Tada K, Okada K, *et al*. Canal diameter, anterior posterior compression ratio, and spondylotic myelopathy of the cervical spine. *Spine* 8(1):1-15, 1983.

4. La Rocca H. Cervical spondylotic myelopathy: Natural history. *Spine* 13:854-855, 1988.

5. Clarke E, Robinson PK. Cervical myelopathy: A complication of cervical spondylosis. *Brain* 79(Pt 3):483-510, 1956.

6. Epstein JA, Carras R, Epstein BS, Levine LS. Myelopathy in cervical spondylosis with vertebral subluxation and hyperlordosis. *J Neurosurg* 32(4),:421-426, 1970.

7. Kadanka Z, Mares M, Bednanik J, *et al*. Approaches to spondylotic cervical myelopathy: Conservative versus surgical results in a 3-year follow-up study. *Spine* 27(20):2205-2211, 2002.

8. Kadanka Z, Bednanik J, Novotny O, Urbanek I, Dusek L. Cervical spondylotic myelopathy: Conservative versus surgical treatment after 10 years. *Eur Spine J* 20(9):1533-1538, 2011.

9. Oshima Y, Seichi A, Takeshita K, *et al*. Natural course and prognostic factors in patients with mild cervical spondylotic myelopathy with increased signal intensity on T2-weighted magnetic resonance imaging. *Spine* 37(22):1909-1913, 2012.

10. Epstein JA, Janin Y, Carras R, Lavine LS. A comparative study of the treatement of cervical spondylotic myeloradiculopathy: Experience with 50 cases treated by means of extensive laminectomy, foraminotomy, and excision of osteophytes during the past 10 years. *Acta Neurochir* 61(1-3):89-104, 1982.

11. Sampath P, Bendebba M, Davis JD, Ducker TB. Outcome of patients treated for cervical myelopathy: A prospective, multicenter study with independent clinical review. *Spine* 25(6):670-676, 2000.

12. Fehlings MG, Wilson JR, Kopjar B, *et al*. Efficacy and safety of surgical decompression in patients with cervical spondylotic myelopathy: Results of the AOSpine North America Prospective Multi-Center Study. *J Bone Joint Surg Am* 95(18):1651-1658, 2013.

13. Kowalczyk I, Duggal N, Bartha R. Proton magnetic resonance spectroscopy of the motor cortex in cervical myelopathy. *Brain* 135(Pt 2):461-468, 2012.

14. Duggal N, Rabin D, Bartha R, *et al*. Brain reorganization in patients with spinal cord compression evaluated using fMRI. *Neurology* 74(13):1048-1054, 2010.

15. Holly LT, Matz PG, Anderson PA, *et al*. Clinical prognostic indicators of surgical outcome in cervical spondylotic myelopathy. *J Neurosurg Spine* 11(2):112-118, 2009.

16. Li FN, Li ZH, Huang X, *et al*. The treatment of mild cervical spondylotic myelopathy with increased signal intensity on T2-weighted magnetic resonance imaging. *Spinal Cord* 52(5):348-353, 2014.

17. Bucciero A, Vizioli L, Tedeschi G. Cord diameters and their significance in prognostication and decisions about management of cervical spondylotic myelopathy. *J Neurosurg Sci* 37(4):223-228, 1993.

18. Morio Y, Yamamoto K, Kuranobu K, Murata M, Tuda K. Does increased signal intensity of the spinal cord on MR images due to cervical myelopathy predict prognosis? *Arch Orthop Trauma Surg* 113(5):254-259, 1994.

19. Naderi S Ozgen S, Pamir MN, Ozek MM, Erzen C. Cervical spondylotic myelopathy: Surgical results and factors affecting prognosis. *Neurosurgery* 43(1):43-49, 1998.

20. Benzel EC, Lancon, J, Kesterson L, Hadden T. Cervical laminectomy and dentate ligament section for cervical spondylotic myelopathy. *J Spinal Disord* 4(3):286-295, 1991.

21. Revanappa KK, Rajshekhar V. Comparison of Nurick grading system and modified Japanese Orthopaedic Association scoring system in evaluation of patients with cervical spondylotic myelopathy. *Eur Spine J* 20(9):1545-1551, 2011.

22. Youstry TA, Schmid UD, Alkadhi H, *et al*. Localization of the motor hand area to a knob on the precentral gyrus: A new landmark. *Brain* 120(Pt 1):141-157, 1997.

23. de Graaf AA, van Dijk JE, Bovee WM. QUALITY: quantification improvement by converting lineshapes to the Lorentzian type. *Magn Reson Med* 13(3):343-357, 1990.

24. Bartha R, Drost DJ, Menon RS, Williamson PC. Spectroscopic lineshape correction by QUECC: combined QUALITY deconvolution and eddy current correction. *Magn Reson Med* 44(4):641-645, 2000.

25. Bartha R, Drost DJ, Williamson PC. Factors affecting the quantification of short echo in vivo 1H MR spectra: prior knowledge, peak elimination and filtering. *NMR Biomed* 12(4):205-216, 1999.

26. Kassem MN, Bartha R. Quantitative proton short-echo time LASER spectroscopy of normal human white matter and hippocampus at 4 Tesla incorporating macromolecule subtraction. *Magn Reson Med* 49(5):918-927, 2003.

27. Klose U. In vivo proton spectroscopy in presence of eddy currents. *Magn Reson Med* 14(1):26-30, 1990.

28. Puri BK, Smith HC, Cox IJ, *et al*. The human motor cortex after incomplete spinal cord injury: an investigation using proton magnetic resonance spectroscopy. *J Neurol Neurosurg Psychiatry* 65(5):748-754, 1998.

29. Holly LT, Freitas B, McArthur DL, Salamon N. Proton magnetic resonance spectroscopy to evaluate spinal cord axonal injury in cervical spondylotic myelopathy. *J Neurosurg Spine* 10(3):194-200, 2009.

30. Blinkenberg M, Bonde C, Holm S, *et al*. Rate dependence of regional cerebral activation during performance of a repetitive motor task: A PET study. *J Cereb Blood Flow Metab* 16(5):794-803, 1996.

31. Rao SM, Bandettini PA, Binder JR, *et al*. Relationship between finger movement rate and functional magnetic resonance signal change in human primary motor cortex. *J Cereb Blood Flow Metab* 16(6):1250-1254, 1996.

32. Schlaug G, Sanes JN, Thangaraj V, *et al*. Cerebral activation covaries with movement rate. *Neuroreport* 7(4):879-883, 1996.

33. Talairach J, Tournoux P. Co-Planar Stereotactic Atlas of the Human Brain. New York: Thieme Medical Publishers, Inc., 1998.

34. Holly LT, Dong Y, Albistegui-DuBois R, Marehbian J, Dobkin B. Cortical reorganization in patients with cervical spondylotic myelopathy. *J Neurosurg Spine* 6(6):544-551, 2007.

35. Dong Y, Holly LT, Albistegui-Dubois R, *et al*. Compensatory cerebral adaptations before and evolving changes after surgical decompression in cervical spondylotic myelopathy. *J Neurosurg Spine* 9(6):538-551, 2008.

36. Cramer SC, Nelles G, Benson RR, *et* al. A functional MRI study of subjects recovered from hemiparetic stroke. *Stroke* 28(12):2518–2527, 1997.

37. Weiller C, Chollet F, Friston KJ, Wise RJ, Frackowiak RS. Functional reorganization of the brain in recovery from striatocapsular infarction in man. *Ann Neurol* 31:463-472, 1992.

38. Bates TE, Strangward M, Keelan J, Davey GP, Munro PMG, Clark JB. Inhibition of N-acetylaspartate production: Implications for 1H MRS studies in vivo. *Neuroreport* 7(8):1397-1400, 1996.

39. Moffet JR, Ross B, Arun P, Madhavarao CN, Namboodiri AM. N-Acetylaspartate in the CNS: from neurodiagnostics to neurobiology. *Prog Neurobiol* 81(2):89-131, 2007.

40. De Stefano N, Matthers PM, Arnold DL. Reversible decreases in N-acetylaspartate after acute brain injury. *Magn Reson Med* 34(5):721-727, 1995

41. Geurts JJ, van Horssen J. The brake on neurodegeneration: Increased mitochondrial metabolism in the injured MS spinal cord. *Neurology* 74:710-711, 2010.

42. Ly CV, Verstreken P. Mitochondria at the synapse. *Neuroscientist* 12(4):291-299, 2006.

43. Tong JJ. Mitochondrial delivery is essential for synaptic potentiation. *Biol Bull* 212(2):169-175, 2007.

44. Mattson MP. Mitochondrial regulation of neuronal plasticity. *Neurochem Res* 32(4-5):707-715, 2007.

45. Myer DJ, Gurkoff GG, Lee SM, Hovda SM, Sofroniew MW. Essential protective roles of reactive astrocytes in traumatic brain injury. *Brain* 126(Pt 10):2761-2772, 2006.

46. Si X, Miguel-Hidalgo JJ, O'Dwyer G, Stockmeier CA, Rajkowska G. Age-dependent reductions in the level of glial fibrillary acidic protein in the prefrontal cortex in major depression. *Neuropsychopharmacology* 29(11):2088-2096, 2004.

47. Rajkowska G. Cell pathology in mood disorders. *Semin Clin Neuropsychiatry* 7(4):281-292, 2002.

48. Gruber S, Frey R, Mlynarik V, *et al.* Quantification of metabolic differences in the frontal brain of depressive patients and controls obtained by 1H-MRS at 3 Tesla. *Invest Radiol* 38(7):403-408, 2003.

49. Garnett MR, Blamire AM, Corkill RG, Cadoux-Hudson TAD, Rajagopalan B, Styles P. Early proton magnetic resonance spectroscopy in normal-appearing brain correlates with outcome in patients following traumatic brain injury. *Brain* 123(Pt 10):2046-2054, 2000.

50. Honda M, Nagamine T, Fukuyama H, Yonekura Y, Kimura J, Shibasaki H. Movement-related cortical potentials and regional cerebral blood flow change in patients with stroke after motor recovery. *J Neurol Sci* 146(2):117-126, 1997.

51. Cohen LG, Roth BJ, Wassermann EM, *et al*. Magnetic stimulation of the human cerebral cortex, an indicator of reorganization in motor pathways in certain pathological conditions. *J Clin Neurophysiol* 8(1):56-65, 1991.

52. Green JB, Sora E, Bialy Y, Ricamato A, Thatcher RW. Cortical motor representation after paraplegia: an EEG study. *Neurology* 53(4):736-743, 1999.

CHAPTER 5:

GENERAL DISCUSSIONS, LIMITATIONS, FUTURE DIRECTIONS AND CONCLUSIONS

5.1 General Discussions

CSM is a devastating disorder resulting in a wide array of symptoms ranging from mild, numbness or subtle problems with dexterity, to severe, such as quadraparesis and incontinence. The pathways mediating the efferent and afferent flow of communication between the brain and spinal cord are disrupted and alterations within the neural circuits may occur. A large amount of current research has concentrated on the local changes occurring in the spinal cord. This thesis provides new knowledge of advanced non-invasive MRI techniques used to explore the functional, metabolic, and structural changes of the primary motor cortex changes of CSM patients in the context of injury and recovery.

Chapter 2 describes the result of the first study to measure metabolite concentrations in the primary motor cortex of CSM patients. The following clinical and metabolic profile was established: CSM patients had decreased neurological function, and decreased NAA/Cr concentration in the primary motor cortex compared to healthy controls. This study concluded that CSM patients undergo pathophysiological changes in the cortex, remote to the site of injury, and that MRS is a sensitive technique that can detect these alterations. Furthermore, the NAA/Cr decreases suggested neuronal damage or dysfunction, and proposes the use of NAA as a future biomarker.

Chapter 3 details the first longitudinal study that used MRS and DTI to investigate the metabolic alterations and fibre tract integrity involved in injury and recovery in CSM patient population undergoing decompressive surgery. In previous studies, our group has utilized fMRI to demonstrate cortical reorganization in SCC patients prior to and following surgical decompression. To understand why recruitment of adjacent cortex was necessary post surgery in

the setting of clinical improvement, MRS and DTI were utilized to measure the potential for remote changes in the metabolite concentrations and WM integrity of the brain. The most striking finding is that NAA/Cr concentrations decreased in the motor cortex in the context of clinical recovery after surgery, suggesting metabolic dysfunction persists following surgery. The intact WM integrity with decreased NAA/Cr concentration suggests mitochondrial metabolic dysfunction rather than axonal damage occurs in the primary motor cortex. This study provided crucial information that the brain does not metabolically recover following successful surgery. The neurological recovery may be attributed to brain reorganization and recruitment of surrounding cortex, rather than the reversal of cellular metabolic abnormalities.

Chapter 4 characterizes the use of MRS and fMRI to create objective biomarkers that will help stratify CSM patients along a spectrum of injury severity and recovery. The following distinct profiles were established: In mild CSM, the metabolic profile of the motor cortex did not recover, despite successful surgery and clinical improvement. The mild CSM group also had a larger activated region in the primary motor cortex than moderate CSM prior to surgery. The moderate CSM patients, who were more severely impaired prior to surgery, demonstrated the largest interval improvement following surgery and a drop in NAA/Cr levels post-operatively. Following surgery, the activated areas were comparable between the mild and moderate groups and had shifted towards the primary sensory cortex. This study establishes that it is possible to differentiate between the mild and moderate CSM groups using clinical examination and advanced imaging biomarkers. These distinct patterns of remote injury of the sensorimotor cortex in mild and moderate CSM patients could be a critical factor underlying natural history and determining the timing and need for intervention.

The ultimate goal was to develop advanced imaging biomarkers that could be used to assess the severity of CSM and predict the outcome of decompressive surgery. This work identified the application of new imaging techniques in examining the prognostic ability of MRS, DTI and fMRI. This data can be used to more accurately identify a specific point in injury severity that will have the most benefit from surgical intervention. Furthermore, the use of NAA as a biomarker may be useful in providing prognostic information to patients, and in implementing appropriate treatment plans, especially in early stage mild CSM. Equally important in this work, is the notion that areas distal from the site of injury are affected, should not be ignored, and further investigated.

5.2 Limitations

The limitations of each of the studies presented in this thesis have been discussed in detail in their respective chapters. However, a general limitation of searching for predictors of surgical outcome for the CSM population is the classification into severity subgroups. CSM patients are highly heterogeneous with symptoms ranging from mild to severe and affecting both upper and lower limbs. Stricter categorization determinants are required in identifying the difference between the CSM subgroups: mild, moderate and severe. Currently, the categorization of CSM to a severity subgroup is strictly based on the mJOA score. However, the mJOA score is a subjective questionnaire completed by the patient and does not take into account the findings from the neurological exam or the imaging results. A classification system should consider all findings during a clinic visit, specifically: the new updated JOAMCEQ-L questionnaire, neurological signs and symptoms, and findings on MR imaging.

This thesis introduced great insight into the cortical changes of the CSM patient population that can be measured non-invasively using MR techniques. Specifically, changes in the NAA concentrations were found in the primary motor cortex CSM patients suggesting neuronal death and/or mitochondrial dysfunction. The differences in the NAA concentration were between the mild and moderate CSM group at the pre-operative time point. The NAA concentrations could be used as predictors of outcome or biomarkers reflecting an underlying structural or physiological event. However, this cannot be confirmed until the affected neurons (with decreased NAA) are directly evaluated in the cortex. This is not possible as it would involve an invasive operation and damaging the white matter itself. Instead, animal models of CSM may prove to be useful in understanding the basic mechanisms of neuronal death or dysfunction in the motor cortex in hopes of devising a marker that can predict conservative and surgical outcome.

5.3 Future Directions

This thesis introduced important findings regarding the cortical changes of the CSM patient population that can be measured using novel non-invasive MRI techniques. It is important to address the injury occurring at the level of the spinal cord, and downstream in the cortex. The measured cortical changes, specifically NAA and VOAs, were able to discriminate between the mild and moderate CSM groups. However, in order to create a predictor of outcome in the CSM patient population, we must first look at the mild CSM population who do not receive surgical intervention. Research has shown that some patients are able to benefit from conservative treatment and do not need to undergo surgical intervention. Measuring the longitudinal metabolite and functional changes in the mild CSM group who do not undergo decompressive surgery builds on the early work of this thesis in an effort to understand the natural history of

CSM. Following an exploration into the natural progression of CSM, accurate predictors and biomarkers can be evaluated in aiding the evaluation and management of the patient population.

Secondly, the metabolite concentrations were only measured in the primary motor cortex contralateral to the greater deficit side in the CSM population. It would be valuable to investigate the metabolite alterations in mild CSM patients treated conservatively, and mild and moderate CSM patients treated surgically, bilaterally in the primary motor cortex. This would provide a further understanding of the pathophysiology of CSM and the adaptations the cortex makes to accommodate for the loss in function. It would be interesting to determine whether the same changes occur bilaterally, or if the greater deficit side experiences more injury. Following these three groups longitudinally would provide insight into the possible role of brain plasticity in the preservation or recovery of neurological function. The metabolite concentrations should also be correlated to functional changes measured by fMRI during a finger tapping task and clinical status measured by the new updated JOACMEQ-L.

5.4 Conclusions

Each of these studies offered new information on cortical adaptations in the primary motor cortex and identified possible biomarkers to better understand and classify CSM based on injury severity. The most pertinent findings presented in this thesis are as follows: 1) The primary motor cortex undergoes cortical reorganization in CSM patients; 2) NAA/Cr is decreased in CSM patients prior to and following surgical intervention despite neurological recovery; 3) Mild and moderate CSM patients present different metabolic concentrations and functional activations; and 4) Following surgery, both groups experience neurological improvement and show an activation

centered on the primary sensory cortex and same low levels of NAA/Cr. Each of these studies presented a new approach at identifying and classifying the severity of CSM. These novel non-invasive imaging assessments are able to provide adjunctive information and hopefully will provide a more precise understanding of the functional and metabolic pathways that may ultimately be incorporated into clinical decision making. The goal is to gain further understanding of the pathophysiology of CSM and evaluate new diagnostic tools. These sensitive imaging biomarkers may foreshadow clinical deterioration and provide predictive information to further tailor the treatment of CSM on a patient-by-patient basis.

APPENDIX A:

RESEARCH ETHICS BOARD APPROVAL

Western Research

Research Ethics

Use of Human Participants - Ethics Approval Notice

Principal Investigator: Dr. Neil Duggal
File Number: 1340
Review Level: Delegated
Approved Local Adult Participants: 35
Approved Local Minor Participants: 0
Protocol Title: Mapping of the Sensorimotor Cortex in Cervical Myelopathy using fMRI, MRS and DTI
Department & Institution: Schulich School of Medicine and Dentistry/Clinical Neurological Sciences, London Health Sciences Centre
Sponsor:
Ethics Approval Date: October 05, 2012 Expiry Date: January 31, 2014
Documents Reviewed & Approved & Documents Received for Information:

Document Name	Comments	Version Date
Revised Study End Date		

This is to notify you that The University of Western Ontario Research Ethics Board for Health Sciences Research Involving Human Subjects (HSREB) which is organized and operates according to the Tri-Council Policy Statement: Ethical Conduct of Research Involving Humans and the Health Canada/ICH Good Clinical Practice Practices: Consolidated Guidelines; and the applicable laws and regulations of Ontario has reviewed and granted approval to the above referenced revision(s) or amendment(s) on the approval date noted above. The membership of this REB also complies with the membership requirements for REB's as defined in Division 5 of the Food and Drug Regulations.

The ethics approval for this study shall remain valid until the expiry date noted above assuming timely and acceptable responses to the HSREB's periodic requests for surveillance and monitoring information. If you require an updated approval notice prior to that time you must request it using the University of Western Ontario Updated Approval Request Form.

Members of the HSREB who are named as investigators in research studies, or declare a conflict of interest, do not participate in discussion related to, nor vote on, such studies when they are presented to the HSREB.

The Chair of the HSREB is Dr. Joseph Gilbart. The HSREB is registered with the U.S. Department of Health & Human Services under the IRB registration number IRB 00000940.

Signature

Ethics Officer to Contact for Further Information

☑ Janice Sutherland (jsutherl@uwo.ca)	☐ Grace Kelly (grace.kelly@uwo.ca)	☐ Sharon Wilcox (swilcox@uwo.ca)

This is an official document. Please retain the original in your files.

APPENDIX B:

COPYRIGHT ACKNOWLEDGMENT

Subject: **RE: Permission to use article in PhD thesis**
To: Izabela Kowalczyk

Date: 08/14/14 07:06 AM
From: JOURNALS PERMISSIONS

Dear Izabela Kowalczyk

Izabela Kowalczyk et al. Proton magnetic resonance spectroscopy of the motor cortex in cervical myelopathy Brain (2012) 135 (2): 461-468 first published online December 15, 2011 doi:10.1093/brain/awr328

Thank you for your recent email requesting permission to reuse all or part of your article in a thesis

As part of your copyright agreement with Oxford University Press you have retained the right, after publication, to use all or part of the article and abstract, in the preparation of derivative works, extension of the article into a booklength work, or in another works collection, provided that a full acknowledgement is made to the original publication in the journal. As a result, you should not require direct permission from Oxford University Press to reuse you article.

However, as per the journal self-archiving policy, you may only include your accepted manuscript in an online thesis, along with the following acknowledgment and a link to the final published version.

This is a pre-copyedited, author-produced PDF of an article accepted for publication in [insert journal title] following peer review. The version of record [insert complete citation information here] is available online at: [insert URL that the author will receive upon publication here].

For full details of our publication and rights policy please see the attached link to our website:

http://www.oxfordjournals.org/en/access-purchase/rights-and-permissions/publication-rights.html

If you have any other queries, please feel free to contact us.

Yours sincerely

Emma Thornton
Permissions Assistant
Academic Rights & Journals

-----Original Message-----
From: Izabela Kowalczyk [
Sent: 13 August 2014 16:47
To: JOURNALS PERMISSIONS
Subject: Permission to use article in PhD thesis

Good morning,

My name is Izabela Kowalczyk. Our group recently had the privelage of having our manuscript published in Brain. The title is, "Proton Magnetic resonance spectroscopy of the motor cortex in cervical myelopathy" (Brain 2012; 135: 461-468).

This manuscript was part of my PhD thesis. I am currently writing my thesis and require a copy of this paper as one of my chapters. Could you please let me know what the steps are to receive permission to do so?

Thank you
Izabela Kowalczyk

APPENDIX C:

CURRICULUM VITAE

IZABELA ALEKSANDEREK (nee KOWALCZYK)

EDUCATION

Toronto Western Hospital
Post-Doctoral Fellow **September 2014 – Present**
Supervisor: Dr. Michael Fehlings, MD, PhD

The University of Western Ontario
Doctoral Degree in Medical Biophysics **September 2008 – Present**
Thesis: Evaluation of the sensorimotor cortex in Cervical Spondylotic Myelopathy patients using functional MRI, Magnetic Resonance Spectroscopy and Diffusion Tensor Imaging
Supervisors: Drs. Neil Duggal, MD and Robert Bartha, PhD

The University of Western Ontario
Certificate in Clinical Trials Management **September 2008 -April 2010**

The University of Western Ontario
BHSc Honours Specialization in Health Science **September 2004 -April 2008**
and Minor in Pharmacology/Toxicology
Thesis: Exercise for the treatment of depression in older adults: Prescribing the best F.I.T.T.

WORK EXPERIENCE

Department of Neurosurgery, University Hospital, London Health Sciences Centre
Senior Research Assistant Dr. Neil Duggal **September 2005-August2014**

Manufacturing and Technology Centre
Computer technician **June 2007 - August 2007**

VOLUNTEER EXPERIENCE

University Hospital, London Health Sciences Centre
CNS Clinic Volunteer **September 2005–August2014**

Let's Talk Science Partnership Program
Coordinator Volunteer **January 2011 – June 2012**

Chelsey Park Retirement Community, London
Physiotherapy Assistant **January 2011 – June 2012**

The University of Western Ontario – Anatomy 203b
Teaching Assistant to Professor Timothy Wilson **January 2006 - April 2007**

The University of Western Ontario – Polish 030

Teaching Assistant to Professor Grzegorz Danowski **September2005 - Dec 2006**

MEMBERSHIPS

Canadian Association for Neuroscience	January 2013 - Present
Society for Brain Mapping and Therapeutics	March 2012 - Present
Biomedical Imaging Research Centre	January 2011 - Present
International Society for Magnetic Resonance in Medicine	November 2010 - Present
Canadian Organization of Medical Physicists	September 2009 – Present

MANAGEMENT

Undergraduate Students

Minnie Rai	September 2007 - April 2008
Daniella Dimitri	September 2008 - April 2009
Emily Yung	September 2009 - April 2011
Sandy Goncalves	September 2010 - April 2011

Graduate Students

Sandy Goncalves	May 2011 – December 2012

Medical Students

Won Hyung A. Ryu	February 2009 - August 2012
Stuart M.K. M^{c}Gregor	May 2010 - August 2012

AWARDS

1) **Southern Ontario Neuroscience Association (SfN) - $200**
   1st place Winner in PhD/Post-Doctoral Category (poster)
   May 13, 2013

2) **Publication of the Month – Schulich Medicine & Dentistry**
   http://www.uwo.ca/schulich/gradstudies/current/student_research.html
   Proton magnetic resonance spectroscopy of the motor cortex in cervical myelopathy
   May 18, 2012

3) **3MT – 3 Minute Thesis Competition - $500**
   Predicting Surgical Outcome in Spinal Cord Compression Patients Using Magnetic Resonance Spectroscopy
   Finalist - April 26, 2012

4) **Western Research Forum - $100**
   2nd Place in Biotechnology and Computer Sciences Category (oral presentation)
   March 27, 2012

5) **Graduate Thesis Research Award - $1,300**
Mapping of the Reorganization of the Sensorimotor Cortex in Cervical Myelopathy Patients Using fMRI, MRS and DTI
May 1, 2011 – August 31, 2012 (Awarded Jan 18, 2012)

6) **J. Allyn Taylor Prize in Medicine Day - $100**
1st Place in PhD Category (poster)
November 3, 2010

7) **Western Research Forum - $100**
2nd Place in Biological Sciences Category (oral presentation)
February, 2010

8) **Western Research Forum - $150**
1st Place in Biological Sciences Category (Poster)
Featured in The Graduate Review: www.uwo.ca/sogs/WGR/IKowalczyk
January 2009

9) **Queen's National Undergraduate Conference in Medicine - $250**
1st Place in Poster Category and Delegate's Choice Award
November 2007

SCHOLARSHIPS and GRANTS

Academic Development Fund Small Research Grant **$7,150**
July 1, 2011 – June 30, 2012
MR Diffusion Tensor Imaging of Sensorimotor Cortex in Cervical Myelopathy
Co-PI: Dr. Neil Duggal

LHRI Internal Research Fund Studentship **$15,000**
January 1, 2011 – December 31, 2011
Impact of Spinal Cord Compression Decompression Surgery on Brain Metabolism
Co-PI's: Dr. Neil Duggal, Dr. Robert Bartha

Western Graduate Research Scholarship **Tuition**
September 2008 - August 2013

INVITED TALKS

1) Magnetic Resonance Spectroscopy and Diffusion Tensor Imaging in Cervical Myelopathy Patients Following Spinal Decompression Surgery. *AC Burton Day.* April 12, 2012.

COMMUNITY OUTREACH

1) Western News: New Research Identifies changes in spinal cord compression. December 16, 2011. http://communications.uwo.ca/western_news/stories/2011/December/new_research_identifies_changes_in_spinal_cord_compression.html

2) CTV2 Local News: Proton Magnetic Resonance Spectroscopy of the Motor Cortex in Cervical Myelopathy. Aired December 16, 2011.

3) Western University YouTube Channel: Spinal Cord Compression & the Brain. December 15, 2011. http://www.youtube.com/watch?v=M9WFrRtEA54&feature=share

PUBLICATIONS

1) **Aleksanderek I**, Stevens TK, Goncalves S, Bartha R, Duggal N. Mild and moderate cervical spondylotic myelopathy: Are they metabolically and functionally different? In preparation to *The Lancet Neurology*, November, 2014.

2) **Aleksanderek I,** McGregor SMK, Stevens TK, Goncalves S, Bartha R, Duggal N. Metabolite changes in the primary motor cortex after surgery in cervical spondylotic myelopathy. Submitted to *Radiology*, October 16, 2014.

3) **Kowalczyk I**, Ryu WHA, Rabin D, Arango M, Duggal N. Reduced endotracheal tube cuff pressure to assess dysphagia after anterior cervical spine surgery. Accepted to *Journal of Spinal Disorders & Techniques*, August 18, 2014 [Epub ahead of print]

4) **Kowalczyk I,** Navjot C, Duggal N. Kinematic Analysis Following Implantation of the Prestige LP. The International Journal of Spine Surgery 7(1):e118-e122, 2013.

5) Ryu WHA, **Kowalczyk I**, Duggal N. Long-term kinematic consequences following single-level implantation of Bryan cervical disc prosthesis. The Spine Journal 13(6):628-634, 2013.

6) **Kowalczyk I**, Duggal N, Bartha R. Proton Magnetic Resonance Spectroscopy of the Motor Cortex in Cervical Myelopathy. Brain 135(Pt2):461-468, 2012.

7) **Kowalczyk I**, Lazaro BCR, Fink M, Rabin D, Duggal N. Analysis of *in vivo* biomechanics of three different cervical devices: Bryan disc, ProDisc-C and Prestige LP. Journal of Neurosurgery: Spine 15(6):630-635, 2011.

8) Duggal N, Bertagnoli R, Rabin D, Wharton N, **Kowalczyk I**. ProDisc-C: An In-Vivo kinematic study. Journal of Spinal Disorders & Techniques 24(5):334-339, 2011.

9) Lazaro BCR, Yucesoy K, Yuksel KZ, **Kowalczyk I**, Rabin D, Fink M, Duggal N. Effect of arthroplasty design on cervical spine kinematics: analysis of the Bryan Disc, ProDisc-C, and Synergy Disc. Neurosurgical Focus 28(6):E6, 2010.

10) Duggal N, Rabin D, Bartha R, Barry RL, Gati JS, **Kowalczyk I**, Fink M. Brain reorganization in patients with spinal cord compression evaluated using fMRI. Neurology 74(13):1048-1054, 2010.

ABSTRACTS (*Presenter)

1) **Kowalczyk I*,** Stevens TK, Goncalves S, Bartha R, Duggal N. Unique metabolic and functional profiles in mild and moderate cervical myelopathy. *Southern Ontario Neuroscience Association (SfN).* London, Ontario; May 5, 2014. (poster)

2) **Kowalczyk I*,** Stevens TK, Goncalves S, Bartha R, Duggal N. Unique metabolic and functional profiles in mild and moderate cervical myelopathy. *Imaging Network Ontario, 12th Imaging Network Symposium.* Toronto, Ontario; March 24-25, 2014. (poster)

3) **Kowalczyk I*,** Stevens TK, Goncalves S, Bartha R, Duggal N. Unique metabolic and functional profiles in mild and moderate cervical myelopathy. *London Health Research Day.* London, Ontario; March 18, 2014. (poster)

4) **Kowalczyk I*,** Bartha R, Duggal N. Magnetic Resonance Spectroscopy and Diffusion Tensor Imaging in Cervical Myelopathy Patients Following Spinal Decompression Surgery. *Canadian Association for Neuroscience*. Toronto, Ontario; May 21-24, 2013. (poster)

5) **Kowalczyk I*,** Bartha R, Duggal N. Magnetic Resonance Spectroscopy and Diffusion Tensor Imaging in Cervical Myelopathy Patients Following Spinal Decompression Surgery. *Southern Ontario Neuroscience Association (SfN)*. Waterloo, Ontario; May 13, 2013. (poster)
WINNER: First place in PhD/Post-Doctoral Category ($200)

6) **Kowalczyk I***, Bartha R, Duggal N. Magnetic Resonance Spectroscopy and Diffusion Tensor Imaging in Cervical Myelopathy Patients Following Spinal Decompression Surgery. *London Health Research Day*. London, Ontario; March 19, 2013. (poster)

7) **Kowalczyk I***, Bartha R, Duggal N. Magnetic Resonance Spectroscopy and Diffusion Tensor Imaging in Cervical Myelopathy Patients Following Spinal Decompression Surgery. *Western Research Forum*. London, Ontario; March 15, 2013. (oral)

8) **Kowalczyk I***, Duggal N, Bartha R. Magnetic Resonance Spectroscopy and Diffusion Tensor Imaging in Cervical Myelopathy Patients Following Spinal Decompression Surgery. *9th Annual Congress of SBMT on Brain, Spinal Cord Mapping and Image Guided Therapy.* Toronto, Ontario; June 2-4, 2012. (oral and poster)

9) **Kowalczyk I***, Duggal N, Bartha R. Decreased *N*-Acetylaspartate in the Motor Cortex of Cervical Myelopathy Patients Following Decompressive Surgery: A Magnetic Resonance Spectroscopy Study. *Western Research Forum.* London, Ontario; March 26-27, 2012. (oral)
WINNER: Second place in Biotechnology and Computer Sciences Category ($100)

10) **Kowalczyk I***, Duggal N, Bartha R. Decreased *N*-Acetylaspartate in the Motor Cortex of Cervical Myelopathy Patients Following Decompressive Surgery: A Magnetic Resonance Spectroscopy Study. *London Health Research Day.* London, Ontario; March 20, 2012. (poster)

11) **Kowalczyk I***, McGregor SMK, Bartha R, Duggal N. MRI Diffusion Tensor Imaging in Cervical Spondylotic Myelopathy. *London Imaging Discovery Day.* London, Ontario; June 23, 2011. (poster)

12) **Kowalczyk I***, Duggal N, Bartha R. MR Diffusion Tensor Imaging in Cervical Spondylotic Myelopathy. *International Society for Magnetic Resonance in Medicine*. Montreal, Quebec; May 7-13, 2011. (e-poster)

13) **Kowalczyk I***, Duggal N, Bartha R. MR Spectroscopy of the Motor Cortex in Cervical Spondylotic Myelopathy: Pre and Post Surgery Observations. *International Society for Magnetic Resonance in Medicine*. Montreal, Quebec; May 7-13, 2011. (e-poster)

14) **Kowalczyk I**, Goncalves S*, Yung E, Lazaro BCR, Fink M, Rabin D, Duggal N. Analysis of *in vivo* biomechanics of three different cervical discs: Bryan Disc, ProDisc-C and Prestige LP. *Margaret Moffat Research Day.* London, Ontario; March 29, 2011. (poster)

15) **Kowalczyk I***, McGregor SMK, Bartha R, Duggal N. MRI Diffusion Tensor Imaging in Cervical Spondylotic Myelopathy. *Margaret Moffat Research Day.* London, Ontario; March 29, 2011. (poster)

16) Ryu WHA*, **Kowalczyk I**, Duggal N. Long-term kinematic consequences following single-level implantation of Bryan cervical disc prosthesis. *Clinical Neurological Sciences Research Day*. London, Ontario; March 8, 2011. (oral)

17) McGregor SMK*, **Kowalczyk I**, Bartha R, Duggal N. Examination of the Structural Integrity of White Matter in Cervical Spondylotic Myelopathy Patients Using Diffusion Tensor Imaging. *Clinical Neurological Sciences Research Day*. London, Ontario; March 8, 2011. (oral)

18) **Kowalczyk I***, Bartha R, Duggal N. Metabolic Changes in the Motor Cortex in Cervical Spondylotic Myelopathy Followed by Proton Magnetic Resonance Spectroscopy. *Clinical Neurological Sciences Research Day*. London, Ontario; March 8, 2011. (oral)

19) **Kowalczyk I***, McGregor SMK, Bartha R, Duggal N. MRI Diffusion Tensor Imaging in Cervical Spondylotic Myelopathy. *Western Research Forum.* London, Ontario; February 26, 2011. (oral)

20) **Kowalczyk I***, Duggal N, Bartha R. Proton Magnetic Resonance Spectroscopy of the Motor Cortex in Cervical Spondylotic Myelopathy. *J. Allyn Taylor International Prize in Medicine.* London, Ontario; November 3, 2010. (poster)
WINNER: First place in PhD Category ($100)

21) **Kowalczyk I***, Duggal N, Bartha R. Proton Magnetic Resonance Spectroscopy of the Motor Cortex in Cervical Spondylotic Myelopathy. *Congress of the Canadian Neurological Sciences Federation.* Quebec City, Quebec; June 2010. (oral)

22) **Kowalczyk I***, Duggal N, Bartha R. Proton Magnetic Resonance Spectroscopy of the Motor Cortex in Cervical Spondylotic Myelopathy. *5th Annual London Imaging Discovery Day.* London, Ontario; June 2010. (poster)

23) Duggal N*, **Kowalczyk I**, Rabin D. In-Vivo Kinematic Comparison of Prodisc-C, Prestige LP and Bryan Cervical Disc. *Spine Arthroplasty Society*. New Orleans, Louisana; April, 2010. (poster)

24) **Kowalczyk I***, Duggal N, Bartha R. Proton Magnetic Resonance Spectroscopy of the Motor Cortex in Cervical Spondylotic Myelopathy. *Clinical Neurological Sciences Research Day.* London, Ontario; March 2010. (oral)

25) **Kowalczyk I***, Duggal N, Bartha R. Proton Magnetic Resonance Spectroscopy of the Motor Cortex in Cervical Spondylotic Myelopathy. *Margaret Moffet Research Day.* London, Ontario; March 2010. (poster)

26) **Kowalczyk I***, Duggal N, Bartha R. Proton Magnetic Resonance Spectroscopy of the Motor Cortex in Cervical Spondylotic Myelopathy. *Western Research Forum.* London, Ontario; February 2010. (oral)
WINNER: Second place in Biological Sciences Category

27) **Kowalczyk I***, Duggal N, Bartha R. Proton Magnetic Resonance Spectroscopy of the Motor Cortex in Cervical Spondylotic Myelopathy. *Imaging Network Ontario, 8th Imaging Symposium.* Toronto, Ontario; February 2010. (poster)

28) Duggal N*, **Kowalczyk I**, Rabin D. In-Vivo Kinematic Comparison Of Prodisc-C, Prestige LP, Bryan Cervical Disc And A Discectomy With Fusion. *North American Spine Society*. San Fransisco, California; November, 2009. (oral)

29) Duggal N, **Kowalczyk I***. In-vivo Kinematic Comparison of ProDisc-C, Prestige LP and Bryan Cervical Disc and Discectomy with Fusion. *Congress of the Canadian Neurological Sciences Federation.* Halifax, Nova Scotia; June 2009. (oral)

30) Chaudhary N, Bajares G, Oliva A, **Kowalczyk I**, Duggal N*. Kinematic Analysis Following Implantation of the Prestige LP Cervical Disc System. *Spine Arthroplasty Society*. London, England; May 2009. (poster)

31) **Kowalczyk I***, Chaudhary N, Bajares G, Oliva A, Duggal N. Kinematic Analysis Following Implantation of the Prestige LP Cervical Disc System. *Margaret Moffet Research Day*. London, Ontario; March 2009. (poster)

32) **Kowalczyk I***, Fink M, Duggal N. Minimally Invasive Equipment: Does it make sense? Cost analysis comparing minimally invasive surgery with standard instrumented open surgery? *Western Research Forum*. London, Ontario; January 2009. (poster)
WINNER: First place in Poster Category
WINNER: http://www.uwo.ca/sogs/WGR/IKowalczyk/index.html

33) **Kowalczyk I***, Chaudhary N, Bajares G, Oliva A, Duggal N. Kinematic Analysis Following Implantation of the Prestige LP Cervical Disc System. *Queen's National Undergraduate Conference on Medicine*. Kingston, Ontario; November 2008. (poster)

34) Duggal N*, **Kowalczyk I**, Rabin D, Fink M. Minimally Invasive Equipment: Does it make sense? Cost analysis comparing minimally invasive surgery with standard instrumented open surgery. *Canadian Congress of Neurological Sciences.* Victoria, British Columbia; June 2008. (oral)

35) **Kowalczyk I***, Fink M, Duggal N. Minimally Invasive Equipment: Does it make sense? Cost analysis comparing minimally invasive surgery with standard instrumented open surgery? *Queen's National Undergraduate Conference on Medicine*. Kingston, Ontario; November 2007. (poster)
WINNER: First place in Poster Category;
WINNER: Delegate's Choice Award

LANGUAGES

Polish – Speak/read/write fluently
English – Speak/read/write fluently